Application of Superconductors to Improve the Performance of PMSG based WECS

By

Amjad Ali

CIIT/SP18-REE-016/LHR

MS Thesis

In

Electrical Engineering

COMSATS University Islamabad,

Lahore Campus, Pakistan

SPRING 2021

COMSATS University Islamabad, Lahore Campus

Application of Superconductors to Improve the Performance of PMSG based WECS

A Thesis Presented to

COMSATS University Islamabad, Lahore Campus

In partial fulfillment

Of the requirement for the degree of

MS Electrical Engineering

By

Amjad Ali

CIIT/SP18-REE-016/LHR

SPRING, 2021

Application of Superconductors to Improve the Performance of PMSG based WECS

A Post Graduate Thesis submitted to the Department of Electrical and Computer Engineering as partial fulfillment of the requirement for the award of Degree of M.S Electrical Engineering.

Name	Registration Number
Amjad Ali	CIIT/SP18-REE-016/LHR

Supervisor

Dr. Muhammad Jawad

Assistant Professor
Department of Electrical and Computer Engineering
Lahore Campus
COMSATS University Islamabad (CUI),
Lahore Campus

June, 2021

Final Approval

This thesis titled

Application of Superconductors to Improve the Performance of PMSG based WECS

By

Amjad Ali

CIIT/SP18-REE-016/LHR

Has been approved

For the COMSATS University Islamabad, Lahore Campus

External: _____

Dr. _ _ _ _ _ _ _ _ _ _ _ _ _ _

_ _ _ _ _ _ _ _ _ _ _

Supervisor: _____

Dr. Muhammad Jawad

Electrical and Computer Engineering, Lahore

HOD: _____

Dr. Ejaz A. Ansari

Electrical and Computer Engineering, Lahore

DECLARATION

I Amjad Ali, Reg No: CIIT/SP18-REE-016/LHR hereby declares that I have produced the work presented in the thesis, during the scheduled period of study. I also declare that I have not taken any material from any source except referred to where due that amount of plagiarism is within acceptable range. If a violation of HEC rules on research has occurred in this thesis, I shall be liable to punishable action under the plagiarism rules of the HEC.

Date: 05-07-2021

Signature of Student:

_____

Amjad Ali
CIIT/SP18-REE-016/LHR

CERTIFICATE

It is certified that Amjad Ali, Reg No: CIIT/SP18-REE-016/LHR has carried out all the work related to this thesis under my supervision of the Department of Electrical and Computer Engineering, COMSATS University Islamabad, Lahore campus and the work fulfills the requirement for the award of the MS degree.

Date: _____

Supervisor:

_____
Dr. Muhammad Jawad
Assistant Professor
ECE Department
CUI, Lahore Campus

Head of Department:

_____
Dr. Ejaz A. Ansari
ECE Department
CUI, Lahore Campus

DEDICATION

This work is dedicated to my parents, whose encouragement and support was always there along my side to accomplish my dreams.

‘My Lord! Bestow on them Your mercy, as they did bring me up when I was small’.
(Quran 17:24)

ACKNOWLEDGMENTS

First and foremost, I would like to praise and thank Allah Almighty for allowing me to complete this research work. I would like to express my sincere gratitude to my advisor, **Dr. Muahmmad Jawad** for his guidance and continuous supervision of my study and research. The achievement of this master's dissertation is only possible due to his guidance and supervision. Without his encouragement, inspirational guidance, patience and immense knowledge I could not have finished my work. He always extended his unconditional support and clarified my doubts and concerns: despite of his busy schedule he was always available whenever I needed him. His guidance helped me in all the time of research as well as the writing of this thesis and it proved as a great opportunity for me to learn from his research expertise. I could not have found a better mentor than him.

Amjad Ali
CIIT/SP18-REE-016/LHR

ABSTRACT

With ever increasing demand of electricity and depleting conventional energy sources with their environmental concerns, renewable energy sources are an excellent alternative for producing clean energy. Among many renewable energy sources, wind energy has huge potential to contribute part of energy demand. However, as a result of unprecedented integration of wind energy in low voltage and high voltage grids, ensuring stability and power quality following grid codes is a challenge lately. Wind Energy Conversion System (WECS) suffers from two main problems, 1) fluctuations in output power due to unpredictable behavior of wind, and 2) retention of connection during grid faults. The optimal solution to increase Fault Ride Through (FRT) capability and smoothing of output power fluctuations in PMSG based WECS is still a point of research in literature. In this research Work, the application of superconductors to enhance the performance of Permanent Magnet Synchronous Generator (PMSG) based WECS is investigated. The presented work considers optimal integration of Superconducting Coil (SC) with PMSG based WECS. Fractional Order PI (FOPI) control is used for control of SC circuit. Harmony Search (HS) optimization technique is used for finding optimum parameter values of the SC and FOPI controllers. The proposed strategy is then compared with PI based control of SC for disturbance in the form of wind gust and grid fault.

TABLE OF CONTENTS

LIST OF TABLES

LIST OF FIGURES

LIST OF ABBREVIATIONS

List of Acronyms	
PMSG	Permanent Magnet Synchronous Generator
SMES	Superconducting Magnetic Energy Storage
SC	Fault ride Through
FRT	Fault ride Through
FOPI	Fractional Order Proportional Integrator
PI	Proportional Integral
WECS	Wind Energy Conversion System
HTS	High Temperature Superconductor
DFIG	Doubly Fed Induction generator
MPPT	Maximum Power Point Tracking
PCC	Point of Common Coupling
FACTS	Flexible AC transmission system
WTGs	Wind turbine Generators
ESS	Energy Storage System
DVR	Dynamic Voltage Restorer
ELDC	Electric Double Layer Capacitor
PSO	Particle Swarm optimization
PAC	Pitch angle control
SFCL	Superconductor Fault Current Limiter
VSC	Voltage Source Converter
CSC	Current Source Converter
BTB	Back to Back
VC	Vector Control
DTC	Direct Torque control
EWMA	Exponentially Weighted Moving Average
FLC	Fuzzy Logic Control
TSR	Tip Speed Ratio
FOC	Field Oriented Control
GSC	Grid Side Control
MSC	Machine Side Control

VOC	Voltage Oriented Control
DPC	Direct Power Control
PLL	Phase Locked Loop
HS	Harmony Search
HMCR	Harmony Memory Consideration Rate
PAR	Pitch Adjustment Rate
BC	Breaking Chopper
CEPRI	China Electric Power Research Institute
GSC	Grid Side Converter
SMC	Sliding Mode Control
SMAPA	Set-Membership Affine Projection Algorithm

Chapter

1

Introduction

Wind energy is an excellent and feasible solution to continuous demand of world energy with no environmental concers. Increased penertration of wind enegy systems with utility grid creates multiple challenges for grid operators to ensure power quality, stability and realibility. Recently, permanent magnet synchronous generator (PMSG) based wind systems have gained increased application due to technological advancements in power electroics and ferromagnetic material research. However, PMSG suffers from two main problems such as output power fluctuations due to wind gusts and necessity to have better fault ride through capability during grid faults in order to comply with grid codes. The application of supercondcutors presents an excellent solution to improve the performance of PMSG based wind energy conversion systems (WECS).

1.1 Research Background

Traditional resources such as oil, gas and coal have been in predominant use through the world. These resources are depleting at a higher rate as they are responsible for almost 80% of the world's energy demand. Also, the utilization of conventional resources has created issues such as climate change, global warming accompanied with high of emission of CO_2, and high fuel cost. increased air pollution. Moreover, due to increased industrial development, average energy demand per capita have also increased. Increased environmental implications, depletion of fossil fuels, greater energy demand and cost associated with conventional resources have created the need to find alternate energy resources. Energy production from renewable resources have increased rapidly during the last decades as a result of limited fossil resources and their associated environmental concerns. Renewable energy resources provide a sustainable and clean energy alternative for the modern power grids. The contribution of renewable energy in total installed power generating capacity of the world is more than 33%, equivalent to 2,378 GW [1]. The graph showing comparison of installed capacities is given in Figure 1.1.

In recent years, wind energy can play an important role modern power network as it is clean, renewable, and is viable source for meeting global energy demand. Wind energy is of great potential to fulfil increased demand of clean energy. The wind power installed capacity grew from 540 GW in 2017 to 591 GW in 2018 globally [1] and it is expected to reach 800 GW by 2021[2] as given in Figure 1.2.

The concept of modern Wind Energy Conversion Systems (WECS) and their development can be traced back to the year 1970 but only recent decades have shown considerable growth in this field. The increased popularity and application of WECS is mainly due to the technological breakthrough made in the field of power electronics, signal processing and turbine dynamics. These breakthroughs have increased the productivity and decreased the cost of the WECS. However, increased addition of wind power into electrical grids, have created a huge challenge for the grid operators in the form of power quality and transient stability assurance.

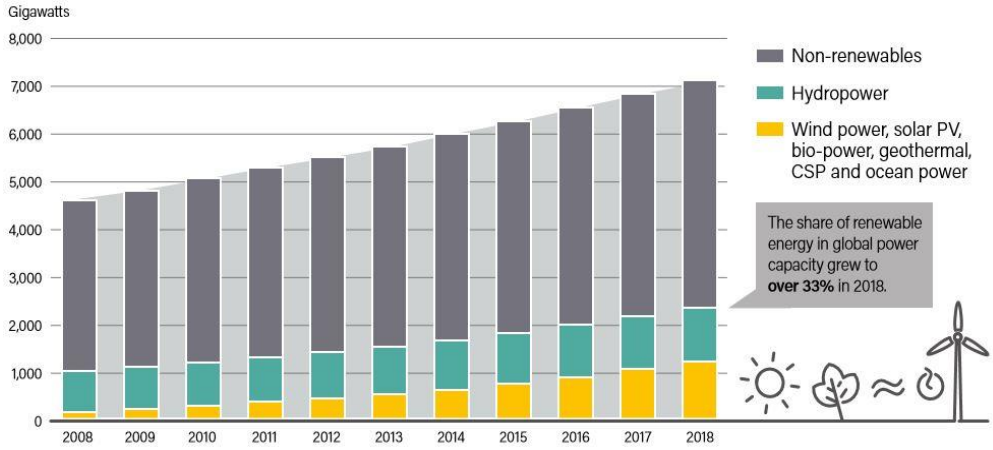

Figure 1.1 Part of energy demand covered by renewable resource in 2018 **[1]**

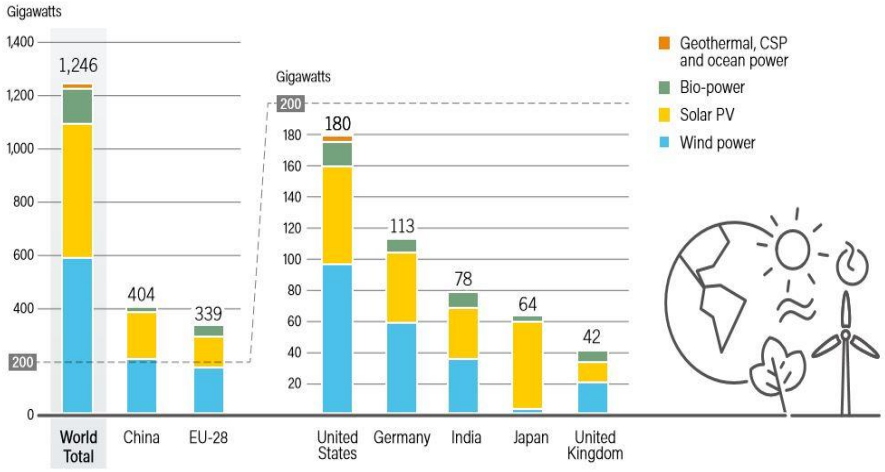

Figure 1.2 Installed capacity of wind energy in 2018 **[1]**

1.2 Challenges

PMSG is popular in wind power industry due to promising features, such as a) higher efficiency, b) high power density, c) self-excitation and d) higher reliability due to

omission of gearbox [3]. However, the PMSG wind turbines are sensitive to disturbances and have two inevitable issues, i.e., fault ride through (FRT) capability and output power fluctuations[4], [5].

Wind output power fluctuations in wind turbines are caused by wind gust during normal operation. Subsequently, it has diverse effects on stability [6], power quality, voltage and frequency of the system [7]. These transients in voltage and frequency can cause cascaded failure in grid, especially during faults at grid side.

Grid codes require that the Wind Turbine Generators (WTGs) should have sufficient FRT capability against disturbances in terminal voltage (PCC) in form of voltage sags and dips. An incident of major blackout happened in state of south Australia on 28th September 2016 due to poor compliance of grid codes. The main reason for this incident was "low voltage ride through (LVRT)" setting on the wind farm. They were set at lower values as compare to required values. Wind power system should have adequate LVRT as most faults create low voltages.

Wind turbine shaft have increased mechanical speed due to transient instability caused by grid faults. The high speed and resulted vibrations can have detrimental effect on shaft. Sudden change in speed acceleration of WTG causes over currents in stator winding and voltage rise in the DC-link bus of WECS [8]. Conventional PMSG wind energy systems employ back to back (BTB) converters to attain full power control. Grid Side Control (GSC) cannot provide all the generated power to grid during grid faults. LVRT is achieved through provision of reactive power to grid by GSC. There is also voltage rise at DC link and fluctuation in frequency due to grid faults. High voltage at DC link can damage capacitor of conversion system. The increase acceleration of the generator is caused by the power imbalance of generated power with that of delivered power to the grid [9]. The high currents can damage generator and power converters if fault condition persists for long time. As result, wind farm will be completely cut out from grid. The loss of large MW wind farm can cause stability risks especially in case of connection with weak grid.

Generators have different LVRT capacities depending upon their sizes. Large generators cannot achieve stable condition quickly after the clearance of fault as they have high inertia. Small capacity generators can get to stable operation very fast due to

their low inertia and fast matching of active power, after recovering from grid fault. The speed variation is much less in case of large generators during faults as they have higher inertia.

To mitigate the rise in voltage at DC link in case of grid faults, either excess active power should be dissipated or the generated power should be reduced so that GSC can give enough reactive power support [10]. LVRT is the process of recovery of WECS from grid faults. The combination of grid variables and generator variables such as votlage profile at DC link, rotor speed, rotor current and grid voltage profile etc., can be used in study for LVRT improvement [11]. The absence of power supply from wind farm during faults can create transient instabilities. In order to protect grid from these transient instabilities , the disconnection of wind farm from grid should be prevented [12].

Numerous techniques have been investigated to improve performance of the PMSG wind turbines and to support grid during disturbances. The performance requirements can be fulfilled either by new modified controls [13] or by utilizing various external devices, such as, FACTS [14], [15] and Energy Storage Systems (ESS) [16]–[18]. In addition, the Dynamic Voltage Restorer (DVR) [19] can be utilized to restore terminal voltage against grid faults by their serial connection with the grid. However, former strategy needs robust controllers and can only be developed for new WECSs. While the latter strategy faces the issue of cost constraint of system due to connection of extra external devices. The control module of these hardware devices further complicates the control of PMSG WECSs.

Recently, application of superconductors in WECS for performance improvement is of great importance [20]. Superconducting Magnetic Energy Storage (SMES) is magnetic field-based energy storage system created with superconducting coil with DC current flowing through it at a cryogenic temperature. A SMES has better cyclic efficiency, quick response for charge and discharge cycles in comparison with other Energy Storage Systems (ESS) [21].

Extensive research have been done to explore the utilization of SMES as a solution to improve power profile and integration of the WECS with grid while ensuring stability of the power system [28]–[31]. However, most of the studies of application of SMES

have been in DFIG based WECS. The integration of SMES with PMSG based WECS by employing control based on advanced meta heuristic Algorithms still need further exploration. SMES can be of better use as compare to other storage devices in multipurpose application, particularly in terms of both FRT and output power smoothing. Moreover, the cost of the Superconducting Coil (SC) is the main issue. Therefore, optimization-based approach is required to get optimal value of SC with the constraint of maintained performance.

This thesis investigates the optimal integration of SMES with PMSG based WECS by utilizing Fractional Order Proportional Integral (FOPI) control and Harmony Search (HS) optimization algorithm. The effect of SMES on the behavior of PMSG system during wind gust and grid fault is investigated.

1.3 Problem Statement

The two main challenges in integration of WECS with primary grid are unpredictable behavior of output power variations and fault ride through capability during grid fault event. There is need to find an optimal solution for both issues.

1.4 Thesis Objectives

The main objectives of this thesis are:

1. Develop a control strategy of SMES unit Integrated with PMSG based WECS.
2. Design of reliable FOPI controllers for regulation of energy between SC and conversion system.
3. Optimization of superconducting coil parameters to minimize the integration cost.
4. Study the effect of wind gust on the PMSG's performance with SC
5. Study the effect of SC on PMSG based WECS's performance during grid fault.

1.5 Summary of Thesis

This thesis consist of six chapters:

- **Chapter 1. Research Background**

  This chapter contains the introduction, challenges, brief discussion on integration of SMES with WECS, thesis objectives and summary of thesis.

- **Chapter 2. Literature Review**

  Extensive literature review of different power fluctuation smoothing and LVRT techniques for PMSG based WECS is presented in this chapter. Moreover, the chapter helps in identifying research gape with respect to use of SMES with PMSG.

- **Chapter 3. Modelling and Control of PMSG based WECS**

  This chapter contains the overall technical attributes of the PMSG based WECS as it is being applied with SMES unit. This chapter contains the complete modelling of the whole WECS.

- **Chapter 4. SMES Unit Configuration and Control Scheme**

  The first part of the chapter contains a brief configurational discussion of SMES power system. This chapter describes the SMES system including proposed control utilizing FOPI controller and Harmony Search (HS) Algorithm for optimization for parameter tunning.

- **Chapter 5. Performance of PMSG Based WECS with integration of Superconducting Coil**

  This chapter contains results and discussion on performance of PMSG based WECS with SMES.

- **Chapter 6. Conclusion and Future Trends**

  Conclusions and brief points of future trends are summarized

Chapter

2

Literature Review

This chapter covers different types of WECS and their fundamental differences. The second part of the chapter deals with literature review of different power smoothing and LVRT techniques being reported for PMSG based WECS over the years. Moreover, different proposed application of SMES in WECS for performance improvement are extensively covered and compared to find the research gap between existing work and future directions.

2.1 Wind Energy Conversion Systems (WECS)

Direct connected WECS were the first generation WECS that used fixed speed turbines to generate power. These systems were much dominated in generation industry that 70% of all installations in 1995 were fixed speed based [26]. This technology lacked high efficiency and could not maximize energy capture. However, tecnological revolution in power electronic have played an important part in improvement of WECS in terms of captured wind energy. Variable speed WECS technology can provide 5% more energy capture as compared to fixed speed technology. Furthermore, variable speed systems can handle wind gusts and corresponding fatigue much better than the fixed speed systems [27], [28]. Based on the wind turbine-generator categories, there are 4 types of WECS that can be found throughout history in wind power generation[29], [30].

2.1.1 Fixed Speed WECS (Type A)

Fixed speed WECS is illustrated in Figure 2.1. It is the first type of WECS making use of asynchronous induction generation for power generation. A gearbox is used to compensate for mismatch of speeds of turbine and generator. In this topology, Direct connection of wind generator with the main power grid is made via a transformer. As a result, generator speed not only depend upon number of poles but also on the system frequency. A soft starter is used to mitigate disturbance caused by the connection of generator with grid. As a result of this disturbance in form of inrush current, drive train ecperiences high torque transients. This configuration has many advantages such as robust, simple, cheap and does not have synchronization problems. However, it has many drawbacks such as, lower efficiency, stress on mechanical parts due to grid fault and requirement of reactive power from grid. To compensate the reactive power need, reactive power compensation devices are used in this configuration.

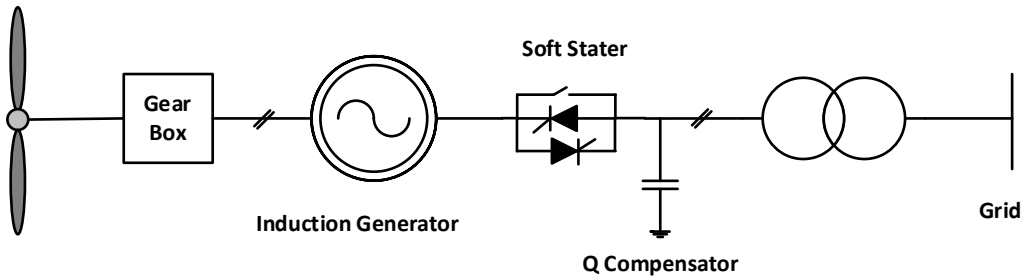

Figure 2.1 Traditional Configuration of Type A WECS

2.1.2 Semi variable speed WECS (Type B)

Type B WECS incorporates the limited variable speed operation of generator to improve conversion efficiency. It has more conversion efficient as compare to Type A system. Typical type B configuration is shown in Figure 2.2. It utilizes wound rotor induction generator in order to use the impact of change of winding resistance on speed torque characteristics of the generator to achieve operation with variable speed. The resistance of the rotor is changed by using an Opti-slip control which allows 0-10% change with respect to nominal speed [31]. This also uses gearbox, soft starter and compensation device.

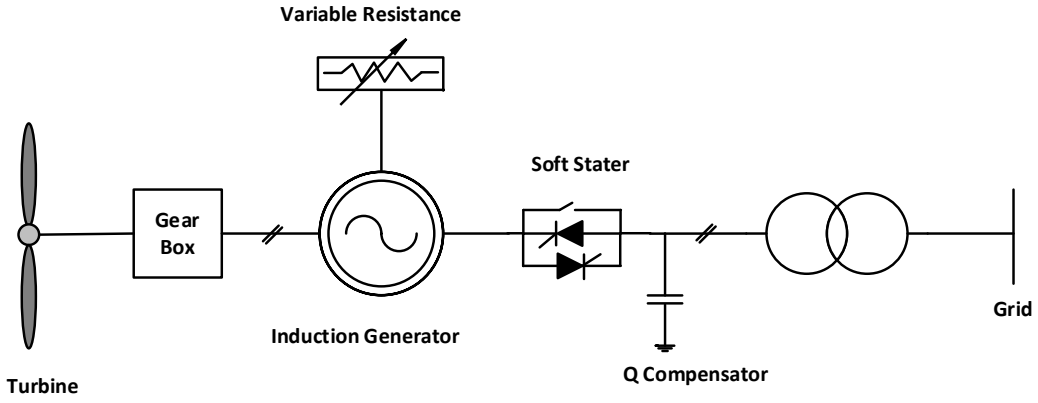

Figure 2.2 Traditional configuration of Type B WECS

2.1.3 Doubly-Fed Induction Generator (DFIG) based WECS (Type C)

This configuration uses DFIG generator with semi control topology as given in Figure 2.3. The generator provides generated power through two windings: stator and rotor winding. The generator has direct connection with grid through the stator winding and rotor winding is connected to BTB converter topology which has rating of about 30% of DFIG rated value [30]. Due to availability of 30% converter rating, variable speed operation of about ±30% can be obtained. The utilization of appropriate control of converter makes the regulation of power much easier. The employment of proposer

Maximum Power Point Tracking (MPPT) technique and 30% variation in speed increase the overall efficiency and improve the dynamic performance of the WECS against the transients. The partial power operation of converters create limitation on FRT capability in case of DFIG.

This configuration does not require a starter and compensation of reactive power as compare to type A and type B [32]. However, the use of slip rings and brushes for connection of rotor winding with converter, creates the dilemma of regular maintenance requirement. The presence of gear box and requirement of maintenance increases the overall cost of WECS.

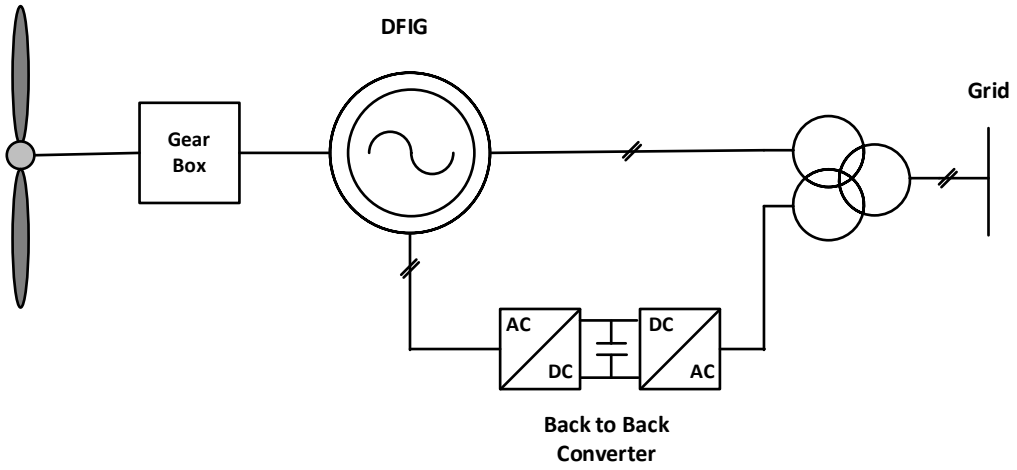

Figure 2.3 Traditional Configuration of DFIG (Type C)

2.1.4 Full converter WECS (Type D)

This variable speed WECS configuration uses full scale 100% power converters and known as type D WECS in market. Gearbox can be removed by using multipole generators in this type of WECS. The rotational speeds of turbine speed and generator speed can be made equal by suitable poles number design of the low-speed multipole generator. The removal of a gearbox has many advantages such as reduced losses, less cost, and increased reliability of system. This scheme can use squirrel cage induction generator, wound rotor synchronous generator and PMSG for generation as shown in Figure 2.4. Full power converter is used to connect generator to the grid. The connection through converter makes the power generation possible at wide range 0-100% speed variation. Moreover, power converter facilitates the system to deliver smooth active power and to compensate reactive power rapidly. PMSG based WECSs are popular in wind power industry due to promising attributes, such as i) high efficiency, ii) large

power density, iii) self-excitation, and iv) higher reliability due to omission of gearbox. Further, technology enhancement in fields of power electronics and ferromagnetic materials will increase the application and popularity of PMSG in wind power industry in coming years.

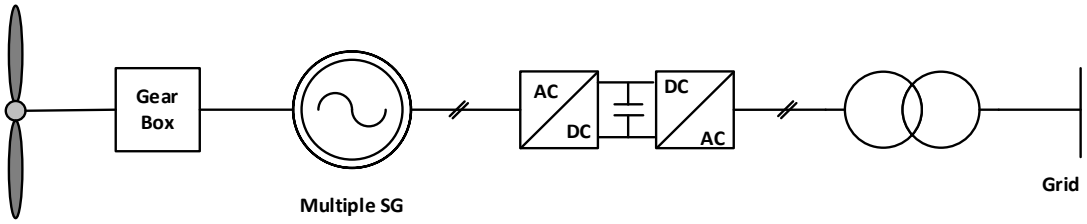

Figure 2.4 Traditional Configuration of Type D WECS

DFIG and PMSG are the most popular generators in wind energy generation industry. The technical difference in operation of the DFIG and PMSG is given in Table 2.1.

Table 2.1 Comparison of DFIG and PMSG

Performance	**Wind Power Generator**	
	DFIG	**PMSG**
Stator	Same	same
Rotor	Coil in rotor	Permanent magnet
Slip ring and carbon brushes	Available	Not needed
Maintenance	High maintenance cost	Maintainance of rotor is not required
Converter power	25-30% power operation	Full power operation
FRT capability	Have appropriate FRT	Have appropriate FRT
Reactive power and adjustment ability	Variation with generator speed	On full range of speed
Connection and support of power grid	Poor	Better
Advantages	Needs lower Initial investment	No rotor coils, low losses Generator is small in size and lighter Higher annual power output

The integration of a WECS with the existing power network must be according to set of rules called grid codes in modern era. Transmission Line Operators (TSOs) have

defined these requirements (grid codes) to accommodate the high penetration of WECSs while ensuring power quality and system stability [33].

The connection of WECS with the grid depend upon voltage at the Point of Common Coupling (PCC), that is crusial part of the grid code. We can enhance the LVRT of the WECS by two strategies. One of the strategies utilizes newly developed coordinated control to achieve the goals of grid code. It is only applicable for new WECS before connecting it to the power grid. Alternatively, flexible AC transmission system (FACTS) devices and energy storage systems can be used for performance improvement and this strategy is suitable for large existing WECS considering the factor of cost [34].

Variable speed WECS can tackle the weaknesses of fixed speed type more efficiently. They can effectively extract maximum possible power from wind and can support the grid with reactive power as well [35]. However, the unpredictable behavior of wind speed in form of wind gust can create power fluctuations in this type of WECSs which ultimately affect power quality. Increased penetration of WECS with low and high voltage power grids have created multiple challenges such as 1) to retain steady supply of power and 2) to maintain LVRT capability following grid codes.

2.2 Power Smoothing Techniques

Wind energy generation suffers from unpredictable power production due to stochastic nature of the winds. This unpredictability will create transient instabilities and power quality issues onto the power grid as a result of voltage and frequency fluctuations. Extensive research has been done to smooth variation of power of the PMSG based WECS due to disturbances in form of wind gust. The power smoothing techniques found in literature can be categorized into two types [36]: 1. Methods utilizing energy storage methods and 2. Methods without energy storage.

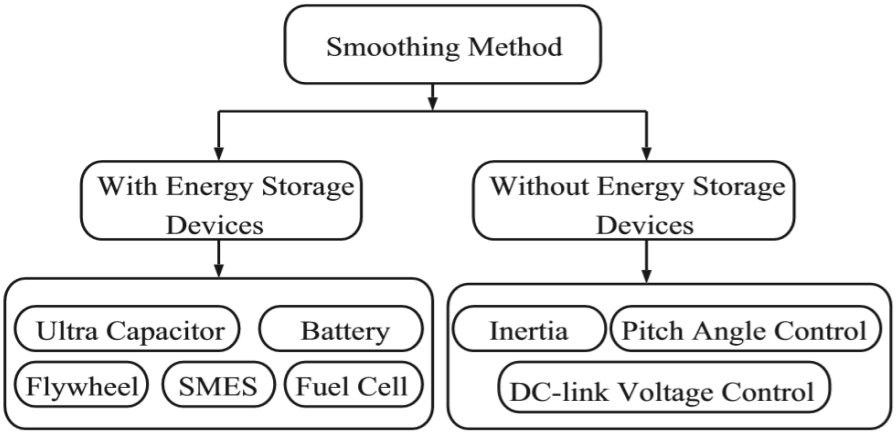

Figure 2.5 Power Smoothing Methods [32]

2.2.1 Energy Storage based Methods

Energy storage systems (ESS) have found application in tackling power fluctuation of WECS [36],[37]. The main target of ESS is to improve power quality of wind energy system operation. it involves mitigating voltage/power fluctuations, load leveling and frequency control. It behaves as great buffer to absorb or discharge energy in case of even fastest fluctuations. ESS equipped with effective control can absorb small power variations and minimize its adverse impact on the power grid. Energy storage systems found in literature are usually Ultra capacitors, Battery energy storage systems (BESS), flywheel ESS, SMES and fuel cells.

These storage systems usually use two configurations of integration with WECS. First one is by using DC chopper at the DC link of the wind energy system and Second configuration utilizes Voltage Source Converter (VSC) and DC chopper. It is attached at PCC of the WECS.

Ultra-capacitor is also called super capacitor or electric double layer capacitor (ELDC). Ultra-capacitor is an electro-chemical capacitor which uses electrodes made of conducting polymers. Application of flying supercapacitor for power smoothing problem of wind power generation can be found in [38]. This article presents direct integration scheme of supercapacitor for WECSs. This topology is based on capacitor clamped three level inverters. This technique gives an alternative as compare to conventional DC link-based conversion system. In [23], PMSG based WECS integrated with Supercapacitor as storage device for FRT improvement and power variation mitigation is proposed. In this technique, buck-boost converter is used for integration

of SC with DC link. During normal conditions, the proposed technique utilizes SCESS to eliminate output power fluctuations. During grid faults, the generated power is forced to store in Super capacitor energy storage system (SCESS), which interns removes DC link voltage rise. The proposed technique is simulated for symmetrical faults and show effective FRT capability. The parameters of the proportional integral (PI) controllers for buck-boost converter and NPC converters are optimized by employing Particle Swarm Optimization (PSO). The MATLAB based Digital Simulator is used for the implementation of the overall system and controllers. SCESS for a five phase PMSG system power smoothing is presented in [39]. The proposed strategy utilized SCESS controlled with model predictive approach with finite set control for power smoothing of the system. Simulation results validated the effectiveness of presented approach for swell effect.

2.2.2 Power smoothing methods without Energy Storage

Power fluctuation smoothing of WECS without ESS lies in the inherent ability of the WECS itself. First technique utilizes the harvesting capability of the pitch angle of wind turbine blades control for power fluctuations removal. Pitch angle control (PAC) is one of the important methods for getting required power from wind energy. One way of getting the appropriate pitch angle value from PAC is by utilizing difference of generated and reference power. Many studies have used conventional PI controller for this purpose as reported in [40]. The gain of PI controller can be adjusted to get improved response. [41] represents a case of PAC utilizing fuzzy logic for power smoothing. However, frequent pitch angle adjustment will create mechanical issues.

Rotor inertia can be used to power smoothing of WECS as presented in [42]–[44]. The rotating mass can absorb or release excessive energy during rotor acceleration or deceleration. Rotor inertial method has an advantage over pitch angle control in energy harvesting as it can store portion of curtailed energy in rotor as kinetic energy. DC link capacitor can be used as a source for power smoothing as temporary variation of voltage at DC can be used to release or absorb energy which ultimately mitigates the power fluctuations. Table 2.2 provides the comparison of output power smoothing techniques.

Table 2.2 Comparison of power smoothing techniques

Method	Advantages	Disadvantages	Remarks
ESS	• Effective power fluctuations mitigation without compromising MPPT • Supply power during peak loads	• Increased Cost of the system • Factor of Storage Capacity	The capacity and cost should be optimized
PAC	• Low cost • Simple Control	• Response is slow • Maintenance cost as it suffers from mechanical stress • Affects the MPPT • Cannot store energy for long time	The combination of PAC with other methods in form of coordination give better performance
Rotor inertia	• Low cost • Faster than PAC • Coordination with other technique provide better performance	• Mechanical stress issue • Short time energy storage	Modification of MSC can provide better performance

Recently, use of combinations of these above-mentioned techniques in form of coordinated control for power smoothing can be found in literature. Coordinated control strategy to mitigate fluctuation in output of PMSG is presented in [45]. The proposed strategy utilized the PAC and DC link voltage exploitation in coordination. It reduced the mechanical strain on turbine blade during high frequency and capacitor size during low frequency operations. A coordinated power smoothing strategy was presented in [46]. The proposed work contains two control strategies for power fluctuations mitigation, 1) combined control of novel DC link voltage control, PAC and rotor speed control at the same time, and 2) Hierarchical Control of above mentioned three controls. A section-based algorithm was designed for hierarchical control.

2.3 Fault Ride Through Techniques

Numerous techniques have been developed over the years to enhance LVRT capability. Most common classification contain two major categories, methods utilizing external devices and methods based on modification of traditional controls of WECS [47] as shown in Figure 2.3. External device-based methods include energy storage systems (ESS) , braking chopper (BC) [18], FACTS devices [12], [14]. While active methods include PAC [48], [49] and modified converter control [50]–[52].

A sliding mode control-based energy storage FRT technique for PMSG based wind was presented in [53]. In the proposed work, MSC controls the DC link voltage through sliding mode control. While GSC controls the maximum power extracted from wind. During fault events, excessive power is stored in rotor inertia. But the limitation of proposed technique is that it transfers stress from the electrical to mechanical.

A coordinated control of PMSG WECS using static synchronous compensator (STATCOM) for severe gird fault scenario was proposed in [54]. The control objectives of converters are swapped such that DC link voltage is maintained by MSC and GSC ensures maximum extraction of wind power. The synchronized STATCOM provides additional reactive power to mitigate voltage dip at the PCC. Results show improvement in synchronization and reactive power supply during symmetric grid faults.

A modified converter-based control for fault ride through handling during asymmetrical faults for PMSG is proposed in [55]. In this work, grid side controls responsible for MPPT and MSC control stabilizes voltage at DC link. Also, GSC control contain dual current controller to maintain sequential currents during asymmetrical faults. Peak current limiter is also being implemented to inject negative sequence current and reactive power to grid.

[56] presents an active power control scheme to achieve better operational performance. In the proposed work, generator side control is based on active power generated during grid disturbances. While, grid side control proposes oscillation cancellations scheme to mitigate distortion in voltage at DC link, active power and reactive power. It is implementation is based on the Positive Synchronous Frame.

A coordinated technique for improving FRT capability of PMSG wind turbine was presented in [51]. In this work, quasi-continuous sliding mode control (SMC) was implemented for MSC to regulated DC link voltage. While a coordinated control for GSC was proposed which have two modes, 1) MPPT for normal conditions, and 2) DC link voltage regulation during grid-side fault cooperative to machine side control. The reference power used for Grid Side Control after fault clearance was previous MPPT value, to reduce rotor load. As a result, converged power is produced that is useful for grid stability right after fault. A combine control (CC) of PMSG wind turbine using vector control (VC) and direct torque control (DTC) was designed in [50]. It has two modes, 1) MSC consists of partial combination of VC (torque and reactive power control) and DTC (hysteresis controllers and switching table) for normal conditions, and 2) swapped duties of back-back converters during fault conditions. MSC maintains the DC link voltage, which has fast transient response due to inclusion of DTC during fault conditions. Genetic algorithm is used to optimization of parameters of all PI controllers. The proposed control results in less fluctuations, less steady state ripples and faster transient response. Performance improvement of PMSG based WECS using adaptive fuzzy logic control (FLC) is presented in [57]. The proposed strategy incorporates adaptive FLC in back-back converter control of wind system. The adaptation of FLC is achieved using continuous mixed-norm adaptive algorithm, which updates the scaling factors of FLC. The technique is compared with control using particle swarm optimization (PSO) optimized PI controllers for symmetrical faults and real wind speed data to evaluate transient and dynamic characteristics of understudy WECS.

2.4 Superconductor Magnetic Energy Storage (SMES) in WECS

SMES technology stores energy in magnetic field formed by DC current passing through the superconducting coil. SMES have gained more application in power sector as a result of increased technological advancements in recent years [58]. Table 2.2 contains the developed/installed SMES systems for various applications in power system around the world. SMES system can store and discharge power in short time even in case of small storage capacity. In addition to power absorb or discharge ability, SMES can also provide reactive power, which in turn makes it suitable for mitigation of voltage fluctuation in grid system.

SMES unit have highest efficiency, which is 90-99% as compare to other storage technologies. The reason behind high efficiency of SMES is that there is minimal resistance and zero frictional loss.

Table 2.3 Application and testing of developed SMES systems

Ref.	Technical Data	Application/features	Organization
[59]	Iron cored HTS coil	Frequency support of PMSG based WECS	University of Wollongong
[60]	1MVA/1MJ SFCL-MES	LVRT capability and power smoothing	wind farm, Gansu province
[61]	1 MJ SMES system	Voltage stability	Chubu Electric
[62]	0.6 MJ SMES system	Voltage quality	Korean Electric Power Research Institute
	2.5 MJ SMES	Power quality	
[63]	20KJ SMES system	Power quality	China Electric Power Research Institute (CEPRI)
[64]	10 kW – 2s SMES with MgB2	Power quality	Research Project University of Bolonga
[65]	A HTS SMES	Power fluctuation Mitigation	Zhangbei test base, China under CEPRI.

An approach to mitigate output power fluctuations through maintaining terminal voltage using SMES was presented in [66]. The output power reference is found by utilizing both simple and exponential moving averages. The proposed control is tested by using actual wind speed data of a wind farm available in Japan. However, as admitted by author, moving averages method required a larger storage capacity of SMES.

A novel high temperature superconductor (HTS) SMES application with PMSG based WECS was proposed in [67]. It proposed a configuration of SMES utilizing a DC chopper for integration at DC link of the WECS. A 2MJ SMES and 3 MW wind turbine were used. Proposed system effectively curves power fluctuation and enhanced LVRT capability of the system. Another case of SMES system for power smoothing by connection at PCC of wind farm was [68]. SMES smooths out output power fluctuations and maintains deviation in grid frequency within an suitable range. An exponentially weighted moving average (EWMA) filter is used to provide output power

reference of the wind farm. However, the proposed system lacked optimization of the SMES parameters.

In [69], power smoothing and LVRT enhancement technique was proposed for DFIG. During normal condition, superconducting coil (SC) is used for power smoothing and during gird fault, SMES is used as fault current limiter in form of inductor. Both Current Source Converter (CSC) and VSC based topology were investigated. The Kalman filter was used for fault detection.

An adaptive SMES controller for PMSG generation system was presented in [70]. The proposed system attached SMES unit at the PCC of the system. The radial basis function neural network was used to find the SMES controller parameters. The weighting functions of the network are determined by training the network with input-output data obtained through an optimum improved particle swarm optimization (IPSO) procedure. Another adaptive control based SMES unit integration with wind farm was proposed in [71]. The configuration of used SMES unit contains a VSC and DC chopper, which handles the transfer of power between SMES and power system. Its unitized set-membership affine projection algorithm (SMAPA) based adaptive PI controllers in converters.

DC chopper controlled SMES for power smoothing of PMSG was presented in [72]. The SMES controlled active power to mitigate power fluctuations and voltage variations of grid inverter during wind gust. Similar topology of SMES unit for performance improvement of DFIG was presented for in [24]. DC chopper is for interfacing SC at DC link of WECS. The duty cycle of the chopper is generated by FLC. However, optimization of controller parameter and SMES sizing were not considered.

SMES can be used as dual function performance improvement unit as energy storage unit and superconductor-fault current limiter (SFCL). Such topology of SMES was presented in [25]. The system used SMES-FCL connected at PCC through a tertiary transformer. SMES coil is modelled as pancakes. During normal conditions, superconducting coil, as connected through VSC and two quadrant choppers, release and absorb energy to smooth output power. During faults, few pancakes from whole SC coil is inserted into main circuit to work as fault current limiter to keep current and

terminal voltage level within feasible value. Trial and error method are employed for finding parameter of PI controllers in SMES control.

The FRT enhancement and power smoothing technique based on cooperative control of the SMES and Fault Current Limiter based on superconducting material was presented in [73]. The proposed system includes resistive type superconductor fault current limiter (SFCL) connected near the GSC and SMES connected at the conversion system through DC chopper. SFCL limits the fault current and helps improve terminal voltage and SMES stores the excess energy to maintain the DC link voltage. The results for symmetrical faults show that SMES-SFCL enhances FRT operation, help smooth output power, mitigate DC link voltage rise and help fast recovery from fault. But the proposed technique does not incorporate parametric optimization of SFCL-SMES. Cooperative control SFCL-SMES was proposed in [74]. In this technique, SFCL limits the fault current and also reduces part of surplus power of DC link. While SMES stores remaining surplus energy. Parameter of SFCL and SMES are estimated to find minimized SMES current capacity and resistance, thereby lowering the overall capital cost. The proposed technique lacks multi-objective function parametric optimization of SMES. Also, the inclusion of SFCL increased complications in the overall estimation process considering cost of SFCL. Similar combined SFCL-SMES technique for FRT capability improvement for DFIG was also proposed in [75]. In this technique, SFCL and SMES were connected at stator and DC link for fault current limitation, terminal voltage restoration and DC link voltage control respectively. Technical discussion was given for parametric optimization of SMES-SFCL but it was not conceived.

Even though SMES is an emerging technology for power quality and stability in WECS, it is still expensive and cost/ratings constraint need to be considered. In light of this, optimization of the SMES parameters is needed. There are multiple literature citing of parametric optimization of SMES. Most of them are based on DFIG WECS. In [76], Optimized technique utilizing SFCL-SMES for FRT capability improvement and output power fluctuations smoothing of DFIG was presented. The proposed work uses PSO to find optimal values for SFCL-SMES and parameter tuning of PI controllers. The objective function used considers factors of terminal voltage, active power and initial stored energy in SC.

Optimal integration of superconducting coil (SC) with DFIG was reported in [77]. The SC is integrated at DC link of conversion system through DC chopper. The chopper controls the exchange of energy between SC and WECS. The power fluctuations of the DFIG are mitigated by SC through charge and discharge modes. During grid faults, the SC behave as the current limiting inductor. It minimizes the rotor and stator overcurrents, and help mitigate the voltage rise at DFIG DC link. The parameters of the SC i.e., coil inductance, initial stored energy and initial coil current are optimized by PSO along with parameters of PI controllers.

An optimal controlled SMES for power smoothing of PMSG based WECS was presented in [78]. SMES unit was integrated at dc link of WECS through DC chopper. The parameters of the PI controllers employed for SMES unit control were optimized using grey wolf algorithm. The proposed control considerably mitigates the power fluctuations. However, objective function did not include the optimization of the SC.
The integration of SMES for power smoothing and FRT can be found in literature [66]–[68], [72] either at dc link through dc-dc chopper or at PCC by using VSC and dc chopper. The control of the SMES unit was carried out by PI controllers. Even though the proposed systems enhanced the performance of the system to some extent, the tunning of the controllers pose a challenge against disturbances. The combination of SMES with SCFL has also been used in PMSG based systems for performance enhancement as given in [73]–[75]. But these studies lacked proper optimization of the parameters of control and SMES. Also, the inclusion of SFCL further complicates the calculations and increases cost of the system. However, the cost of the SC is a negative aspect in its application. And there should be a proper optimization process to determine SC parameters without compromising its performance. There are very few studies that cover both the optimization of the SMES parameters and the controller parameters. Such cases of study can mostly be found in literature for DFIG based WECS [76], [77]. PI controller was used in control of SMES and PSO for optimization. However, PI control lacks robustness against nonlinearities and variarion of parameters. In addition, PI and PSO do not give satisfactory performance when compared with the fractional order proportional integral (FOPI) control and recent optimization techniques. Studies found in literature lacked much emphasis on optimization of SC and control parameters in case of PMSG based WECS. Therefore, solution for optimal integration of SC in PMSG based WECS is proposed in this thesis.

From above Literature survey, The significance and novelity of proposed work as compare to previously done research can be outlined as:

- A topology of SC at DC link of PMSG based WECS without modifying conventional controls of WECS or already installed WECS.
- The sole application of SC in form SMES in PMSG based WECS for handling both issues of output power fluctuations and LVRT capability improvement as compare to studies either proposing solution for only one issue [67], [68] or using combination of SMES with superconductor fault current limiter (SFCL) [73], [74].
- Simple and less computational FOPI based control of SC to regulate energy transfer between SC and conversion system of PMSG based WECS.
- New solution to tackle capacity and cost concerns of application of SMES through optimization of SC size and parameters as previous studies for PMSG lacked emphasis in this regard.
- Use of harmony search optimization for parameter tunning of FOPI (SC control) for better performance.

Chapter

3

Modelling and Control of PMSG based WECS

This chapter describes the working, modeling and control of wind system. The process of energy conversion is illustrated in form of mechanical modeling of the WECS. It involves the description of all components including PMSG, converters to control energy transfer and grid model. The basic principle and working of the conventional control schemes utilizing PI controllers has been discussed and simulated.

3.1 Introduction

Wind energy and its applications has become an attractive and promising solution in market of generation, lately. The typical WECS contain systematic combination of mechanical and electrical components to produce electrical power through controlled operation by harvesting the wind mechanical power [79].

In this chapter, all components of the WECS are discussed and modelled to explain all operational cases. A typical PMSG based WECS is given in Figure 3.1. The structure includes a wind turbine connected to PMSG generator which then delivers power to grid through a conversion system based on BTB converter setup.

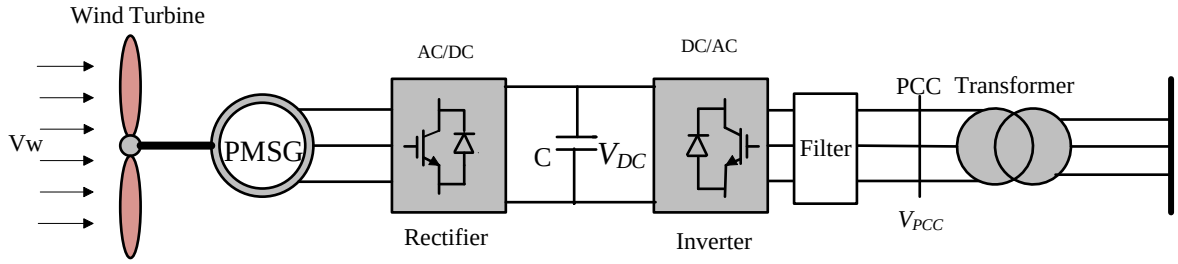

Figure 3.1 Traditional PMSG based WECS

First step is the explanation and modelling of wind turbine aerodynamics. The model of the wind turbine will be formed to get turbine mechanical characteristics. The second part will contain electrical and mechanical modelling of the PMSG generator. Furthermore, it will include converter topology interface along with the control for connection with the power grid. In order to mitigate harmonics, filters can be put in place to improve profile of the output current.

It is also noted that the interface of the system with grid can be made through transformer to get the same voltage level as the power grid.

3.2 Modelling of Mechanical Parts in WECS

3.2.1 Wind Turbine Model

Wind turbine basically transform the wind energy into mechanical energy and then electrical generator convert it to electrical energy. The kinetic energy stored in wind is basically transformed into mechanical energy. Under the assumption that the wind stream is uniform which means it is assumed that each layer of air flow parallel to each other, the kinetic energy stored of the wind can be given as follows [80]:

$$E_{Ki} = \frac{1}{2} m v_w^2 \tag{3.1}$$

Where E_{ki} is the kinetic energy of wind, m is the mass of air and v_w is the wind speed (m/s). By substituting mass as product of density and volume. Then volume can be expressed as product of speed, time and area. The mass in a circular interface area between turbine blades can be derived as:

$$m = \rho v = \rho v_w A t = \rho v_w \pi R^2 t \tag{3.2}$$

Where ρ is the density of air which varies from 1.1 to 1.3 (kg/m^3), R represents the radius of the blades of turbine and t is the time.

The equation of E_{ki} from (3.1) and (3.2) gives:

$$E_{Kin} = \frac{1}{2} \rho v_w^2 \pi R^2 t \tag{3.3}$$

Afterwards, the stream power of wind P_{wind} can be expressed as [81]:

$$P_w = \frac{1}{2} \rho \pi R^2 v_w^3 \tag{3.4}$$

The power that is being captured by turbine from air stream is equal to:

$$P_M = \frac{1}{2} \rho A C_p v_w^3 \tag{3.5}$$

Where P_M denotes the captured wind power, A is the area swept out by turbine blades. where R represents the radius of blades of turbine and ω_m is the mechanical speed of the generator in rad/s.

The power coefficient (Cp) is expression in form of the Tip Speed Ratio (TSR) λ and the pitch angle β as shown below [82]:

$$C_p(\lambda,\beta) = C_1\left(\frac{C_2}{\gamma} - C_3\beta - C_4\right)e^{\frac{-C_5}{\gamma}} + C_6\lambda \tag{3.6}$$

$$\gamma = \frac{1}{(\lambda+0.08\beta)-(0.035\beta^2+1)} \tag{3.7}$$

The constant (empirical) values can be estimated for wind turbine as: C1 = 0.5176, C2 = 116, C3 = 0.4, C4 = 5, C5 = 21, and C6 = 0.0068. The TSR is expressed as follows:

$$\lambda = \frac{\omega_m R}{v_w} \tag{3.8}$$

According to Betz's limit, Cp can have maximum value within the range 59.26 % in an ideal case. Therefore, the captured power from the wind will always be less than the Betz's limit [83]. The actual value of extracted power can very well be less than 50% pertaining to the loss involved in the whole conversion system. These losses are caused by inefficient converter operation or design and construction of the whole setup.

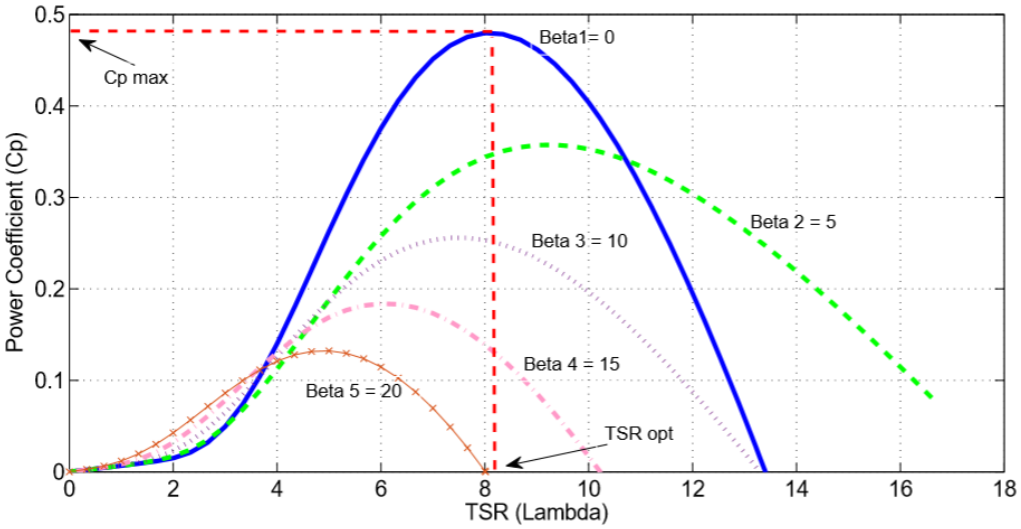

Figure 3.2 Relation of power coefficient with TSR

The relation between power coefficient C_p of wind turbine and TSR indicate that optimum value of power coefficient C_p occurs at optimum value of TSR for all operational situations. MPPT can be obtained by adjusting these values with respect to wind speed variation and pitch angle. Figure 3.2 represents the correlation of the power co-efficient C_p and optimum values of TSR by varying the pitch angle β..

The main target of MPPT is to find optimum angular speed $\omega_m *$ to capture maximum mechanical power from available enegy of wind as much as possible. Therefore, significant relationships of Cp and TSR λ shown in Fig 3.2 should be taken into consideration while designing to get MPPs. The dynamic relation of the wind turbine is expressed below:

$$J\frac{d\omega_m}{dt} = T_e - T_m - F\omega_m \tag{3.9}$$

J represents the total moment of inertia of generator and wind turbine, and Tm is the input mechanical torque to the generator. Where F is the friction of viscosity coefficient. PMSG based WECS can operate in direct driven fashion without the need of gearbox.

3.3 Electrical Modeling of the WECS

Depending upon the operation of system, there are two way of doing electrical modeling of WECS as static or dynamic components.

3.3.1 Reference frame Transformation

The analysis of electric machines can be simplified by using reference frame theory. It can also be handy to facilitete digital implementation of control schemes to get simulation of wind energy conversion system. Many reference frames have been studied and presented over the years. The most commonly approached frames are the three-phase stationary frame (also reffered to as *abc* frame), the two-phase stationary frame ($\alpha\beta$ frame), and the synchronous frame (*dq* rotating frame).

3.3.1.1 abc/dq Reference frame

The representation of three phase values can be done in form of a space vector x in stationary reference frame (abc coordinate system) as shown in Figure 3.3. The space vector is rotating at an arbitrary angular speed *w*.

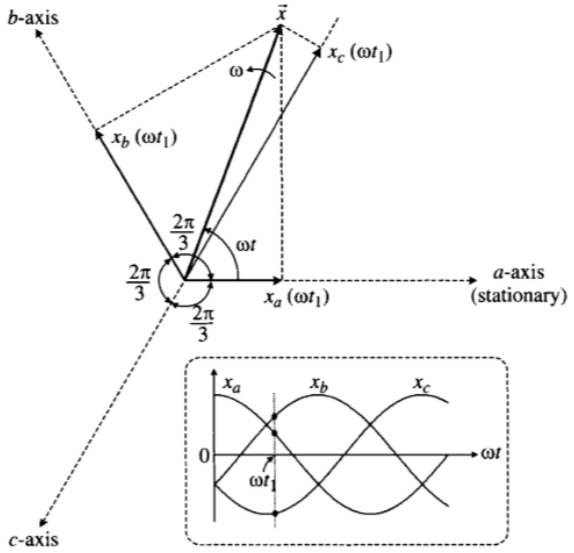

Figure 3.3 space vector x and its three phase variable xa,xb,xc

The two-phase reference frame (*dq* frame) contains two axes being d (direct) and q (quadrature) which are orthognal to each other. Figure 3.4 represents the transformation of three phase variables in stationary frame into *dq* reference frame.

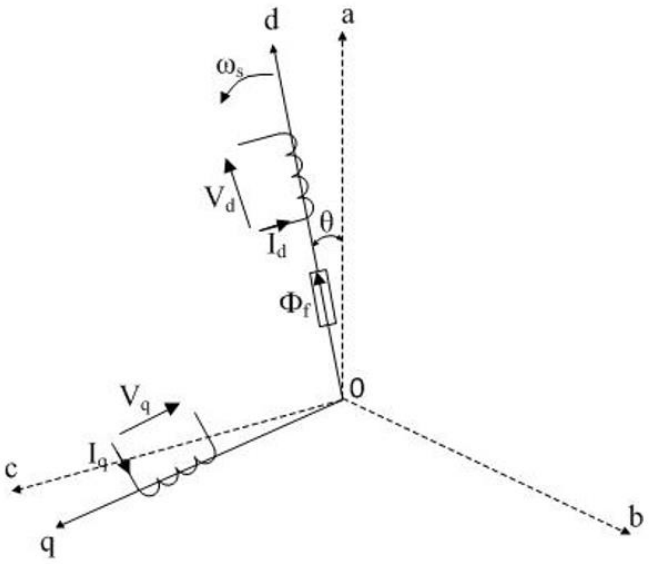

Figure 3.4 abc- dq axis

The position of abc stationary frame as compare to dq reference frame is given by angle θ. And this angle θ is the angle between *d*-axis and *a*-axis. The dq reference frame rotates at a speed ω given by the relation $\omega = \frac{d\theta}{dt}$.

The transformation from abc stationary frame to dq frame can be expressed in form of trigonometric functions derived through orthogonal project method. The sum of

orthogonal projections of each of the x_a,x_b,x_c on the axis of *dq* frame gives the corresponding components of that axis in dq reference frame.

The transformation *abc-dq* can be expressed in a matrix form as shown below:

$$\begin{bmatrix} x_d \\ x_q \end{bmatrix} = \frac{2}{3} \begin{bmatrix} cos\theta & \cos\left(\theta - \frac{2\pi}{3}\right) & cos\left(\theta - \frac{4\pi}{3}\right) \\ -sin\theta & -sin\left(\theta - \frac{2\pi}{3}\right) & -sin\left(\theta - \frac{4\pi}{3}\right) \end{bmatrix} . \begin{bmatrix} x_a \\ x_b \\ x_c \end{bmatrix} \tag{3.10}$$

It should be observed in above transformation that:

- A coefficient of 2/3 is being used in the equation. $\sqrt{2/3}$ can also be used. The benefit of using 2/3 is that in this case the magnitude of transformed variables *dq* is equal to the magnitude of the three-phase variable used for transformation.
- Two variables *dq* contain all information about the three phase *abc* waveforms given that the three phases are balanced.

The equation for inverse transformation of getting *three phase abc (stationary reference frame)* variables back from *dq* transformed variables (*rotating reference frame*) is:

$$\begin{bmatrix} x_a \\ x_b \\ x_c \end{bmatrix} = \begin{bmatrix} cos(\theta) & -sin(\theta) \\ cos(\theta - 2\pi/3) & -sin(\theta - 2\pi/3) \\ cos(\theta - 4\pi/3) & -sin(\theta - 4\pi/3) \end{bmatrix} . \begin{bmatrix} x_d \\ x_q \end{bmatrix} \tag{3.11}$$

The vector angle ϕ between d-axis and x is constant under the assumption that space vector x rotates with same angular speed as the dq reference frame. As a result, dq-axis components (x_d and x_q) received after transformation, are DC variables. Therefore, the advantages of the *abc/dq* transformation, in representing three-phase AC variables in form of two-phase DC variables, has made it effective in modelling and control wind power systems.

For controling of WECS, the synchronous reference frame is usually used. In this reference frame, the synchronous speed (of both synchronous or an induction generator) is matched by the rotating speed of the arbitrary reference frame ω , given by

$$\omega_s = 2\pi f_s \tag{3.12}$$

Where f_s is the stator frequency. The angle θ can be obtained from

$$\theta(t) = \int_0^t \omega_s(t)\, dt + \theta_o \tag{3.13}$$

Where θ_o is the initial angular position.

3.3.2 PMSG Model

Electrical generator is one of the major components of a typical WECS which converts mechanical energy into electrical energy. Permanent magnet synchronous machines (PMSM) are usually manufactured in high power ratings of up to 8 to 10 MW, which constitute new development in wind power generation. PMSM give more efficiency as compare to conventional synchronous machines due to less electrical losses as a result of operation without excitation circuit. These machines also have less mechanical equipment of gear box and have fixed magnetic fluc due to permnent magnets.

Synchronous generator (SG) is more costly as compare to Induction Generator (IG) of the same size. However, it has application in large scale generation due to its numerous advantages. One of these advantages is that magnetic field generated from permanent magnet of the rotor, enables it to operate correctly without the need of reactive magnetizing current. Another cost effective advantage of these machines is that they can be driven directly with wind turbine without gear box by using appropriate number of poles. Thus, synchronous generator is considered a suitable solution for wind turbine generator in spite of drawbacks of cost and complexity. Synchronous generators are especially more suitable for low wind speed setups where required frequency can be achieved by selecting appropriate number of poles [84].

Rotating reference frame in synchronism is used to denote the output voltages of PMSG while q-axis lead the d-axis by 90 degrees considering the rotation [85]. There are three tpes of SG with respect to construction and are explained below :

• Salient pole type: In this particular model, the rotor's windings are represented as a coil and situated around the pole shoe. As a result of this structure, reluctances in d and q axis are different from each other, which ultimately yields different machine reactance values (xd >xq). The most prominent application of this type of SG is in hydro-electric power stations, having lower rotating speed w.r.t wound rotor generators [86].

• Round rotor SG: In this model, The rotor windings are spread in the rotor slots in uniform style. In this configuration, the reactances in d and q are eqaul . Round rotor

SGs have major application in thermal or diesel fueled power plants with speed as high as 3000 rpm [87].

• Multipole PMSG: To achieve low speed operation of wind turbine, the number of poles can be increased in this multipole SG to get to the required rotational speed. Permanent magnets are used to provide magneti field in place of excitation winding in this configuration. Because of equal distribution of surface mounted magnets in this model, there is a difference of only few percent between d and q aixs reactance's. Due to the multi-pole nature, it's suitable for low-speed application (compared to high dynamic drives).

3.3.2.1 Dynamic model of PMSG

The synchronous rotating reference frame, where d-axis trails the q-axis by 90 degrees, can be used to represent the PMSG output voltages. Equations (3.14) and (3.15) represent this generator's d-q stator voltages equations respectively.

$$V_{ds} = R_s I_{ds} + L_{ds}\frac{dI_{ds}}{dt} - \omega_e \psi_q \tag{3.14}$$

$$V_{qs} = R_s I_{qs} + L_{qs}\frac{dI_{qs}}{dt} + \omega_e \psi_d \tag{3.15}$$

$$\psi_q = L_{qs} I_{qs} \tag{3.16}$$

$$\psi_d = L_{ds} I_{ds} + \psi_{PM} \tag{3.17}$$

where *Lds* and *Lqs* are the inductances of the rotor on *dq* reference frame, *ids* and *iqs* are d and q axis components of generator current, Rs is the resistance of the rotor, ψ_{PM} is the flux of the permanent magnet and ω_e is the electrical angular speed of the PMSG which is defined as:

$$\omega_e = P\omega_m \tag{3.18}$$

where *P* is the No. of pole pairs. The electromagnetic torque of the generator can be expressed as:

$$T_e = \frac{3}{2}P\left[\left(L_{ds} - L_{qs}\right)I_{ds}I_{qs} + \psi_{PM}I_{qs}\right] \tag{3.19}$$

T_e can be further simplified by using L_d=L_q assumption that is in case of surface mounted PMSG

$$T_e = \frac{3}{2}P\psi_{PM}I_{qs} \tag{3.20}$$

From above expression, it can be seen that electromagnetic torque can be varied by controlling the value of I_{sq}. Electromagnetic torque follows the mechanical torque and afterwards power to achieve MPPT. The part of modeling of PMSG is the motion equation given by:

$$\frac{d\omega_m}{dt} = \frac{1}{J}(T_e - T_m - F\omega_m) \tag{3.21}$$

The Active and reactive powers of the SG are stated in equations (3.22) and (3.23) respectively:

$$P_{gen} = \frac{3}{2}\left[V_{ds}I_{ds} + V_{qs}I_{qs}\right] \tag{3.22}$$

$$Q_{gen} = \frac{3}{2}\left[V_{qs}I_{ds} - V_{ds}I_{qs}\right] \tag{3.23}$$

Equations (3.14), (3.15) can be rearranged for operation of generator mode for simulation purposes:

$$i_{ds} = \frac{1}{S}\left[-v_{ds} - R_s i_{ds} + \omega_r L_q i_{qs}\right]/L_d \tag{3.24}$$

$$i_{qs} = \frac{1}{S}\left[-v_{qs} - R_s i_{qs} - \omega_r L_d i_{ds}\right]/L_q \tag{3.25}$$

The block diagram representing the model of SG for computer simulation is expressed in Figure 3.5. The SG model's input variables are the dq-axis stator voltages vds and vqs, the rotor flux linkage $\lambda_r = \psi_{PM}$ (in case of PMSG) and the mechanical torque Tm. The output variables of the model are the stator currents in dq axis, electromagnetic torque Te and the rotor mechanical speed ω_m.

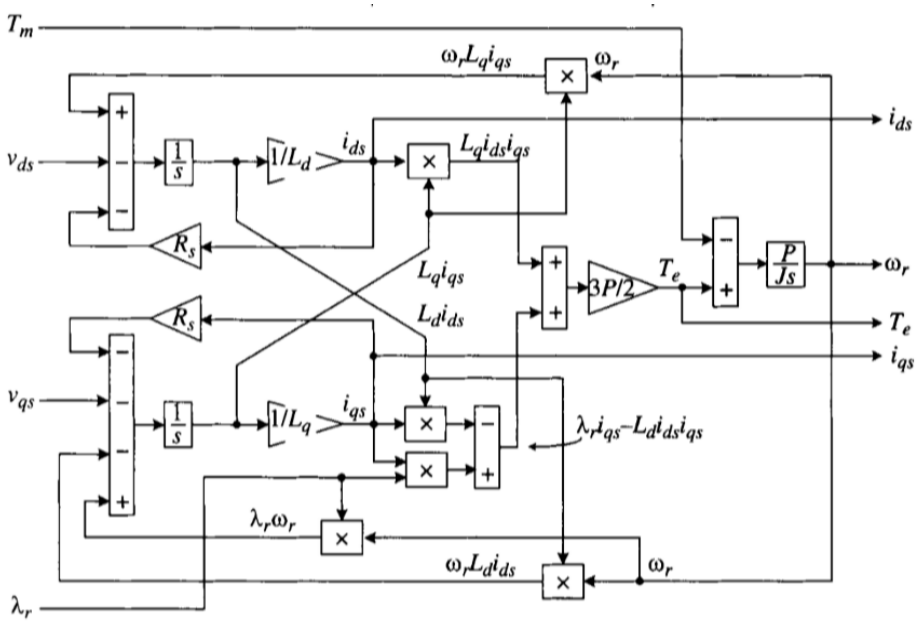

Figure 3.5 Block diagram of SG [88]

Full power operation of the generator can be attained by using BTB converter. The generator's produced reactive power is getting exchanged with grid-side converter instead of the power grid. Therefore, there will be zero net reactive power distributed to the grid and WECS solely supply active power to the grid.

Damper windings are not used for these multipole generators as they are connected to grid through decoupled convertor system. Furthermore, there is no need of excitation circuit as field is provided by permanent magnets. These currents in other SGs can be used to damp current transients. Hence, PMSG cannot contribute damping in all operations for any type of disturbance.

3.3.3 Voltage Source Rectifier Model

In modern WECS, Voltage Source Converters (VSC) are an effective device to convert AC into DC and vice versa. The advantage of the VSC are compact size, can easily be controlled through open loop V/Hz control, low cost, low power losses and give high power factor [89]. The uncontrolled diode rectifier is represented in Figure 3.6, which is low cost, simple and easiest technique of rectification. However, it lacks the ability to provide reactive power due to uncontrolled topology.

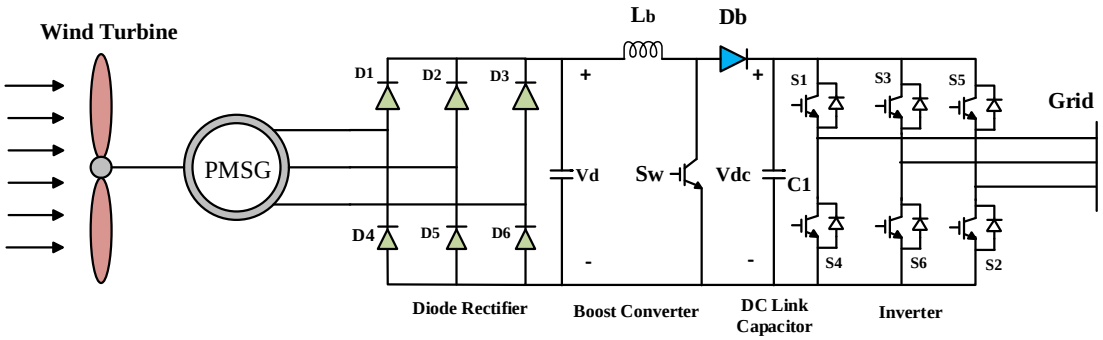

Figure 3.6 Diode Rectifier in WECS

Increased value of torque and load angle will yield increased stator current which in turn will make the stator voltage to drop which in turn will make DC link voltage to drop [10]. The conversion depicted in figure 3.6 must balance the dropped DC voltage. It is going to be possible for only one point of operation as excitation of PMSG is fixed and constant. Also, the inability of diode rectifier to provide/consume reactive power will lead to insufficient usage of PMSG in case of change of operational point. Therefore,In order to achieve best low speed operations of PMSG, fully controlled rectifier and inverter should be used for conversion. Usually, PWM controlled Insulated

Gate Bipolar Transistor (IGBT) voltage source rectifier and inverter are used for full power operation. It has better overall efficiency as it can absorb/supply reactive power. The topology of converters that we can use is BTB converter.

3.3.4 Back-to-Back (BTB) Converter Model

GSC controls the power flow while maintaining the voltage at DC link. The generator side control maintains the maximum capture of the power from the wind. A decoupling capacitor is connected between generator converter and grid inverter. It allows the independent operation (compensation for asymmetry) on sides of generator and grid by ensuring separate operation of rectifier and inverter. [90], [91]. The typical diagram of BTB converter used for WECS's grid connection is shown in Figure 3.7. The full capacity converters facilitate the design of system by ensuring decoupled control of grid and generator side converters. This topology also increases the range of operation of generator.

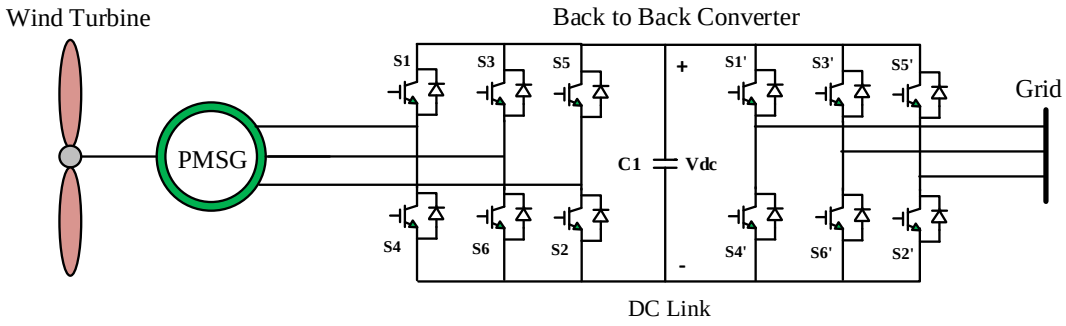

Figure 3.7 BTB Converter topology for WECS

Boost inductance can be used in DC link circuit in some applications which helps in reducing harmonic demands on the grid side harmonic filter. In order to protect converter against disturbance on the grid, commination of capacitor and inductor are also being used as filters [92].

3.4 Grid Model

Grid model will be expressed in mathematical equations in this section [93].

Three phase symmetrical voltage source can be used to represent the grid as shown in Figure 3.8. The three-phase voltage V_a, V_b, V_c are defined as:

$$V_a = V_m cos(\omega t) \tag{3.26}$$

$$V_b = V_m cos\left(\omega t - \frac{2\pi}{3}\right) \quad (3.27)$$

$$V_c = V_m cos\left(\omega t - \frac{4\pi}{3}\right) \quad (3.28)$$

Where the angular frequency is represented by ω and Vm represents amplitude of phase voltage. The three phase currents can be represented as:

$$I_a = I_m cos(\omega t + \varphi) \quad (3.29)$$

$$I_b = I_m cos\left(\omega t - \frac{2\pi}{3} + \varphi\right) \quad (3.30)$$

$$I_c = I_m cos\left(\omega t - \frac{4\pi}{3} + \varphi\right) \quad (3.31)$$

where *phase angle between volage and current is* φ and I_m is amplitude of current

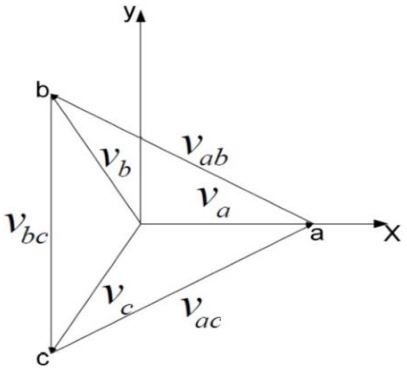

Figure 3.8: Symmetrical three-phase voltage representation

The phase-to-phase voltage can be written as:

$$V_{ab} = V_a - V_b \quad (3.32)$$

$$V_{bc} = V_b - V_c \quad (3.33)$$

$$V_{Ca} = V_c - V_a \quad (3.34)$$

The neutral current is defined as:

$$I_N = I_a + I_b + I_C \quad (3.35)$$

In case of zero neutral current (IN = 0), equations (3.35), (3.36) should be satisfied:

$$I_a + I_b + I_C = 0 \quad (3.36)$$

$$V_a + V_b + V_C = 0 \quad (3.37)$$

Apparent power can be written as product of voltage and current:

$$S = V.I^* \quad (3.38)$$

3.5 Control Schemes of WECS

A control of PMSG side converter can be achieved through Vector Control. In this control, generator phase currents are controlled to either control torque or flux. Various

vector controls can be found in literature. PMSG side control or machine side control (MSC) can either use field-oriented control (FOC) indirectly or Direct Torque Control (DTC). Also grid side control (GSC) can utilize either Voltage Oriented Control (VOC) or Direct Power Control (DPC). In this section, FOC and VOC are being explained for the proposed model of PMSG.

The overall control of WECS involve Grid Side Control (GSC) and Machine Side Control (MSC). MSC incorporates the MPPT to excerpt maximum power from wind. GSC covers the active and reactive power control along with control of DC link voltage in case of VSC. In case of CSC, DC current is controlled.

The overall control involves active power control through MPPT at generator side, voltage control at DC link for VSC or DC current for CSC and control of reative power on grid side.

Synchronous reference frame is used to implement FOC scheme for easier control and this way, the control of special orientation of PM flux can be done. The MSC implementation based on FOC for PMSG is presented in Figure 3.9.
Vector control can be achieved by utilizing *dq* reference frame in such a way that direct axis d is positioned along rotor flux vector. As a result, electromagnetic torque is in direct proportion to the *q*-axis stator current as long as magnetic flux is constant (Equation 3.20). Therefore, in a surface mounted PMSG, i_{sd} should be zero so that maximum torque per ampere can be obtained.

The separate and indirect control of the torque and fluc can be achieved through FOC by using current control loops indirectly. The shaft speed is used as a feedback in control process of FOC. The shaft speed is measured by an encoder. The advantages of this control scheme are as follows: precise speed control, better respose of torque and it can achieve full torque standstill [94].

DTC method controls the torque and flux directly without the current loops. And it facilitates the operation of VSI semiconductor devices as good method. However, DTC suffers from high torque pulsation and require variable switching frequency and higher sampling rates.

3.5.1 Reference Frames for Control Schemes

The control of electrical machines can be implemented by taking into account a reference frame that is rotating with one of space vector of generator. We can get steady state control signal by using this reference frame as compare to normal sinusoidal signals. [189] contains the discussion on various methods that can be implemented for converter controls.

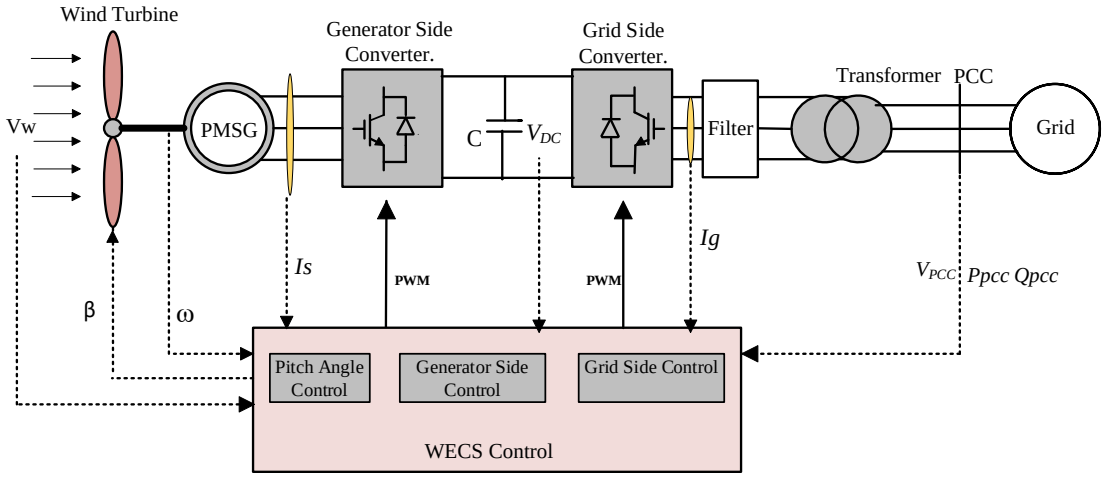

Figure 3.8 Schematic diagram of PMSG Based WECS

3.5.2 Machine Side Control

The aim of MSC is to extract as much power as possible with respect to changing wind speeds. MSC based on FOC is represented in Figure 3.9. It includes an outer control for speed control and the inner one is the *dq* axis current controller. The speed control loop utilizes MPPT technique to generate speed reference ω^* to attain maximum available power at particular wind speed v_w as discussed in next part. The control uses PI controllers to adjust the error of signals where integrator term help reduce steady state error to zero. The inner current loop basically achieves the control of generator through zero d-axis current (ZDC). First d and q-axis components of stator current are determined and then used as feedback in control. The reference value of d component of stator current is zero according to ZDC. As a result, stator current i_s is equivalent to its q component i_{qs}. According to equation (3.20), it can be deduced that electromagnetic torque produced is soley dependent and proportional to the stator current given that the flux produced by magnets is constant. The two PI current

controllers' outputs in addition with coupling term of the network produce the reference dq axis voltages v_{ds}^{*}, v_{qs}^{*} as command values for pulse width modulation (PWM).

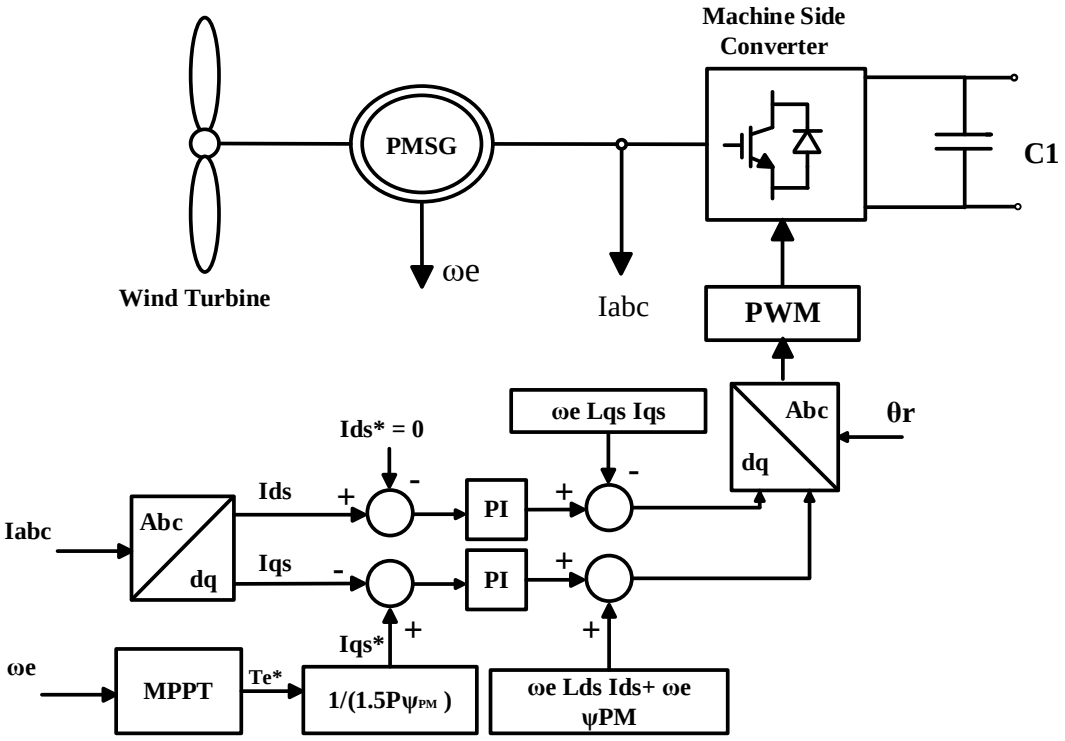

Figure 3.9 Machine Side based on FOC

3.5.2.1 MPPT Implementation

The control of generator is done to attain indirect control of wind turbine below the rated wind speed. The main goal is to capture maximum power from wind power at certain wind speeds. It can be possible by keeping tip speed ratio value at optimum $\lambda_{T,opt}$ value while adjusting the turbine speed.

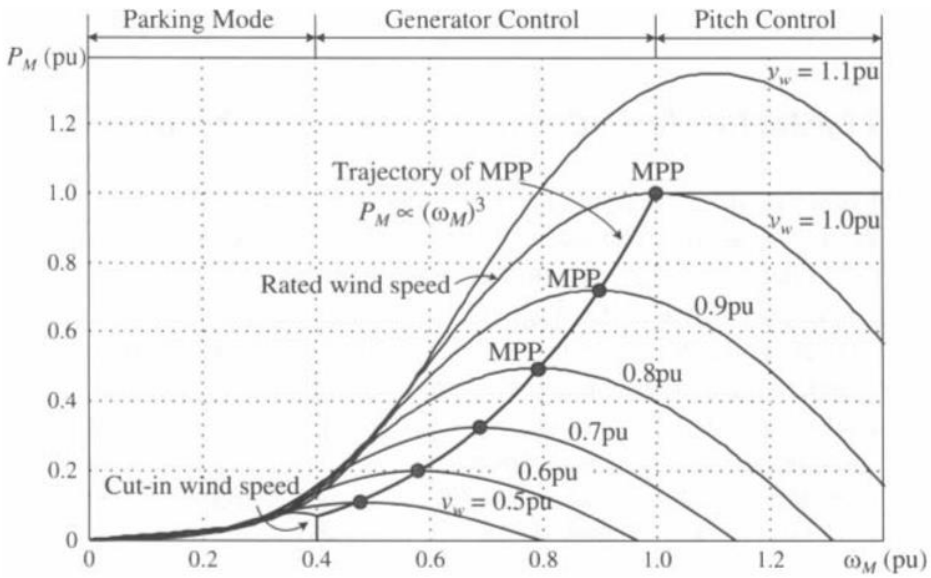

Figure 3.10 Characteristics of wind turbine interms of power and speed [88]

Figure 3.10 shows the relation between power and rotation speed at different wind speeds, where the mechanical power is represented by P_M and ω_M is the turbine's mechanical speed.

As represented in Figure 3.10, each curve of the power-wind characteristic has a peak point (MPP) for a specific wind speed value. And at the MPP, optimum value of TSR $\lambda_{T,opt}$ is obtained. The wind turbine operation must be adjusted to follow all MPPs in order to receive maximum value of power from available wind power at different wind speeds. The trajectory of MPPs can be described as a curve given by:

$$P_M \, \alpha \, \omega_M^3 \tag{3.39}$$

The wind turbine's mechanical power can be written in terms of T_M as:

$$P_M = T_M \omega_M \tag{3.40}$$

Where Tm is the turbine mechanical torque. Substituting eq. () into eq. (), we get:

$$T_M \, \alpha \, \omega_M^2 \tag{3.41}$$

The MPP operation of the generator can be achieved by manipulating the relation of mechanical speed, power and torque of wind turbine. These mechanical quantities of wind turbine are used to generate optimum torque and speed control signals. There are many different MPPT techniques that have been developed over the years. Three are three methods of MPPT depending upon wind power profile, TSR and torque control. The system under study utilizes the optimal torque control.

MPPT with Optimal Torque Control

In this technique, MPPT is attained according to the equation 3.41, where mechanical torque T_M is in direct proportion to square of turbine speed ω_M. The mechanism of this control tecnique is presented in Figure 3.11. In this tecnoque, first the generator speed ω_m is measured. Then it used to yield the reference value of torque T_m^* depending upon the value of the coefficient for the optimal torque K_{opt}. MPPT is realized when generated torque *Tm* is equal to its reference T_m^* in steady state through feedback control.

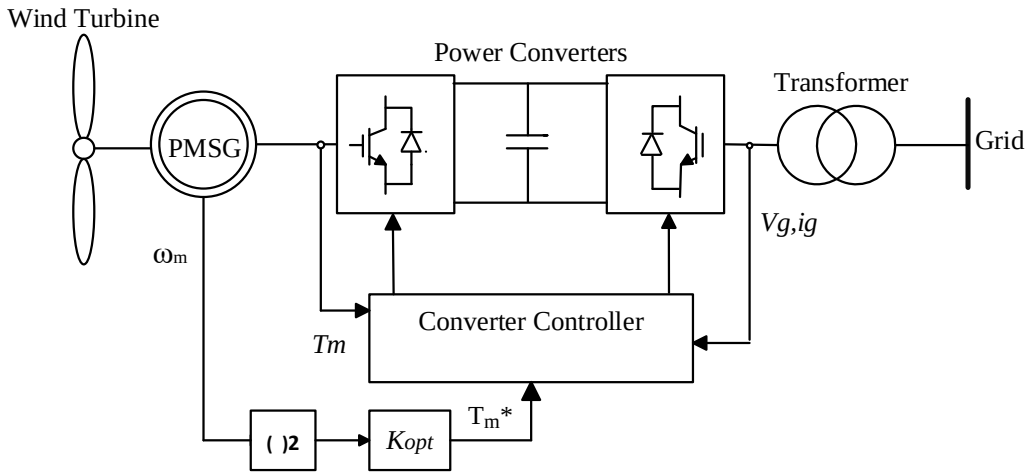

Figure 3.11 Optimal Torque Control for MPPT

3.5.3 Grid Side Control

GSC of converter is implemented by utilizing VOC along with decoupled control is shown in presented in Figuer 3.12. In VOC, outer loop for DC voltage V_{dc} control and inner loop manages the *dq*-axis currents $i_{dg}$and i_{qg}. To realize VOC, Phase Locked Loop (PLL) is applied on the grid voltage to measure its angle θg which in turn used for the *abc/dq* transformation of three phase line currents i_{ag} ,i_{bg} ,i_{cg} to i_{dg} and i_{qg}.
In order to implement VOC technique, the *d*-axis is in phase with the grid voltage vector, hence the (*d*-axis grid voltage is equivalent to its magnitude ($v_{dg} = v_g$) and as a result q-axis voltage v_{qg} is then equivalent to zero. The system's active and reactive power can be expressed for $v_{qg} = 0$ by

$$P_g = \frac{3}{2}\left(v_{dg}i_{dg} + v_{qg}i_{qg}\right) = \frac{3}{2}v_{dg}i_{dg} \tag{3.42}$$

$$Q_g = \frac{3}{2}\left(v_{qg}i_{dg} + v_{dg}i_{qg}\right) = -\frac{3}{2}v_{dg}i_{dg} \tag{3.43}$$

The reference value for q axis current can be obtained by

$$i_{qg}^{*} = \frac{Q_g^{*}}{-1.5 v_{dg}} \tag{3.44}$$

The reference reactive power depends upon the power factor. It is going to zero in case of unity power factor operation. The value of i_{qg}^{*} is negative and positive in case of leading and lagging power factor respectively.

The PI control of V_{dc} control generates the reference signal of *d*-axis current i_{dg}^{*}. The inverter's DC voltage is retained at reference value V_{dc}^{*} during inverter steady state operation. The reference current i_{dg}^{*} is then produced by vdc PI controller according to the operating conditions. The decoupled control makes independent control of i_{dg} and i_{qg} possible which inturn provide independent/separate control of active and reactive powers respectively. It helps make system easily stabilized through convenient design of PI controllers.

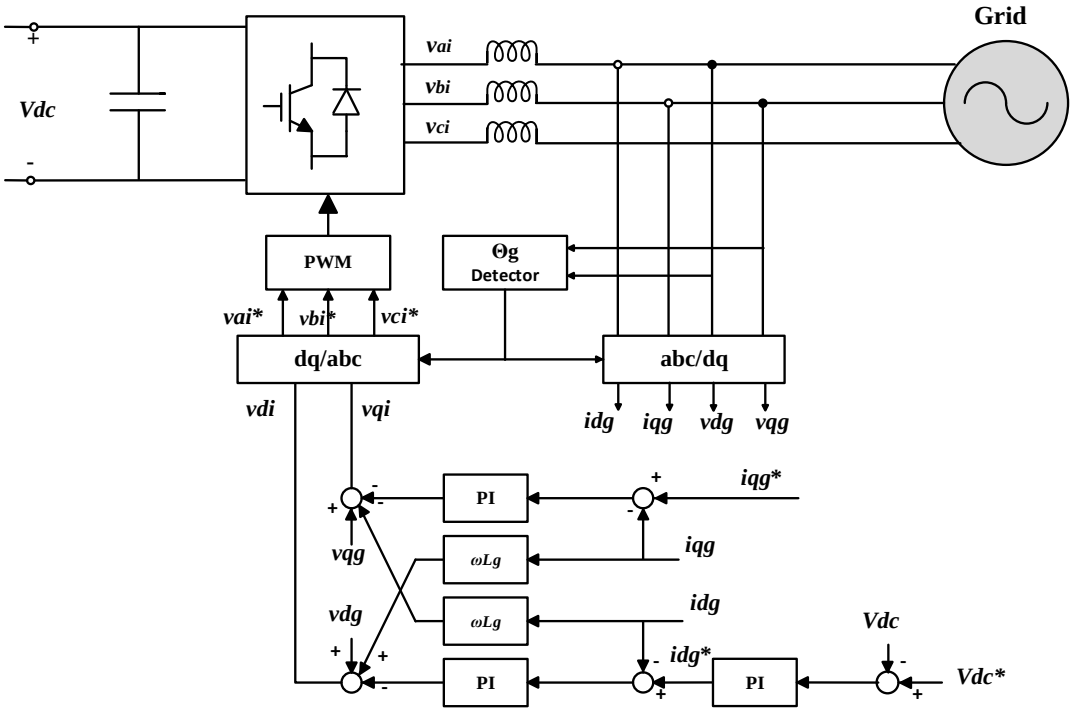

Figure 3.12 Gide side Converter Control

3.5.3.1 Phase Locked Loop

The process of synchronization is essential for grid connected inverter system that helps to get synchronized inverted voltage in terms of amplitude, frequency and phase.

The synchronization process helps in keeping the magnitude and phase of inverted voltage of the VSI with grid voltages in synchronization. To guarantee the correct operation of the grid connected system, fast and accurate detection of inverted voltage of the VSI need to be done to achieve precise generation of reference signals. Moreover, WECSs are made to operate near unity power factor to make sure minimum power loss and grid code standards as well. There are two methods that can be considered to achieve this target: Filtered Zero Crossed Detection (ZCD) and PLL. The phase of generated signal is automatically adjusted by the PLL which is a feedback control system. In this work, phase locked loop method is used, available in Simulink. The main purpose of the PLL is to ensure unity power factor operation through the synchronization of angle of inverter current with phase angle of the grid voltage. The algorithm of the PLL alters the frequency of the inverter current corresponding to the phase shift between inverter current and grid voltage. The most common PLL technique is based on synchronous reference frame *dq*-axis.

3.6 Simulation of PMSG based WECS and Results

The wind energy conversion system shown in Figure 3.9 is implemented and simulated by using Simulink blocks in MATLAB/Simulink 19.

The traditional MSC and GSC of the WECS utilizes PI controllers for control loops. The preliminary conditions of the system are taken into consideration, hence to simulate the system in stable manner.

The parameters used for the simulation of WECS are given below:

a) Wind Turbine.

Table 3.1 Parameters of wind turbine used in simulation.

Wind Turbine Parameter	**Parameter Value Used**
Blade Radius Ro	33.05 m
Air Density	1.205 kg/m^3
Rated Wind Speed	12 m/s
Cut-in Speed	5 m/s
Cut-out Speed	25 m/s

b) Parameters of generator

Table 3.2 PMSG Parmeters used in Simulation

PMSG parameter	Parameter Value Used
Rated Power	1.5MW
Number of Poles	48
Stator Resistance	0.006 Ω
d-axis inductance	0.000395 H
q-axis inductance	0.000395 H
Flux linkage	1.48 V. s

c) Parameters of power converter

Table 3.3 Parameter of power converter

Parameter	Value used
PWM carrier frequency f_p	2700 Hz
Rated DC link voltage V_{dc}	1150 V
DC link capacitor	10000e-6 F

d) Parameters of control Schemes

Table 3.4 The control parameters of MSC and GSC.

MSC				GSC			
Kp_Id	Ki_Id	Kp_Iq	Ki_Iq	Kp_vdc	Ki_vdc	Kp_Idq	Ki_Idq
1.5	0.52	0.75	8.5	8	400	0.83	5

3.6.1 Wind Turbine Results

The wind profile used in simulation of WECS is given in figure 3.13. The rated value of wind speed used for the system simulation is 12 m/s.

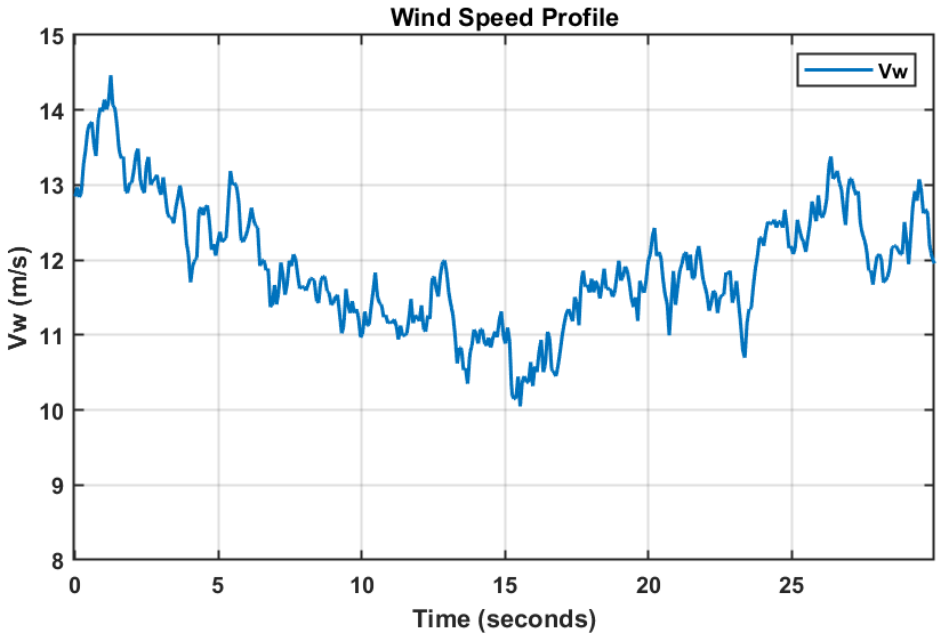

Figure 3.13 Wind speed profile

The power coefficient Cp of the wind turbine is given in Figure 3.14. it can be observed that under PAC, Cp is decreased to get power at rated value. The maximum value of Cp is 0.445 and it is maintained at instances where wind speed is less than 12 m/s. The pitch angle value of turbine is shown Figure 3.15.

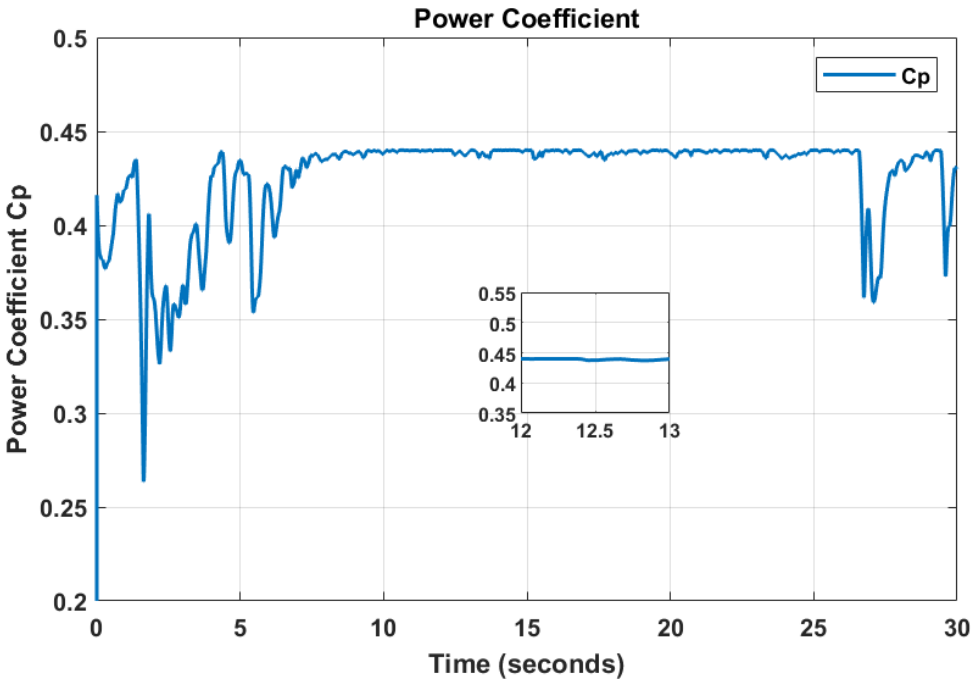

Figure 3.14 Power coefficient Cp

The comparison of reference mechanical speed and actual mechanical speed is used to drive PAC. The PAC is involved in operation when speed of wind is greater than the rated value to curtail production of power.

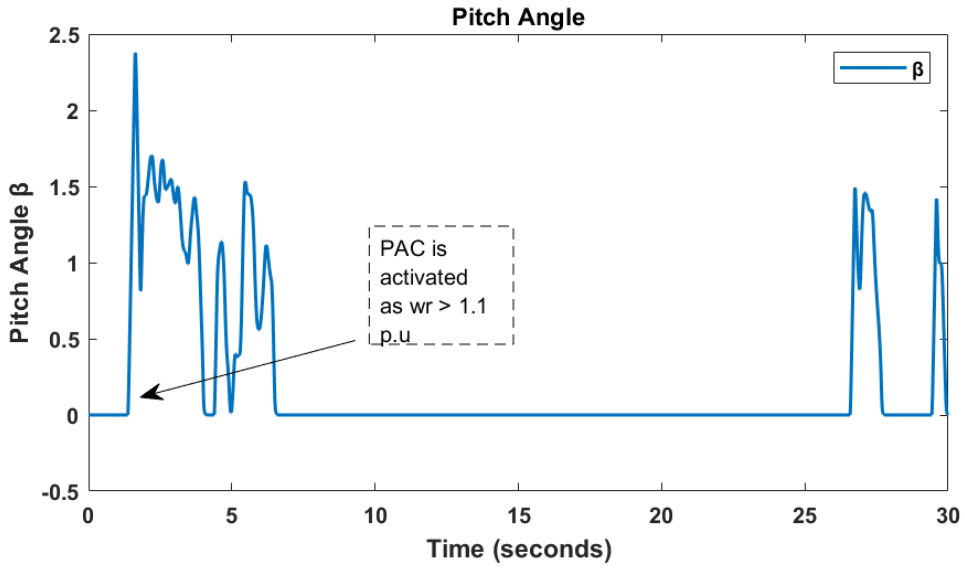

Figure 3.15 Pitch angle of WECS

The reference value of mechanical speed of the rotor used in PAC is 1.1 p.u. As long as the rotor speed is below this value, PAC will remain deactivated and the pitch angle value will be 0. It can be observed incase of start time where rotor speed is less than 1.1 p.u. But the PAC is activiated at 1.3s as the rotor speed becomes greater than 1.1 p.u given in Figure 1.17. The mechanical power Pm obtained by the wind turbine is shown in Figure 3.16. It can be seen that at the start, Pm rises following the wind speed and crest at 1.64 p.u. However, at 1.3s the value of Pm drops around 1 p.u value because of activation of PAC. After 7s, Pm follows the pattern of wind speed.

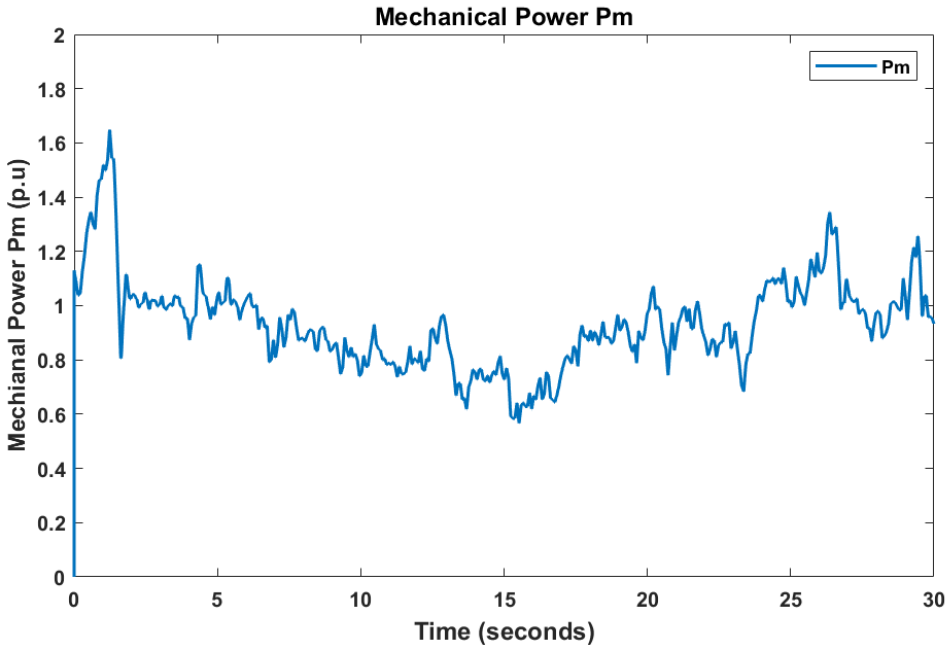

Figure 3.16 Mechanical Power Pm of Simulated System

3.6.2 Wind Generator and Grid Parameters

The overall control of PMSG based WECS is achieved by using PI controllers in MSC and GSC. The behaviour of rotor speed of the generator in illustrated in Figure 3.17. The wind speed is higher than 12 m/s from 1.5s to 6.5s, The mechanical spped of rotor is controlled at 1.2 p.u by PAC during these instances.

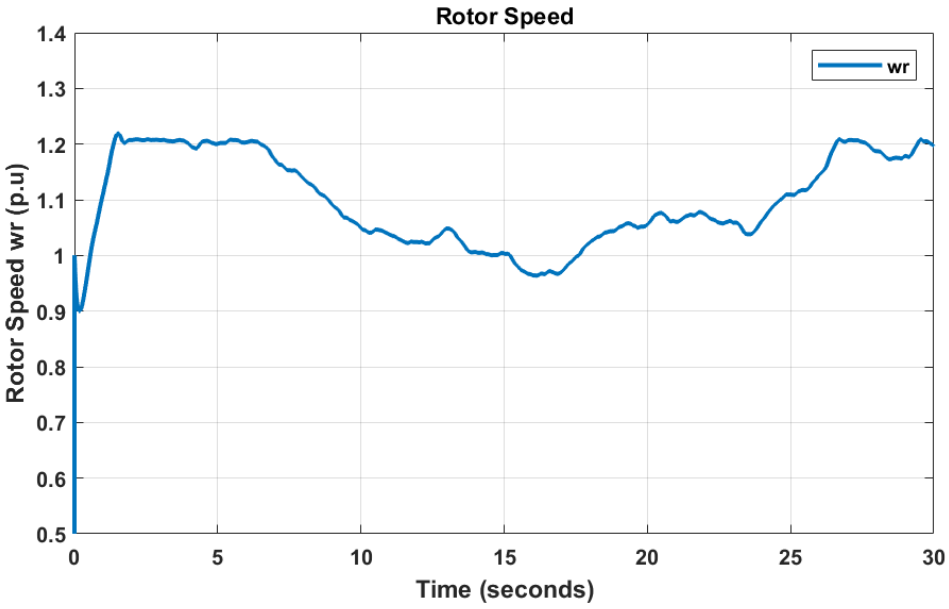

Figure 3.17 Rotor speed of the generator wr

The electromagnetic torque Te of the generator along with reference torque value T_e can be seen in Figure 3.18. T_e^* is generated through MPPT by using optimal torque

control (shown in Figure 3.11). The value of this reference torque value T_e^* is then used to generate reference q axis stator current i_{qs}^* (ZDC shown in Figure 3.9). The generated electromagnetic torque is following the referecen value. The three-phase generator currents during wind variation is presented in Figure 3.19. The value of stator current changes with generated power which in turn follows the values of electric torque and rotor speed. The minimum value of current is at 16.5s as dips in value also happens for rotor speed and torque at that time value.

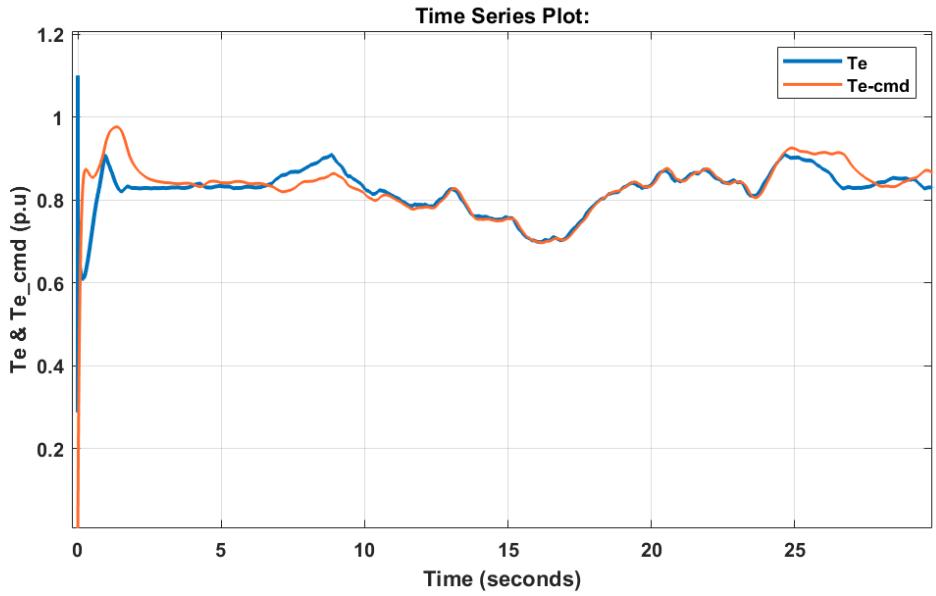

Figure 3.18 Electromagnetic Torque Te

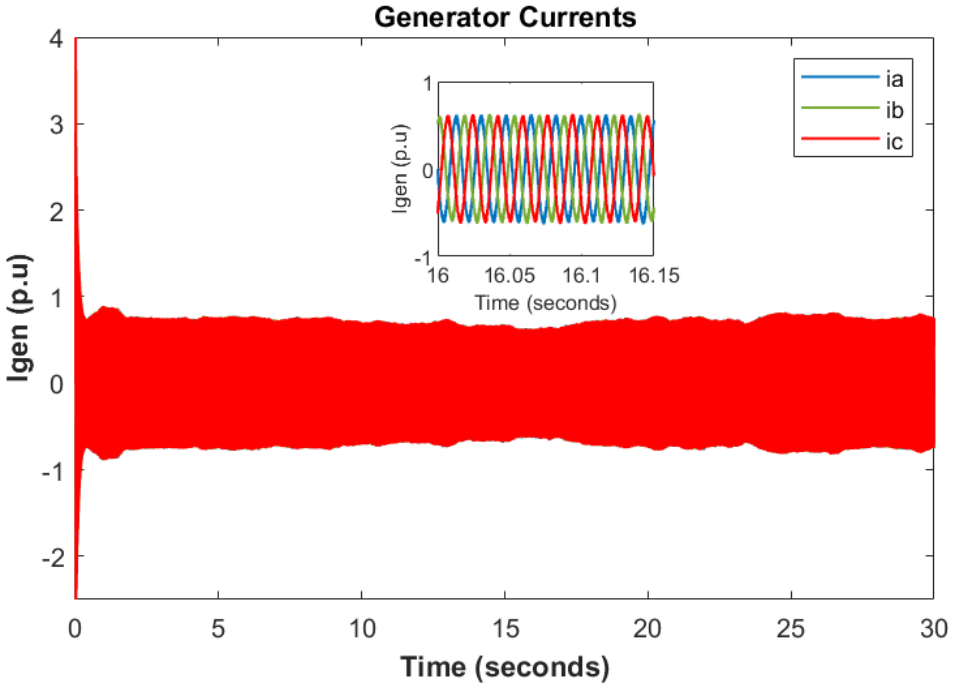

Figure 3.19 3 Phase Generator Currents

The voltage profile at DC link of the conversion system is illustrated in Figure 3.20. The DC link votlage is controlled by the outer loop of GSC according to the reference value of 1150 V. The DC link voltage control produces the reference value of grid current *d* axis i_{gd}^{*}. The active power delivered to the grid by the system during wind profile is shown in Figure 3.21. The operation of GSC is maintained at power factor value of 1 by controlling the q axis grid current i_{gq} at 0 value by the inner loop of GSC. As a result, reactive power of the WECS is 0 as given in Figure 3.21.The three-phase current of the grid under the given wind speed profile are given in Figure 3.22. The variation of grid current values are in correlation with active power supplied to utility grid. Consequently, the changes in wind speed affect the value of grid current.

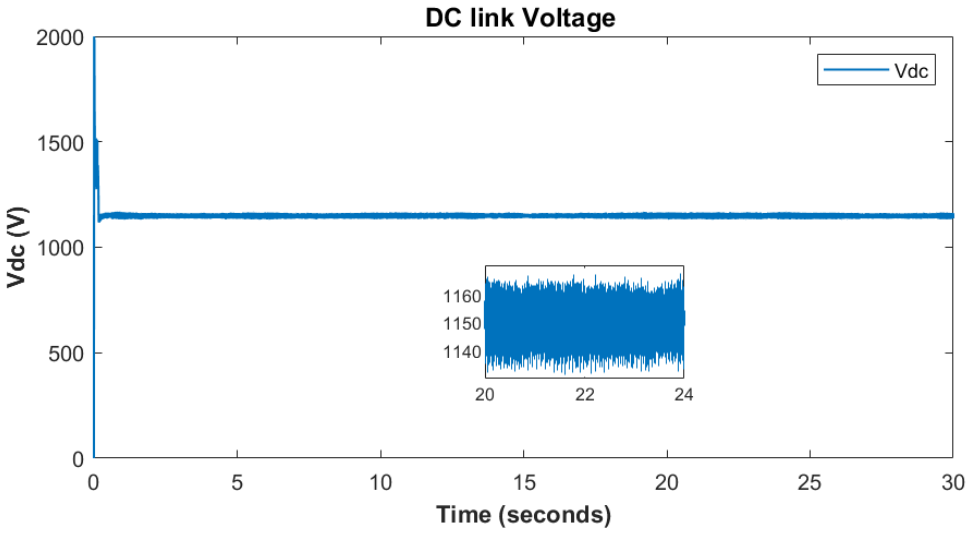

Figure 3.20 DC Link Voltage Vdc

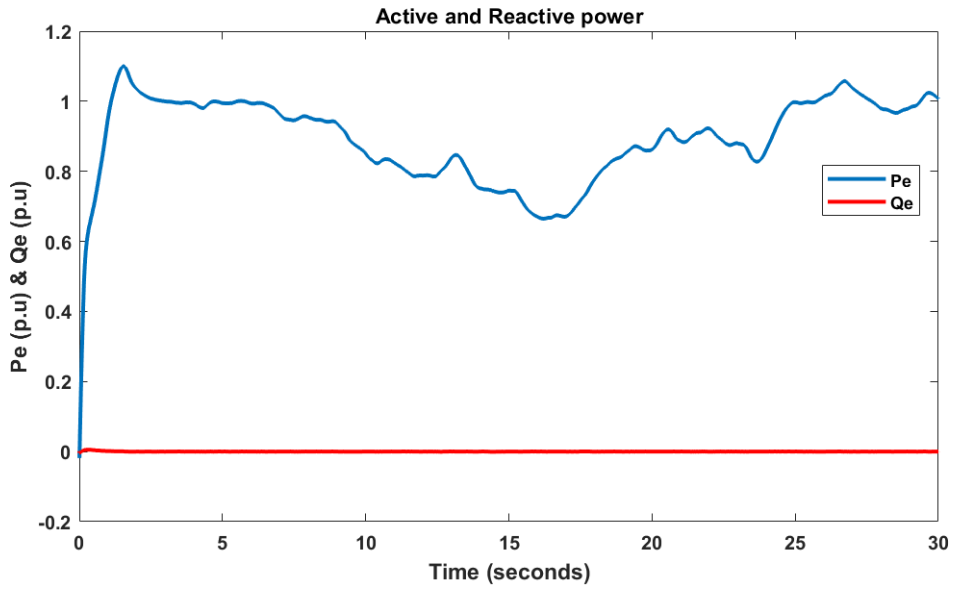

Figure 3.21 Active and Reactive power to the Grid

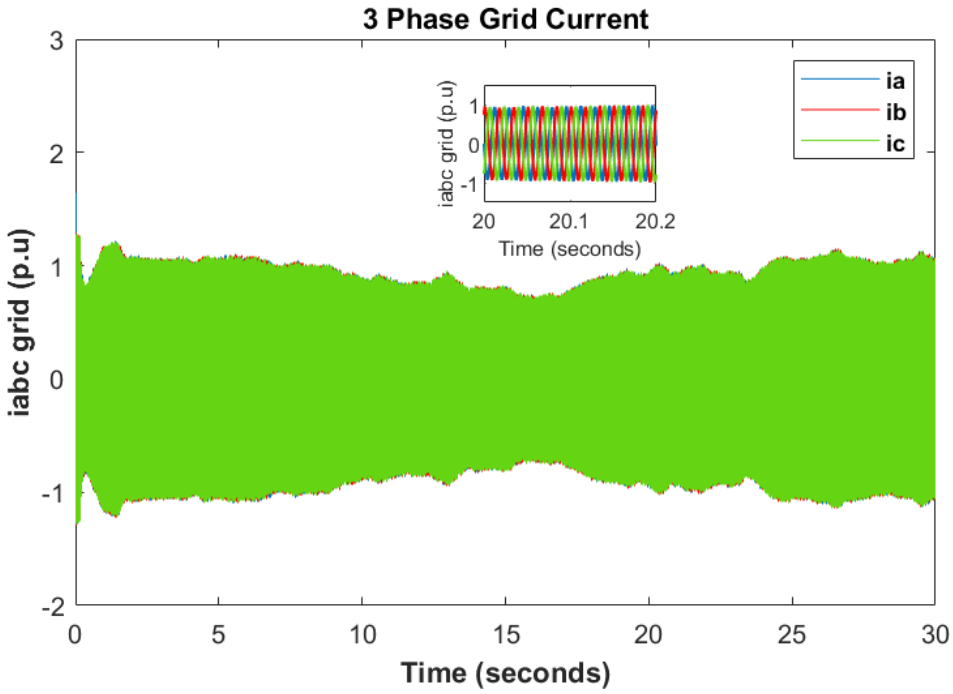

Figure 3.22 Three Phase Grid Currents

Chapter

4

SMES Unit Configuration and Control Scheme

Superconductors have gained popularity for application in WECS over the last decade in terms of power conditioning, frequency support and stability. Many configurations have been proposed for integration of superconductos with the WECS. Most presented techniques utilized the conventional PI controller for control of superconductor unit.

This chapters describes different configurations of SC unit. Furthermore, the proposed control is explained in terms of the control structure and controller used. The last part of the chapter deals with parameter optimization of the SC system.

4.1 Introduction

A SMES unit stores energy in magnetic field produced by superconducting coil due to flowing DC current through the coil. The temperature of the SC is kept below critical temperature value by using cryogenic process. The energy in an electromagnetic field depend upon the current flow and number of turns of the coil N. The electromotive force is the product of current flow and number of turns as NI. Eq. 4.3 represents the calculation of electromotive force of a coil, and the energy produced is expressed in Eq. 4.3.

$$e = -N\frac{d\phi}{dt} \tag{4.1}$$

$$E = \int_0^{\phi} Ni(t)\, d\phi = \int_0^{B} lHA\, dB = \int \int_0^{B} H\, dB \tag{4.2}$$

$$E_{volume} = \frac{B^2}{2\mu} \tag{4.3}$$

where

e is electromotive force (V), E is energy stored by the coil(J), N represents the number of turns of the coil, i is current flowing through the coil (A), ϕ is flux (Wb) produced, l is length (m) of the coil, B illustrates the magnetic induction (Wb/m^2), H depicts strength of the magnetic field (A. turns/m), A represents geometric area (m^2), , and μ represents the permeability (Wb/Am).

After the simplification of the Eq. 4.2, the stored energy of the coil depend upon the inductance and current flowing through the coil and can be expresses as:

$$E = \frac{1}{2}Li^2 \tag{4.4}$$

Where the stored energy is represented by E, L depicts coil inductance and i is the coil current.

Therefore, it can be deduced that with the help of media as air or vacuum, high energy density is possible. However, the electrical resistance is the issue. The resistance falls radically at the value known as the critical temperature. Niobium-Titane (NbTi) material is one commonly used for superconducting coils as it has critical temperature of 9.2K [95]. Electronic converters being interfaced with SMES unit helps in exchange of energy between SMES and grid.

The application of SMES will be more economic in coming years due to rapid research and development of superconducting materials [21]. Superconducting coils can be divided into two groups: high temperature SC (HTS) and low temperature SC (LTS) coils working at 5K [96]. The low temperature-SMES is common and commercially available.

The overall efficiency of SMES is very high as compare to other storage technologies and usually lie within a range of 90-98% [95]–[98]. The low power loss in SMES makes it more efficient.

There are no frictional losses in SMES due to absence of moving parts and minimal resistance of the coil does not create significant enough current losses that may pose as issue for efficiency. SMES has another advantage in form of short and quick time as compare to other storage devices. In other words, It can provide large amount of power immediately, which makes it suitable solution for fast power demand scenarios [44]. In case of load leveling applications, SMES is superior option for managing bulk power.
The typical structure of a SMES system is given in Figure 4.1. It consists of a SC, protection system and cryogenic process to maintain the temperature of the coil.

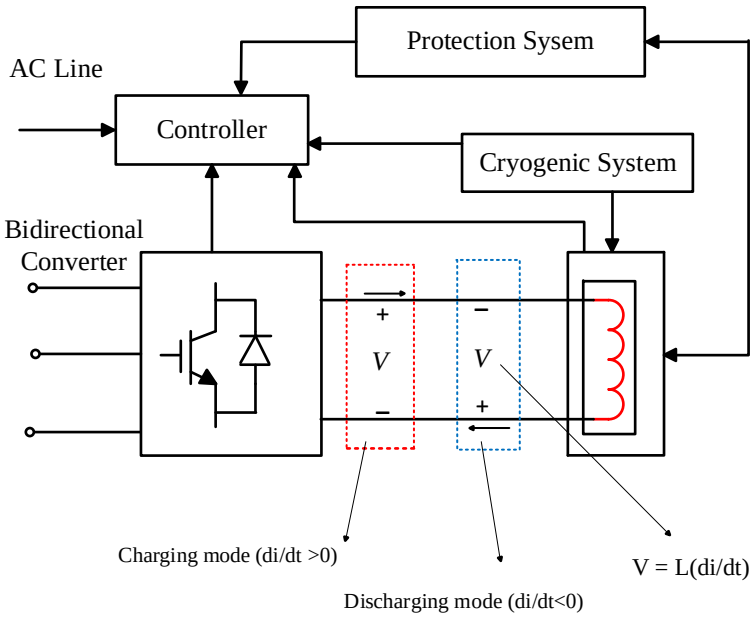

Figure 4.1 Schematic diagram of SMES unit

The high cost of implementation and other environmental concerns related to magnetic fields are the main drawbacks of SMES. The incorporation of SMES unit with renewable energy systems has been illustrated in several studies showing significant benefits. In early days, PV systems also utilized SMES unit to smooth out the output power. SMES also provided support in active and reactive power demand along with reducing transients created due sudden change in load demand. Application of SMES in variable wind energy conversion systems was discussed in chapter 2. However, the configuration of SMES unit and control scheme will be discussed next.

4.2 Configurations of SMES

There are types of configurations of SMES: VSC and CSC. Conventionally, the connection of CSC based SMES is done through a 12-pulse converter, which in turn consider effective for elimination of harmonics on AC and DC side. However, 12 pulse converter configurations are cost ineffective as it uses two parallel 6-pulse CSCs. On the other hand, VSC utilizes DC-DC converter for connection with DC link for facilitation of energy exchange between SMES and AC grid. It has been found in literature that SMES unit can connected with WECS at different locations of the system. The SMES unit can be connected at PCC of WECS through combination of VSI and DC-DC converter. A typical VSC based SMES configuration of this particular connection topology is shown in Figure 4.2. Reference [99] utilized 1 MJ SMES for power fluctuation smoothing 9 MW wind farm. SMES is connected at PCC of wind

farm. VSC utilized Hysteresis Current (HC) controller and for DC chopper control, fuzzy logic controller is used. The presented system mitigated power fluctuations up to 40%. However, addition of VSC and control increase the overall cost of SMES configuration. In addition, in case of fault very near to the PCC, LVRT capability of SMES in this case is less.

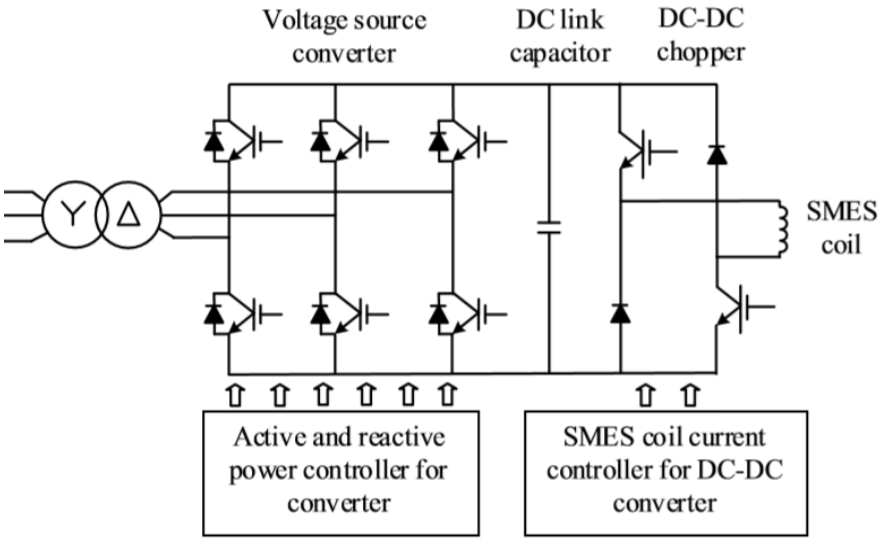

Figure 4.2 SMES connection at PCC

Variable speed WECSs also supports the integration of SMES at DC link of Conversion system. Literature contains many studies that utilized SMES at conversion system of PMSG and DFIG. In this topology, SMES is connected at DC link of the WECS through a two quadrant DC chopper as illustrated in Figure 4.3. CSC based unit does not require converter for this connection and DC chopper is used for VSC based SMES unit configuration. This connection is cost effective and can smooth out power fluctuations.

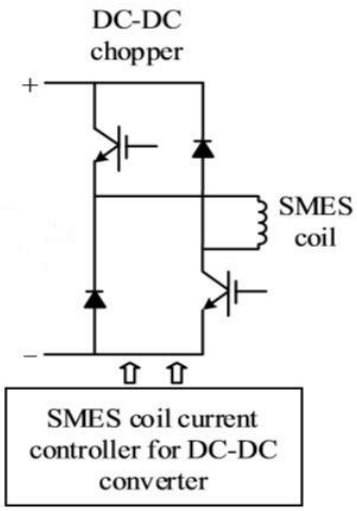

Figure 4.3 Class D DC-DC Chopper SMES connection at DC link

4.3 Operation of Selected SMES configuration

The control scheme in Figure 4.4 provides the duty cycle D to chopper. The duty cycle D decides the direction of flow of power between superconducting coil (SC) and AC. The voltage across SC V_{sc} as a function of DC link voltage V_{dc} and duty cycle D can be given as:

$$V_{SC} = (1 - 2D)V_{dc} \tag{4.4}$$

There are three modes of operation of SC depending upon the duty cycle of chopper as presented in Table 4.1.

Table 4.1 Modes of operation of SC unit

Value of D	**SC Mode**
D = 0.5	Freewheeling Mode
$0 \leq D < 0.5$	Discharging mode
$0.5 < D \leq 1$	Charging mode

When the value of *D* is 0.5, the freewheeling mode is on as shown in Fig. 4.4(a). The average voltage of the SC is zero and I_{SMES} of the coil is held at constant rated value. Therefore, no energy transfer will happen between SC and AC system.

Discharging mode happens when D < 0.5. During this mode, the average voltage across SC is negative due to negative rage of change of SC current and energy is discharged to the AC system. Discharging mode is shown in Fig. 4.4(b). Charging mode is when

$D > 0.5$ at which the surplus energy gets stored in the SC. The charging mode is shown in Fig. 4.4(c). The direction of the current through the Superconducting Coil in SMES remains same during each mode and energy exchange depends upon the change in the slope of SC current (di/dt).

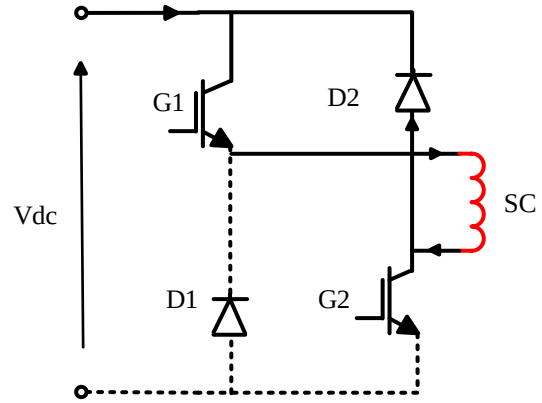

(a)

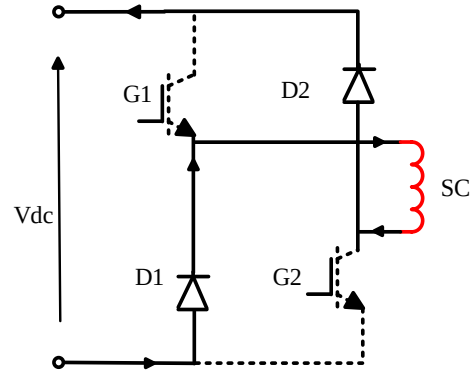

(b)

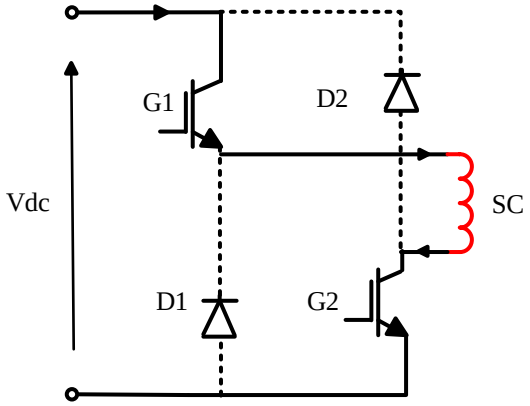

(c)

Figure 4.4 SC operation; (a) Freewheeling mode, (b) Charging mode, (c) Discharging mode [34]

4.4 Control Strategy of SMES unit

The SMES configuration used in this thesis utilizes DC-DC chopper for the connection of SMES at the DC link of the WECSs as represented in Figure 4.2.

The tradition control of DC-DC chopper mostly utilizes PI control for the generation of duty cycle of chopper as found in the literature. The integration of SMES through DC-DC chopper with WECS is given in [67]. In proposed system, PI controllers are used to generate duty cycle according to power generated and reference power. The SMES current I_{SMES} is also included in control along with reference current I_{SMES}^{*} to consider the effect of stored energy on the generated duty cycle. [68] presents SMES system containing VSC and DC chopper. Four PI controllers used for both VSC and DC chopper need more time to properly tune parameters for better performance. The power reference for DC chopper control is generated through EWMA filter which further complicates the computation of the whole system. However, both proposed systems lacked effective tuning process for parameters of PI controller. Another SMES unit connected at PCC for performance improvement is presented in [100]. The SMES control utilizes PI controllers optimized with IPSO optimization algorithm. [101] utilizes PI controlled SMES system to keep DC link voltage of the wind power system constant. The error of the DC link voltage and reference is fed into PI controller which in turn generate PWM signal for the chopper.

The application of PI control in SMES unit used for WECS can be found in so many other studies such as [25], [58], [59], [74], [76], [102]–[104]. However, variable speed WECS suffer from various uncertainties and disturbances such as wind gust, terminal voltage dip and faults at the PCC. PI controller cannot guarantee satisfactory response to such disturbances on WECS. To enhance the operation of such SMES unit many non-linear controls also been employed to achieve better performance of WECSs. For example, FLC in addition to PI controller have found application in control of DC chopper control for SMES unit. Such System is presented for performance improvement of DFIG based WECS in [24]. In this system, Fuzzy Logic control is used to generate duty cycle for the chopper. Fuzzy logic is developed through comparison of generated power and SMES current with their respective references. In recent years, Fractional Order control is been considered as one of the effective and robust techniques to curtail the effect of disturbances.

The control strategy used in this thesis is shown in Figure 4.5. It employs Fractional order Proportional Integrator Controller (FOPI) for control of DC-DC chopper to exchange energy between SC and AC System.

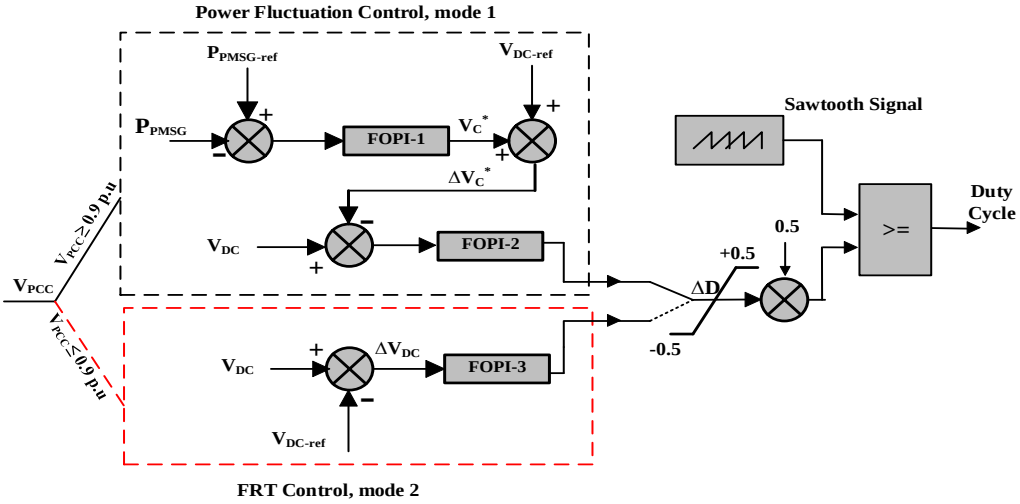

Figure 4.5 Proposed control Scheme of SC (SMES)

Based on the level of PCC voltage, there are two control modes; power fluctuation control and fault ride through control. Mode 1 is responsible for output power fluctuations smoothing due to wind gust, given that PCC voltage is within limits of ±10% (IEEE standard).

The selection of mode of operation depends upon the V_{pcc} value. If the value of V_{pcc} is greater than or equal to 0.9, then power smoothing mode is activated. On the other hand, mode 2 of LVRT enhancement is triggered when V_{pcc} falls below 0.9.

Power Fluctuation Control mode

The target of this control mode is to achieve smooth output power during wind gust while maintaining voltage at the PCC within ±10% (IEEE standard) [105]. Two FOPI controllers are utilized in this control as represented in Fig. 4.5. The difference of PMSG output power and reference power is fed into first FOPI. The output of FOPI-1 is voltage value (VC*) that represents change in PMSG power with respect to variation in wind speed. An error signal ΔVC* is generated through the comparison of value VC* with reference DC link voltage. The difference of the error signal ΔVC* and measured voltage value at DC link is fed to FOPI-2 which then generates duty cycle deviation

ΔD. The final duty cycle value D is then produced by comparing normalized duty cycle deviation and sawtooth signal.

FRT Control mode

Power cannot be provided to the grid network by the GSC during faults at PCC and voltage of the DC link will experience oscillations. However, with the presence of controlled SC, the voltage profile of DC link is improved by the rapid energy release from the SC during grid fault condition. The duty of the FOPI-3 controller used, is to keep constant value of voltage at DC link which in turn improves the FRT capability of the PMSG. This mode is activated when voltage at the PCC becomes less than 0.9 p.u. First, the voltage of DC link is measured, error value of DC link voltage is fed to the FOPI-3 controller as shown in Figure 4.5. Then the duty cycle deviation generated by the FOPI-3 controller can be normalized between 0 and 1 as stated above.

4.4.1 Fractional Order Proportional Integral (FOPI) Control

Fractional Calculus (FC) have found significant application in different science and engineering domains in the last decade. FC is the generalization of order of Derivative and integral from integer to real value. In FC, notation to represent fractional order of integral-derivative is written as:

$$D_t^{\alpha} f(t) = \begin{cases} \frac{d^{\alpha}}{dt^{\alpha}} f(t) & \alpha > 0 \\ f(t) & \alpha = 0 \\ \frac{d^{\alpha}}{dt^{\alpha}} = I^{\alpha} f(t) & \alpha < 0 \end{cases} \tag{4.5}$$

Where alpha is the fractional order of the derivative and integral. The transfer function of Fractional Order Proportional Integral and Differential (FOPID) is based on definition given in eq. 4.1, which is further represented by Riemann-Lieuville (R-L) and Grunwald Letnikov (G-L) approximations.

R-L definition for α > 0 is given by[106]:

$$D_t^{\alpha} f(t) = \frac{1}{1-\Gamma(n-\alpha)} \frac{d^n}{dt^n} \int_{\alpha}^{t} \frac{f(\tau)}{(t-\tau)^{(\alpha-n+1)}} d\tau \tag{4.6}$$

Where ($n\text{-}1 < \alpha < n$) and $\Gamma(n)$ represents the gamma function

The definition of G-L is expressed as:

$$D_t^{\alpha} f(t) = \lim_{t \to 0} \left(\frac{1}{h^{\alpha}}\right) \sum_{j=0}^{\infty} (-1)^j \binom{\alpha}{j} f(t - jh) \tag{4.7}$$

Where

$$\binom{\alpha}{j} = \frac{\Gamma(\alpha+1)}{\Gamma(j+1)\Gamma(\alpha-j+1)}$$

The Laplace transfer function for fractional order derivative *f(t)* expressed as*:*

$$LD^{\pm}\,\alpha f(t) = s^{\pm\alpha}F(s). \tag{4.8}$$

The definition of transfer function of FOPID can be made through following differential integral equation according to the equation 4.1.

$$u(t) = k\left(e(t) + \frac{1}{Ti}D^{-\lambda}e(t) + T_d D^{\mu}e(t)\right) \tag{4.9}$$

where k represents the proportionality constant, T_i depicts the integral time constant, T_d denotes the derivative time constant, λ represents the fractional order of the integral term, μ depicts the corresponding fractional order of the derivative term, e(t) denotes the error signal and u(t) depicts the control signal. After applying the Laplace transform on Eq. 4.9 according to the fractional Laplace transform given in Eq. 4.8, the transfer function of the FOPI controller can be stated as:

$$C(s) = K_p + \frac{K_i}{s^{\lambda}} \tag{4.10}$$

The Figure 4.6 represents the relationship between the simple PID and FOPID. FOPID can be converted into conventional PID controller by using values as λ = μ = 1. Therefore, conventional PID can be a specific case of FOPID controller as can be seen in the Figure 4.5. FOPI and FOPD can be obtained by setting K_i or K_d in FOPID equal to zero respectively. Consequently, they can be considered as subset of FOPID and enhanced or detailed version of traditional PI and PD controllers.

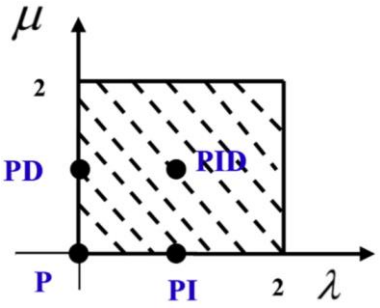

Figure 4.6 Range of Integral PID and Fractional PID

From this figure, it can be seen that conventional PID controller can modify parameters at only four specific points, whereas FOPID controller can change its parameters in this whole quadrant. As a result of flexible nature of these two parameters μ and λ, FOPID or FOPI controller can give better performance and robustness against disturbances on

the whole system. However, the presence of more parameters in case of FOPID, make its tunning process more time consuming and complex [107].

There are many methods available for the tunning of parameters of the FOPI. Recently, the main methods used for this purpose are dominant pole method, phase and amplitude margin method, optimization methods, etc. Phase and amplitude margin method for parametric tunning of FOPI is presented in [108]. Hybrid fractional controller for grid connected WECS is given in [109]. The presented study used Frequency method The FOPI design ensuring robustness according to phase and gain margin criterion. The parameters of the FOPI were then attenuated by PSO algorithm. The cost function is formulated by using settling time, Rise time and max overshoot values. [110] represents another study utilizing Optimization method for parametric tunning of FOPI controller. FOPI control is utilized to improve the power control of the DFIG. In this study, PSO algorithm is used for the calculation of parameter of FOPI controllers. The objective function being used for the optimization process is the integral of time weighted square error (ITWSE).

In this thesis, the parameters of FOPI utilized in SC control are determined by an optimization method.

4.4.2 Harmony Search (HS) Algorithm

The Harmony Search (HS) algorithm being nature inspired metaheuristic mimics the underlying principles of musical improvisations. It is an emerging optimization method, first proposed by Green et. All in [111]. It has found application in areas such as optimization benchmark, cost minimization tool in power systems, industry applications, medical science, robotics and image processing [112]. The process of finding better harmony can be considered similar to attaining an optimal result for a given engineering problem. Figure 4.7 depicts the flow chart representing basic steps of HS algorithm.

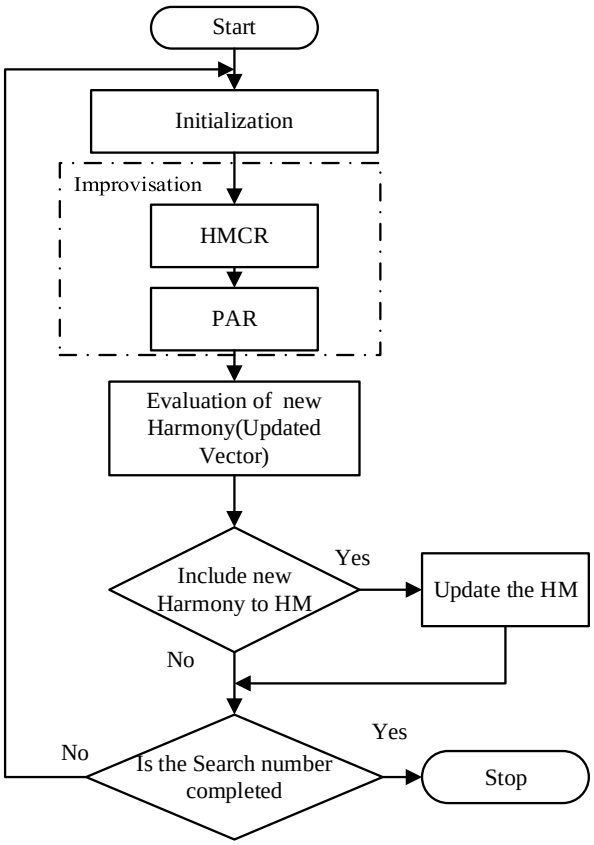

Figure 4.7 Flow Chart of HS

The HS algorithm uses stochastic random searching technique instead of gradient one. In this algorithm, solution vector is found in the search space by using Harmony Memory Considering Rate (HMCR) and Pitch Adjustment Rate (PAR) [112]–[114]. The procedure of the HS algorithm includes following steps:

1) Formulation of objective function and setting parameters of algorithm.
2) Setting of harmony memory (HM).
3) Finding a new Harmony.
4) Harmony Memory modification
5) Stopping criteria check. Otherwise, repeat step 3 to 4.

A. Formulation of optimization problem and setting HS parameters

In this stage, the objective function is formulated as

$$Min\ f(x) \tag{4.11}$$

Given

$$g(x) = 0$$

$$x_{k,min} \leq x \leq x_{k,max} \quad k = 1,2,\cdots,N$$

Where *f(x)* represents the cost function and equality constraint are defined by *g(x).* x depicts the set of deciding variables with x_{min} and x_{max} as the minimum and maximum limits respectively. The HS parameter such as size of Harmony Memory (HMS), HMCR, bandwidth rate (BW), PAR and number of improvisations NI, are also being set in this step.

B. *Setting of Harmony Memory (HM)*

The harmony memory is the matrix containing all the solution vectors. In this step, Randomly produced solutions are stored in HM by following constraints on the decision variables

$$HM = \begin{bmatrix} x_1^1 & x_2^1 & x_3^1 & x_4^1 & x_5^1 & \cdots & x_N^1 \\ x_1^2 & x_2^2 & x_3^2 & x_4^2 & x_5^2 & \cdots & x_N^2 \\ \vdots & \vdots & \vdots & \vdots & \vdots & \cdots & \vdots \\ x_1^{HMS} & x_2^{HMS} & x_3^{HMS} & x_4^{HMS} & x_5^{HMS} & \cdots & x_N^{HMS} \end{bmatrix} \quad (4.12)$$

C. *Finding new harmony memory*

The new solution vector also called new harmony vector, $X' = (x_1', x_2', \dots, x_N')$ is determined based on three values: 1) HMCR 2) PAR and 3) Random Selection.

First step is the selection of decision variable X' for new solution vector from $(x' - x^{HMS})$ according to the HMCR. HMCR is defined as the probability of selecting value from historical values stored in HM and it can vary between 0 and 1. On the other hand, (1-HMCR) represents the rate of random selection of value from available rang as

$$x_i' = \begin{cases} x_i' \in \{x_i^1, x_i^2, \dots, x_i^{HMS}\} & if\ rand \le HMCR \\ x_i' \in X_i' & otherwise \end{cases} \quad (4.13)$$

Where rand represents random value among 0 and 1. X' is set of range of values of each decision variable.

After memory consideration, pitch adjustment is the next process. Pitch adjustment rate (PAR) is used to in this process as;

$$x_i' = \begin{cases} x_i' \pm rand * BW & if\ rand \le PAR \\ x_i' & otherwise \end{cases} \quad (4.14)$$

where BW represents the arbitrary bandwidth.

The response of HS algorithm can be further improved by modification of PAR and BW values during each iteration by using following expressions;

$$PAR(g) = PAR_{min} + \frac{PAR_{max} - PAR_{min}}{NI} * g \quad (4.15)$$

where *PAR(g)* depicts the pitch adjusting rate while g represents the current number of generations, PAR_{min} and PAR_{max} are the lower and upper limits of PAR respectively and NI represents the improvisations' number.

$$BW(g) = BW_{max} \exp\left(\frac{Ln\left(\frac{BW_{min}}{BW_{max}}\right)}{NI} * g\right) \quad (4.16)$$

D. Harmony Memory Modification

If the new solution from previous step produces better fitness as compare to the worst solution in HM, it will replace that one.

E. Stopping criterion

The process is stopped when iteration number is equal to the improvisation number (NI) or Step C and Step D are repeated.

4.4.3 Integration of HS in Proposed Control

HS has been very popular in optimization techniques for application in several power and renewable fields. HS optimization technique can give higher efficiency and better performance as compare to traditionally used PSO and Genetic Algorithm (GA) as shown in [115]. HS has a prominent feature of computational simplicity as compare to other population-based techniques as it uses a single search memory to evolve. In this thesis, HS is utilized to find parameters of FOPI/PI controllers and to optimize size of Superconducting Coil (SC) as shown in Figure 4.7. The target is to minimize the initial stored energy rating in SC in SMES by minimizing its size. HS is used to find the parameters of 3 FOPI utilized in control scheme presented in Figure 4.5.

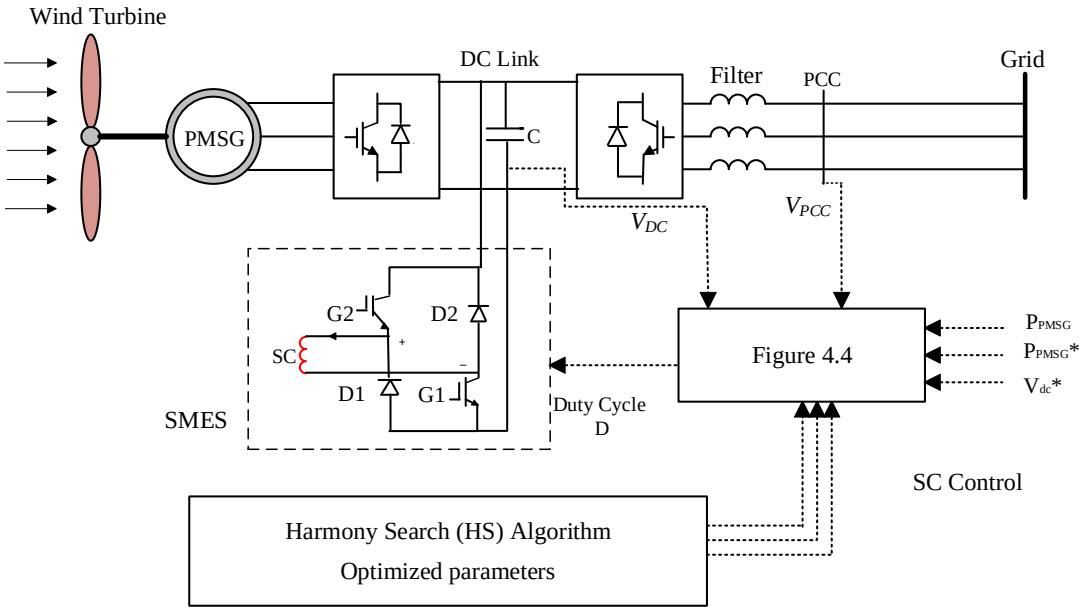

Figure 4.8 Proposed system integrated with PMSG based WECS

In order to find optimum size of SC (Inductance L_{sc}), minimized initial current value of SC (I_{sco}), and optimized parameters of FOPI, an objective functions J is formed which is given by:

$$J = w_1 E \quad + w_2 \int |\Delta V_{dc}| dt + w_3 \int |\Delta P| dt + w_4 \int |\Delta I_R| \, dt \tag{4.17}$$

Subjected to the following constraints:

$$L_{sc_{min}} \leq L_{sc} \leq L_{sc_{max}}$$

$$I_{sc0_{min}} \leq I_{sco} \leq I_{sc0_{max}}$$

Where $E_0 = 0.5 L_{sc} I_{sc0}^2$ is initial energy of the SC and w_1 to w_4 are random weighting factors (0,1).

In equation 4.17, ΔV_{dc} represents the difference among actual and reference value of voltage at DC link, ΔP represents the deviation of power of the PMSG, ΔI_R is change in value of current of Grid converter. I_{sco} is initial current of the SC and w_1 to w_4 are random weighing factor values range from 0 to 1. The disturbances in the form of wind gust and fault at PCC will create changes in form of ΔV_{dc} at DC link and ΔP. The purpose of the cost function is to minimize these deviations.

The first term in function (Eq. 4.17) is related to the size of the SC and initial stored energy. The weighing factor are selected depending upon the importance of individual terms for the optimization. The term of $w_2 \int |\Delta V_{dc}| dt$ being the representation of FRT

control mode, is used for parametric tunning of third FOPI controller shown in Figure 4.4. The last two terms in objective function are representation of power smoothing control of the PMSG proposed in Figure 4.4. related to the power fluctuation smoothing control of the PMSG. The parameters of first and second FOPI are tunned through the minimization of last two terms in objective function.

Optimum parameters would be determined by minimizing the cost function through harmony search algorithm. The first step in HS involves initialization of required parameters (11 in total in case of FOPI) with random values within the admissible range. Then Harmony Memory (HM) matrix contain parameter (to be optimized) in rows as shown below:

$$HM = \begin{bmatrix} L_{sc}^{1} & I_{sco}^{1} & K_{p1}^{1} & K_{i1}^{1} & \lambda_1^1 & \cdot & \cdot & \lambda_3^1 \\ L_{sc}^{2} & I_{sco}^{2} & K_{p1}^{2} & K_{i1}^{2} & \lambda_1^2 & \cdot & \cdot & \lambda_3^2 \\ \cdot & \cdot & \cdot & \cdot & \cdot & \cdot & \cdot & \cdot \\ \cdot & \cdot & \cdot & \cdot & \cdot & \cdot & \cdot & \cdot \\ L_{sc}^{HMS} & I_{sc}^{HMS} & K_{p1}^{HMS} & K_{i1}^{HMS} & \lambda_1^{HMS} & \cdot & \cdot & \lambda_3^{HMS} \end{bmatrix} \quad (4.18)$$

Second step involves improvisation method in which each row in HM is updated based on two probabilistic factors: i) HMCR, ii) PAR. The relation between new solution vector (harmony) x_i^{n+1} and current solution (harmony) vector x_i^n is written as:

$$x_i^{n+1} = x_i^n + rand * BW \quad (4.19)$$

The next steps, that are going to be followed, are given above.

Chapter

5

Performance of PMSG based WECS with Integration of Superconducting Coil

The impact of integration of superconducting coil on the perfromace of the PMSG based is invertigated in this chapter. The two main challenges faced by the WECS are fluctuation of output power and fault ride through. Wind gust lead to output power fluctuation. The fluctuation of output power create many issues in form of poor power quality, voltage and frequency transients etc. The WECS should have FRT capability to withstand grid faults. Many techniques have been investigated for performance improvement of PMSG based WECS over the years as reported in chapter 2. And, the use of superconductors to enhance the operation and performance of WECSs can be effective technique. Superconductor based storage systems called SMES have various technical advantages in form of high efficiency, quick response for charging and discharging.

This chapter contains discussion investigating the effect of superconducting coil on the performance of the PMSG based WECS against disturbances in form of wind gust and grid faults.

5.1 Performance of PMSG based WECS during Disturbances

5.1.1 Simulation Result of WECS

MATLAB/Simulink 19 is used for modelling and simulation of the whole WECS. The modeling details of wind turbine model, PMSG with BTB converter system and the two main controls are given in chapter 3. The PMSG based WECS with connection of SMES at DC link is given in Figure 5.1. It consists of WECS connected at PCC to grid via transformer. An ideal 3 phase supply with constant frequency is used to represent AC grid. The reactive power of the system is maintained at 0 under unity power factor. The implemented system under the average speed of 12 m/s gives 1 p.u turbine power and 1 p.u of rotor speed wr. The simulation results of WECS under variable wind speed are also presented in chapter 3.

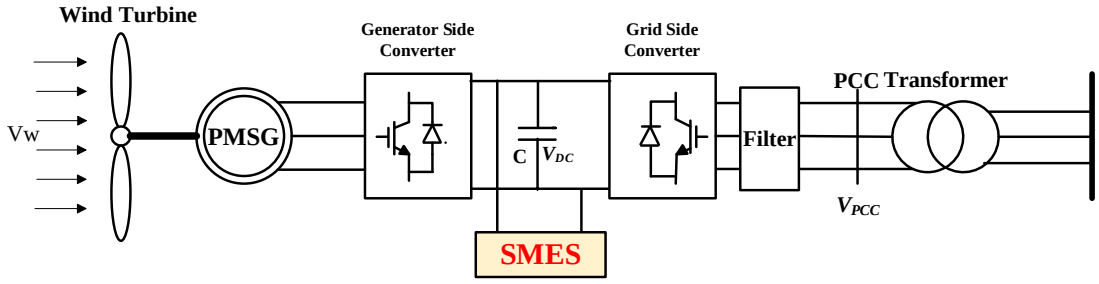

Figure 5.1 Connection of SC at DC link in Simulink

5.1.2 SMES with proposed control

The details of superconducting coil (SC) integration topology and the working of proposed control scheme are explained in chapter 4. The model of the configuration of SMES containing superconducting coil built in Simulink is given in Figure 5.2. It utilizes two quadrant D type DC chopper to integrate superconducting coil at the DC link of the WECS.

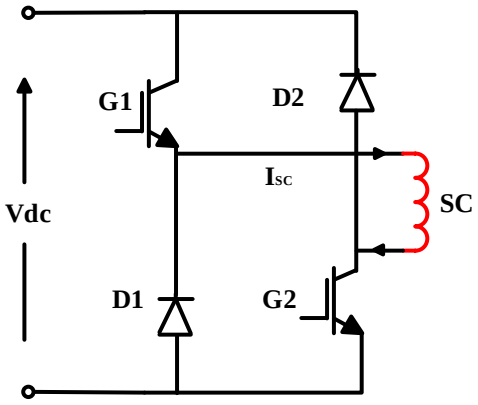

Figure 5.2 SC Unit in Simulink

The control Scheme of SMES buil in MATLAB/Simulink is shown in Figure 5.3. The fractional order controller is used from FOMCOM block available in simulink.

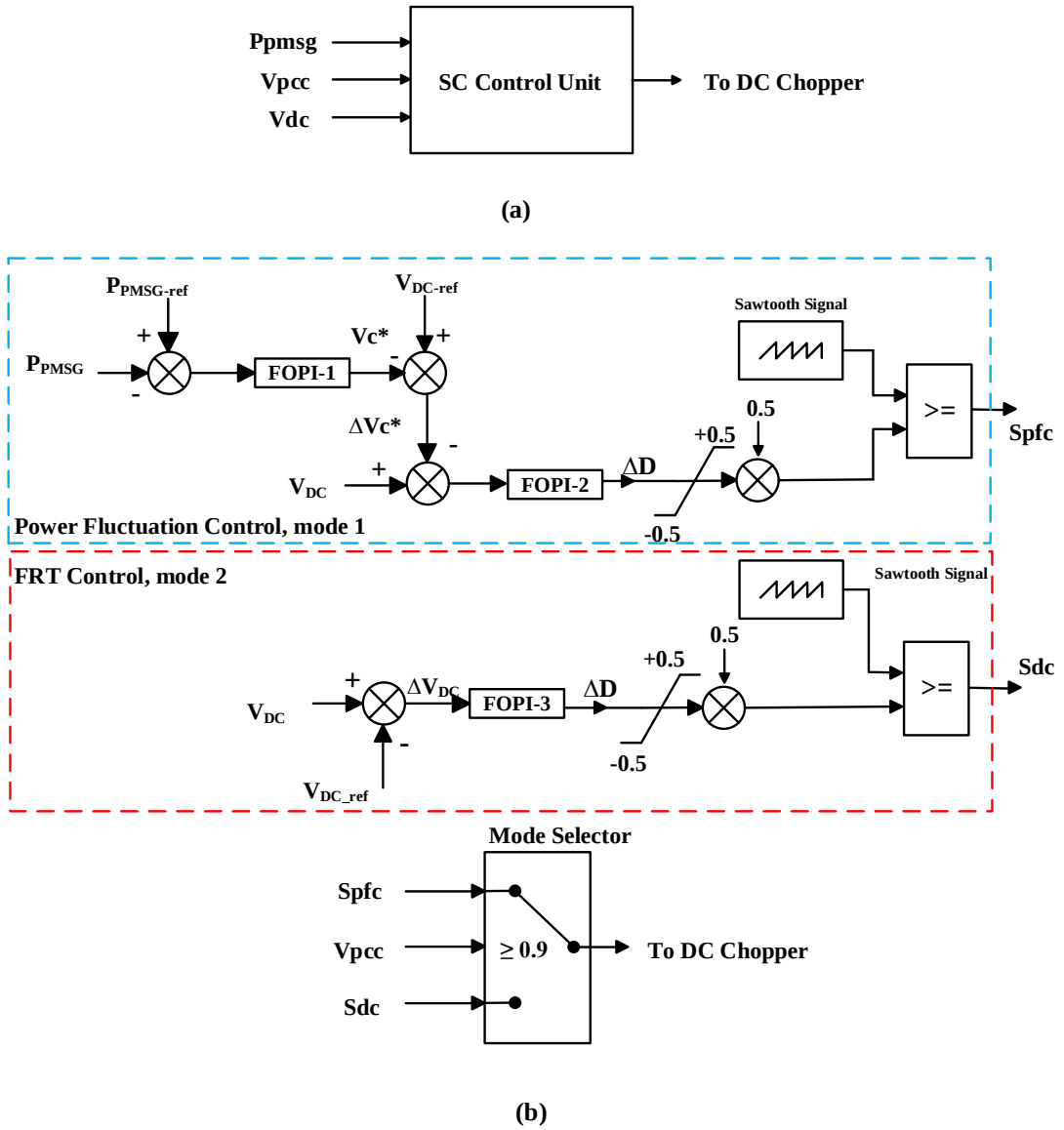

Figure 5.3 The proposed control of SC in Simulink (a) SC control Unit (b) Internal Control

The parameters of FOPI and superconducting coil are obtained from HS optimization algorithm. The parameters of HS used for optimization are in Table 5.1

Table 5.1 HS Parameters

HS Parameter	Value
HMS	15
BW	0.2
HMCR	0.93
PAR	0.3

The parameters of FOPI/PI controllers and superconducting coil values used for the simulation are given in Table 5.2.

PMSG wind system is tested with disturbances in form of wind gust and grid fault to investigate the impact of superconducting coil.

Table 5.2 Parameters of FOPI/PI controller and SC

	SC parameters		**Controller Values**								
PI	Lsc (H)	I_{sco} (kA)	Kp_p1		Ki_p1	Kp_p2		Ki_p2	Kp_p3		Ki_p3
	2.4	1.55	0.85		0.45	0.98		0.23	0.26		0.02
FOPI	L_{sc} (H)	I_{sco} (kA)	Kp_1	Ki_1	λ1	Kp_2	ki_2	λ2	Kp_3	Ki_3	λ3
	1.3	1.32	0.56	0.045	0.7	1.5	0.56	0.67	0.78	0.07	0.76

5.1.3 Power Regulation of PMSG based WECS

One of the issues of variable wind system is their fluctuating output power against unpredictable nature of wind. These power fluctuations are harmfull for stable and efficient operation of grid. These fluctuations crease voltage and frequency instabilities which in turn result in losses in grid. The WECS should contribute smooth power to ensure power quality by following the requirements given by TSO. The increased integration of WECS with grid have created the need of power mitigation process. In this thesis, the proposed system and control robustness is tested for following case studies: 1) step change in wind speed and 2) quick random change in wind speed in short time.

5.1.3.1 CASE 1 - Step Change in Wind Speed

The proposed power fluctuation mitigation control mode 1 is tested for a sudden variation in wind speed from normal average speed in this case. The wind speed changes from average value of 12 to 14 m/s in between 12 to 14 s as given in Figure 5.4. The voltage at the PCC remains within 10% of nominal value, as given in Figure 5.5. Thus, activating the mode 1 of the proposed control.

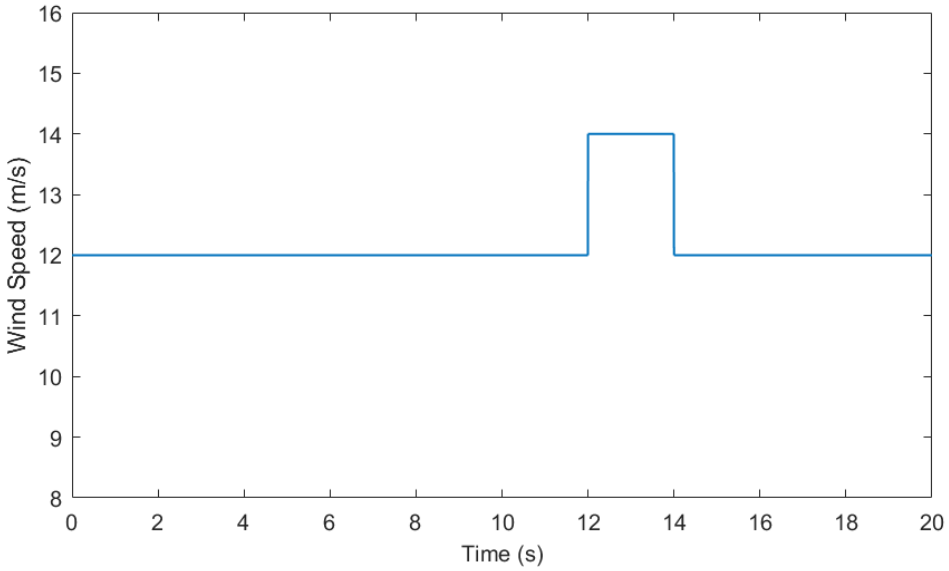

Figure 5.4 Step Change in Wind Speed

The voltage profile at the PCC of PMSG during sudden abruption in wind speed is comparatively better in case proposed control. The active power of the PMSG wind system during change in wind speed is given in Figure 5.6. There is a rise in active power of the system which creat at 1.18 p.u value and falls down at 14s time as clearly seen in Figure 5.7. The SC control employing FOPI effectively suppres the rise in active power down to almost 1.03 p.u.

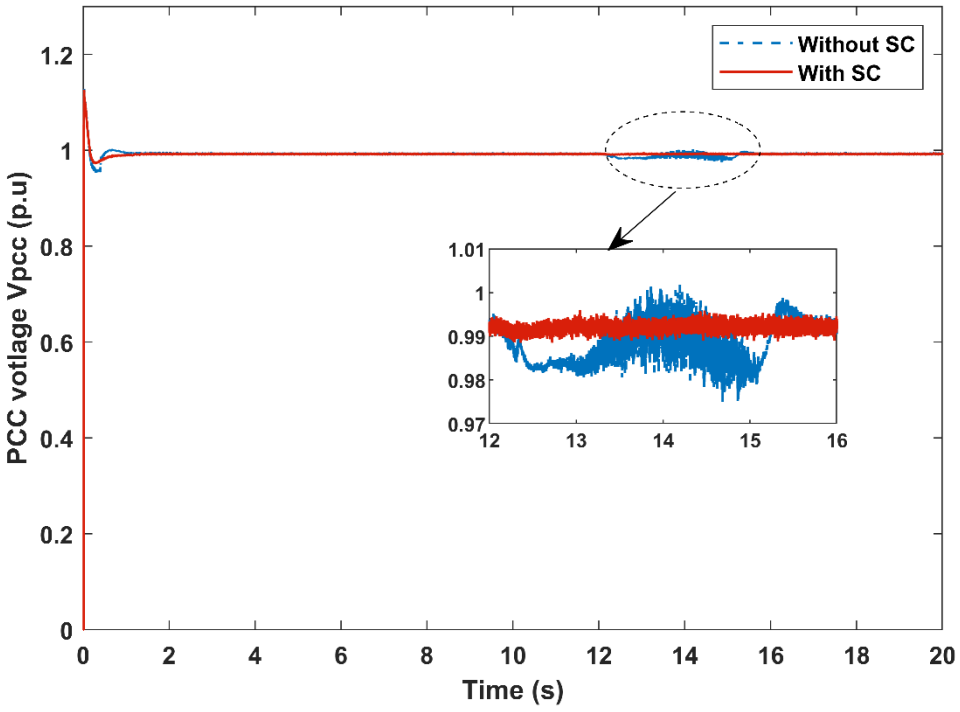

Figure 5.5 PCC voltage in case of step change of wind

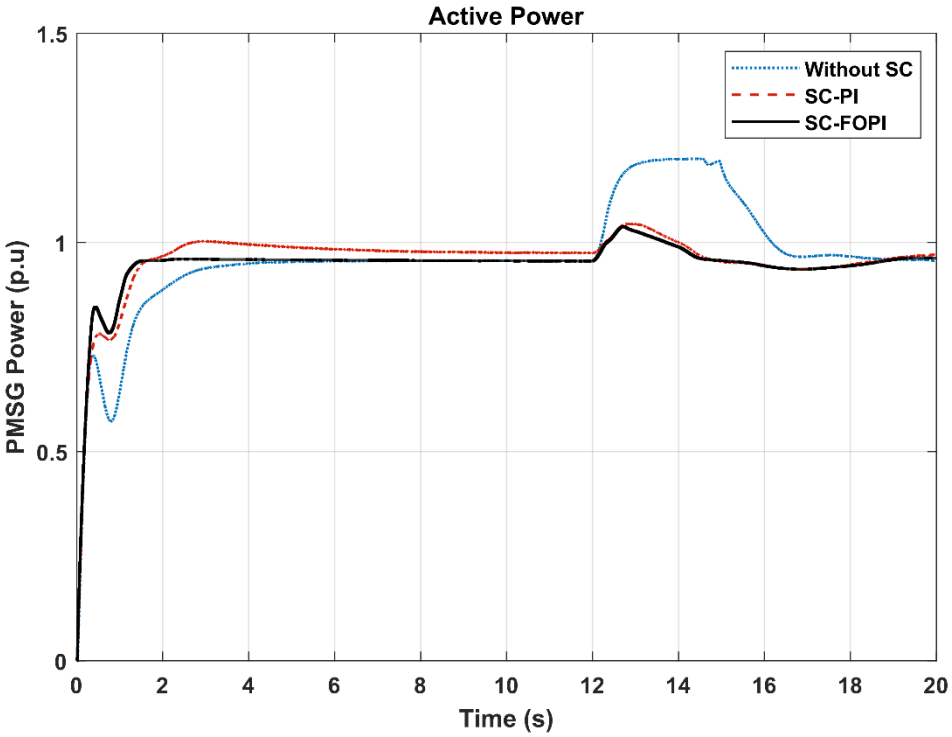

Figure 5.6 Active power of the PMSG during step change in wind speed

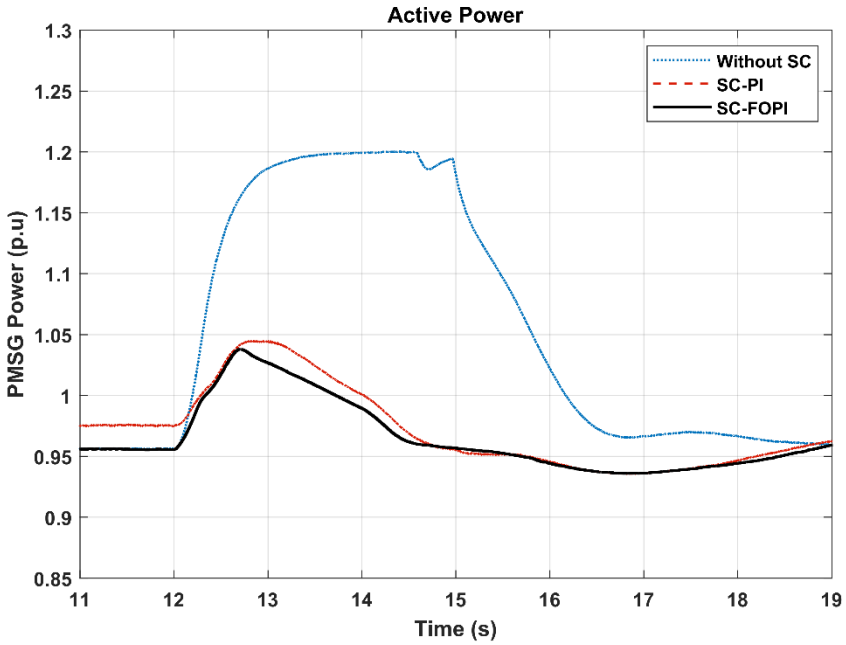

Figure 5.7 Active power response for step change in wind speed

5.1.3.2 CASE 2- Application of Wind gust

The under study WECS is subjected to quick wind speed change in order to check the working of presented superconducting setup. In this case, the impact of SC integrated with PMSG is tested with the wind profile given in Figure 5.8. The quick variation in wind speed produces oscillations in PCC voltage as given in Figure 5.9. However, the variation in terminal votlage still remains within 10% of nominal PCC voltage requirement according to IEEE standard. Thus, the power fluction control mode is utilize for this case.

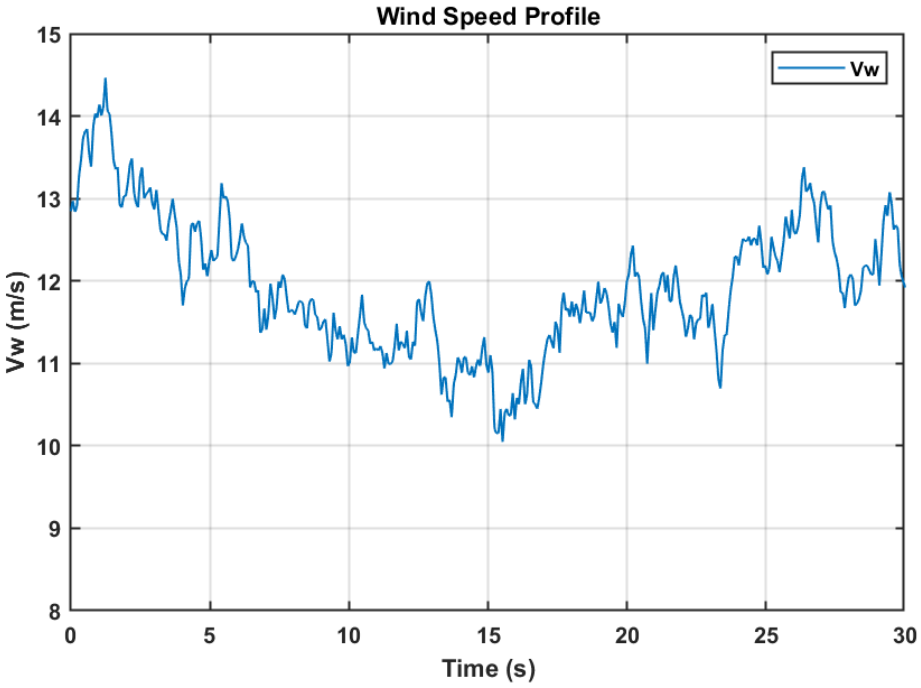

Figure 5.8 Wind Profile for case 2

The active power of the PMSG is fluctuating during wind gust as shown in Figure 5.10. The PMSG power reaches the maximum value of 1.195 p.u due to wind gust. there is variation of 54.3% between max and min peak, w.r.t rated value of PMSG ouput power without SC integration. These fluctuations of output power are reduced to 17.7% with PI based proposed SC control. In this case, proposed FOPI based SC control gives better response of keeping power variations within minimum range as compare to the PI based control and reduces output power fluctuations of PMSG to 15% with respect to rated value.

The voltage at DC link of the PMSG based WECS during wind gust is illustrated in Figure 5.11. The wind gust caused considerable oscillation in DC link upto 10% of

nominal value in case of no SC integrated. The oscillations are slightly reduced in case of PI controller.

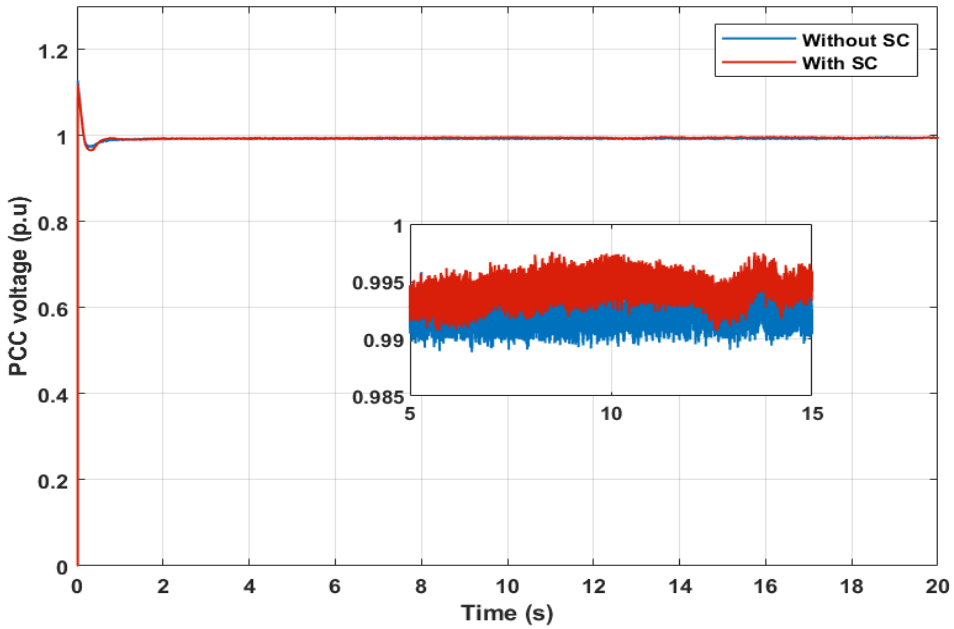

Figure 5.9 PCC voltage during wind gust with and without SC

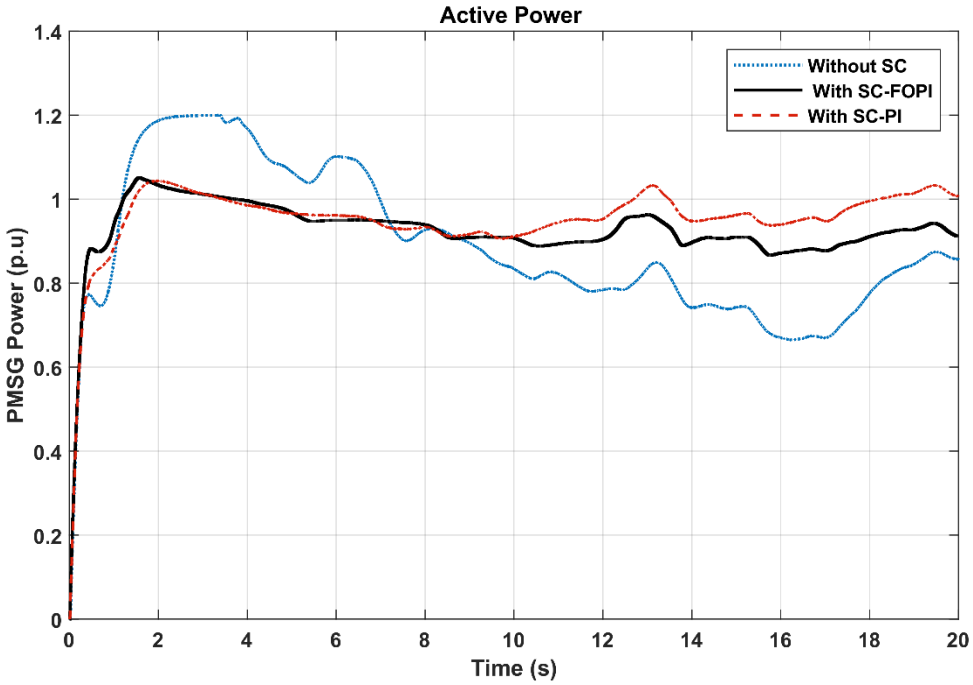

Figure 5.10 PMSG system Power with and without SC

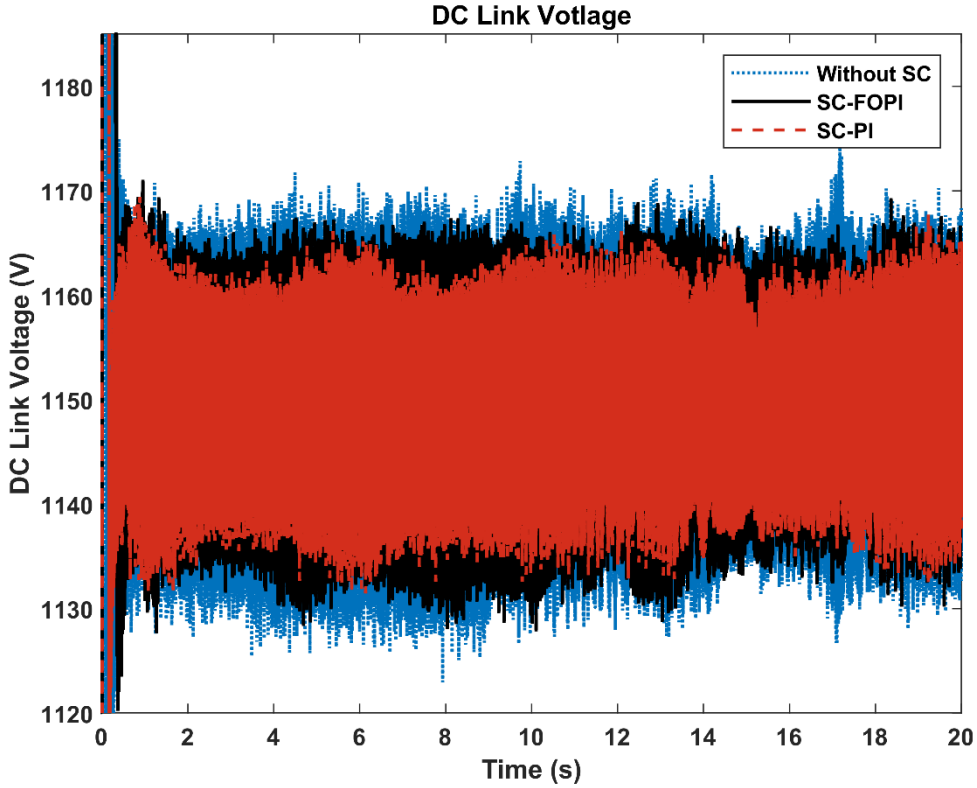

Figure 5.11 DC link voltage during Wind Gust

5.1.4 FRT of PMSG based WECS during grid fault

During grid fault, Wind turbine shaft will experience increased mechanical speed due to transient instability. The high speed and resulted vibrations can have detrimental effect on shaft. Sudden change in speed of WTG causes over currents in the stator winding and overvoltage in the DC-link bus of WECS [8]. Conventional PMSG wind energy systems employ BTB converters to achieve full power control. GSC cannot provide all the generated active power to the grid during grid fault. LVRT is achieved through provision of reactive power to grid by GSC. There is also the rise in voltage at DC link and fluctuation in frequency due to fault. High DC link votlage can damage capacitor of conversion system. The increase acceleration of the generator is caused by the power imbalance of generated power with that of delivered power to the utility grid [9]. DC link voltage rise need to be mitigated to within allowable range to acieve LVRT.

The proposed control of SC is investigated in its ability to provide support to PMSG based WECS during grid faults. In this regard, 3 phase short circuit fault is applied at PCC from 12s to 12.25s. The average value of 12 m/s wind speed is considered for this scenario. Fault will create 100% voltage dip at the PCC. The performace of The SC in

terms of PCC voltage profile against fault is illustrated in Figure 5.12. Without SC, the PCC voltage of the system falls to 0 p.u. The WECS does not follows either of Germany or US code and will be disconnected from the grid against the requirement. PI-SC control recovers the PCC voltage to 0.11p.u which is satisfactory for only germany grid code for continued connection with the grid. The FOPI based control gives a better response with PCC voltage recovered to value 0.4 p.u which is suitable for both Germany and US grid codes. It is satisfactory for FRT of the PMSG based WECS during short circuit fault at PCC according to grid code standards also given in Figure 5.13. The active power of the PMSG during fault with and without SC is illustrated in Figure 5.14. The overshoot of the power is at 1.18 p.u in case of without SC. The active power of the PMSG reduces to 0.42 p.u during grid fault. And during recovery from fault, the output power rises to 1.16 p.u. The highest value of recovered active power during fault is in case of FOPI controlled SC which is at 0.7 p.u. The ouput power goes back to normal value at 14.2s. However, the active power have peak at 1.3 p.u during recovery from fault and take some time to go back to normal value in case of SC-PI.

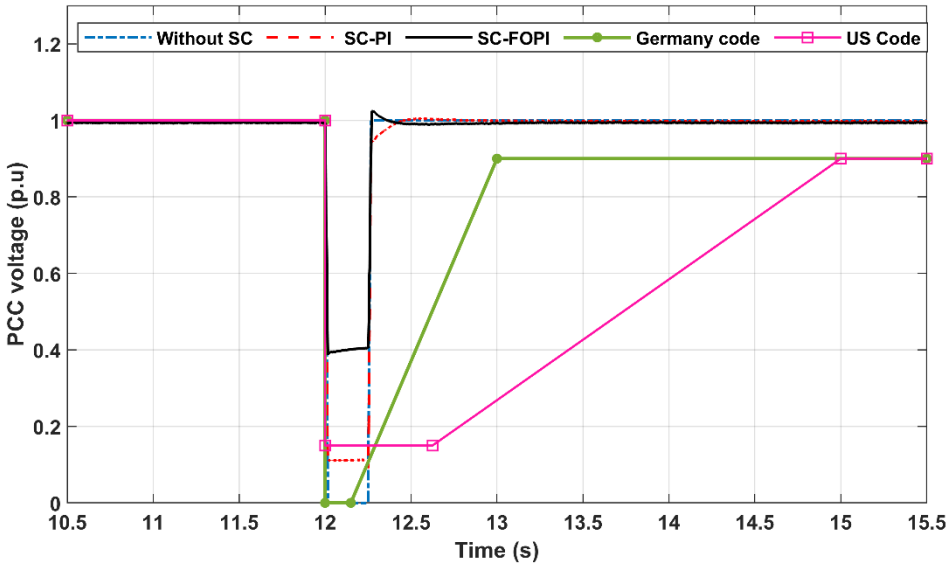

Figure 5.12 PCC voltage during grid fault

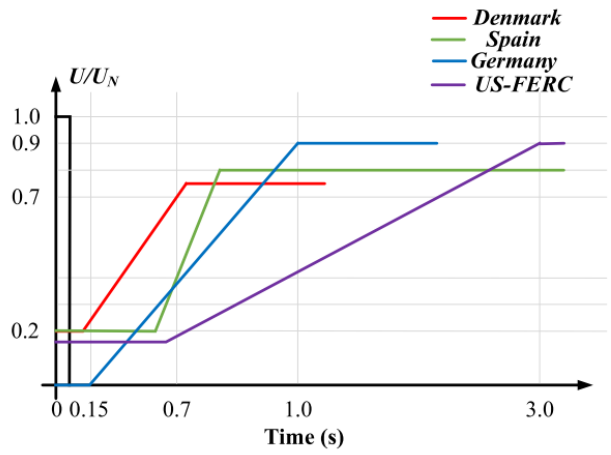

Figure 5.13 Grid codes representation of various countries **[73]**

The behavior of the mechanical speed of the PMSG during grid fault is shown in given in Figure 5.15. The mechanical speed of the generator increases to cover the loss of active power due to fault. The rotor speed of the PMSG increase to 1.138 p.u from normal 1.09 p.u due to grid fault and speed response have oscillations that continue right after 16.5s as depicted in Figure 5.16. The proposed SC-PI reduces the peak in rotor speed to 1.105 p.u. But the response from SC-FOPI is much better with peak at 1.1 p.u and fast normalization (reduction of oscillations) of speed 15s. The corresponding electromagnetic torque Te is given in Figure 5.17. Te oscillations are removed and response is cleaned in case of SC-FOPI as depicted in Figure 5.18.

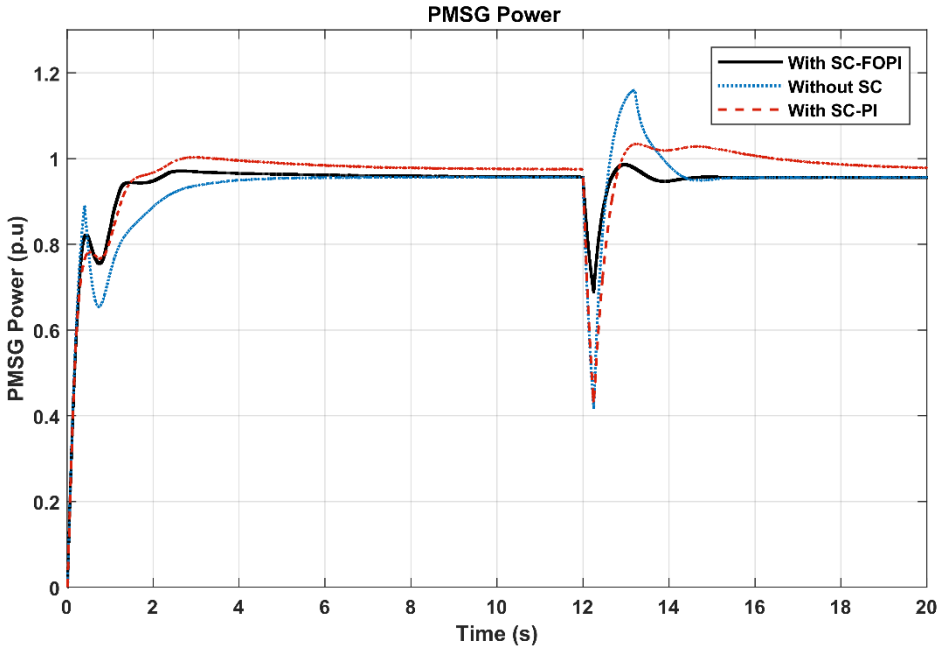

Figure 5.14 PMSG System Active Power during 3 phase Short Circuit fault

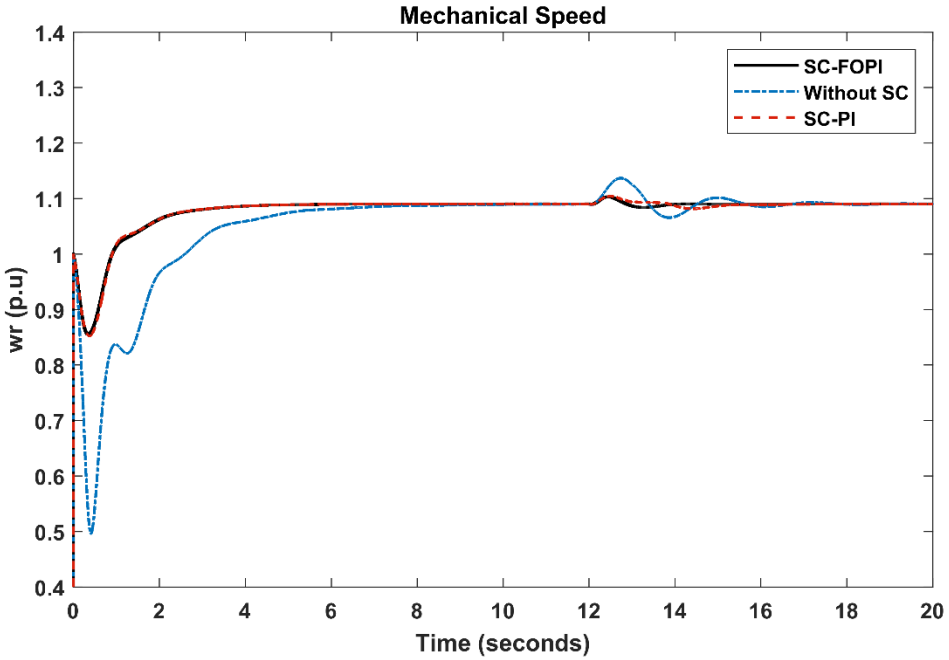

Figure 5.15 Mechanical Speed of PMSG

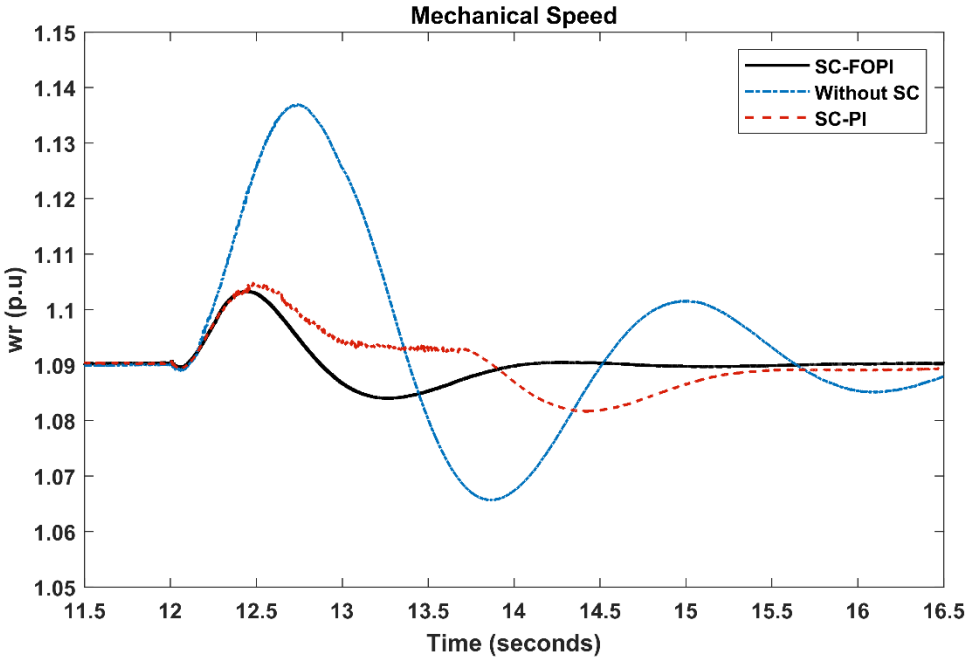

Figure 5.16 Rotor Speed during Grid Fault

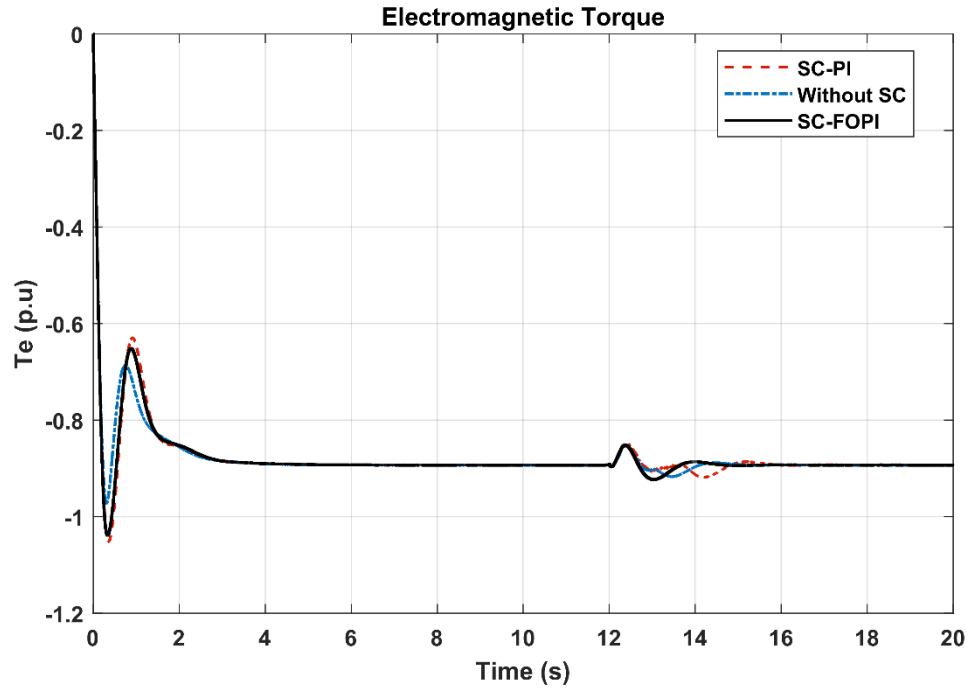

Figure 5.17 Electromagnetic Torque of PMSG

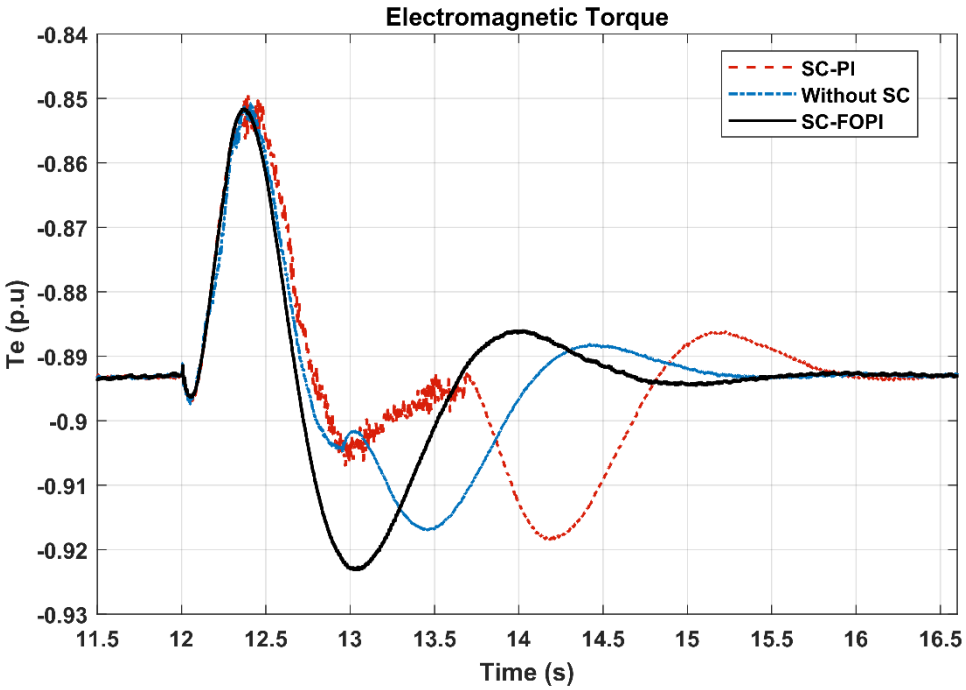

Figure 5.18 Te of PMSG during FRT control mode

5.1.4.1 Mitigation of voltage Rise at DC link During Grid Fault

The voltage at the DC link of WECS rises during grid faults, due to the mismatch between power generated by generator and delived power to the grid. And GSC cannot provide the generated active power to the grid. Also the voltage rise at DC link is harmful for the capacitor at the link. The use of SC at DC link to reduce the voltage rise as a result of faults is presented in [74], [116]. The SC can effectively store the stranded power to mitigate voltage rise at DC link within suitable values. The voltage profile at DC link of the WECS integrated with SC is given in Figure 5.19.

It can be observed that during grid fault, the voltage at DC link rises to very high value of 7.3 p.u. The integration of SC with WECS effectively reduced the voltage rise and bring it within acceptable range. The PI based SC unit reduces the voltage rise at DC link to 1.94 p.u as depicted in Figure 5.20. But the FOPI based SC topology effectively mitigate the voltage rise to 1.3 p.u of rated value and improving the LVRT of the PMSG based WECS. Thus, representing the robust charging in case of SC-FOPI as compare to SC-PI controller. The peak values at the start of simulation are due to the under study WECS response. And as the voltage at the PCC is more than 0.9 p.u at the start of the simulation. So they are covered by the power fluctuation mode of the proposed control. Therefore, peaks at the start are also being reduced by the proposed SC unit.

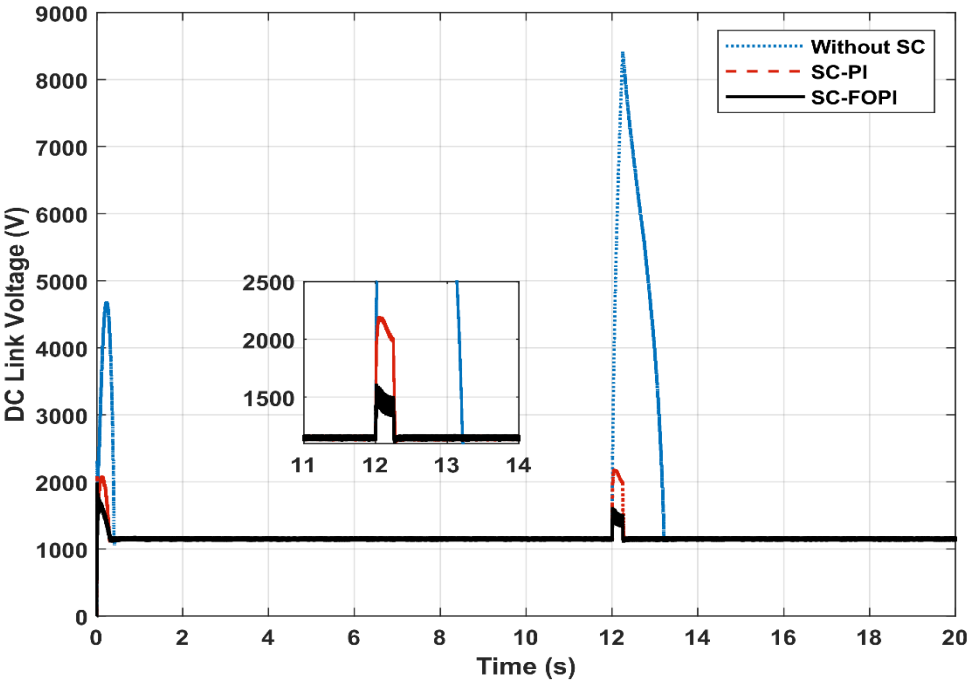

Figure 5.19 DC link voltage minimization with proposed SC unit

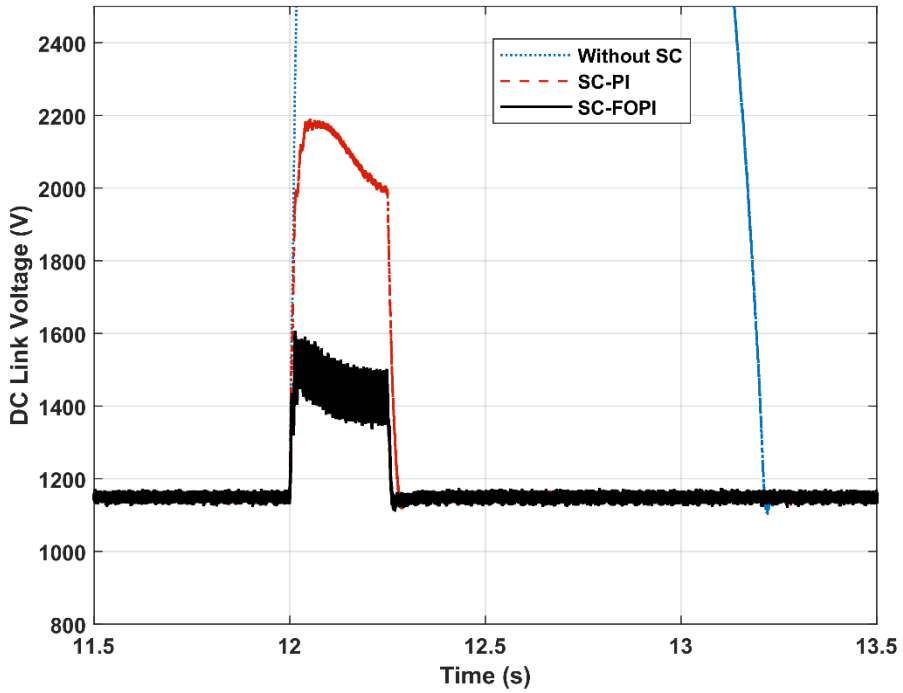

Figure 5.20 DC link Voltage during Grid Fault

5.1.4.2 SC Response During Grid Fault

The superconducting coil SC charging and discharging depend upon the duty cycle D of the chopper. When the value of D is greater than 0.5, the charing of SC happens. For value of D < 0.5, the SC goes into discharging mode. The SC current during grid Fault is given in Figure 5.21. During normal operation, the coil current almost remains constant. When faults is applied at 12s, FRT mode of the proposed technique is activated because PCC voltage goes below 0.9 p.u. The DC link voltage becomes greater than rated value which produces the duty cycle of > 0.5. The superconducting coil absorbs the extra energy generated by the PMSG. The avergage voltage across the SC during this instance is positive due to positive rate of change of SC current. When the fault clears at 12.25s, the stored energy is discharged back to the system for the recovery of the active power of the PMSG as illustrated in Figure 5.21(b). The negative slope of SC produces negative value of average voltage across SC during the recovery from the fault as given in Figure 5.22.

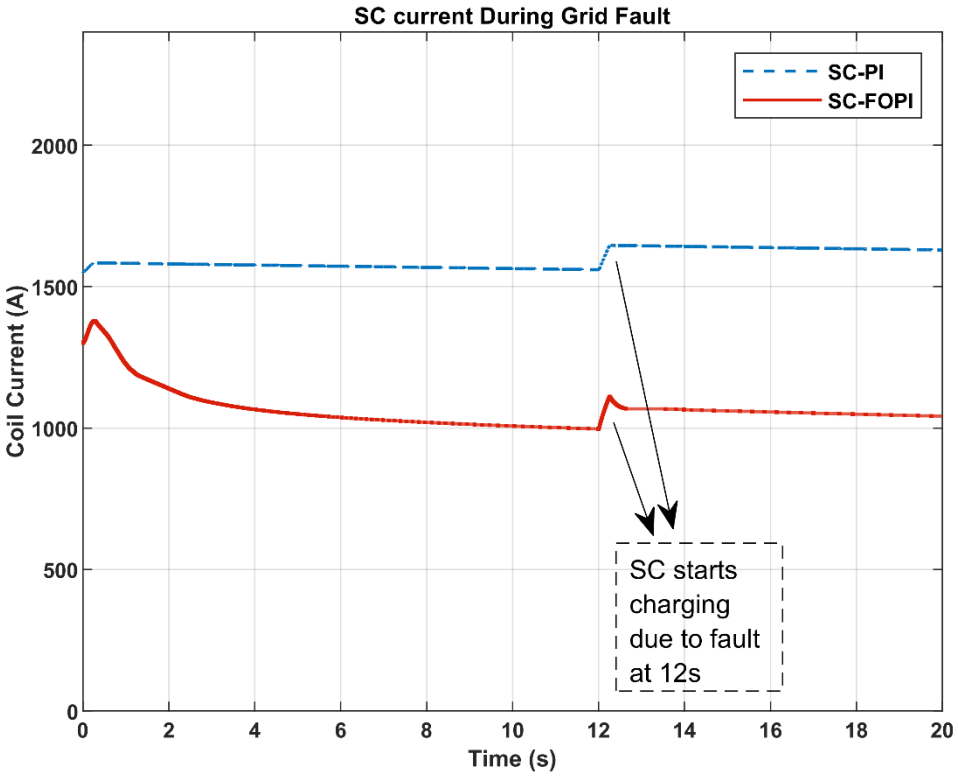

(a)

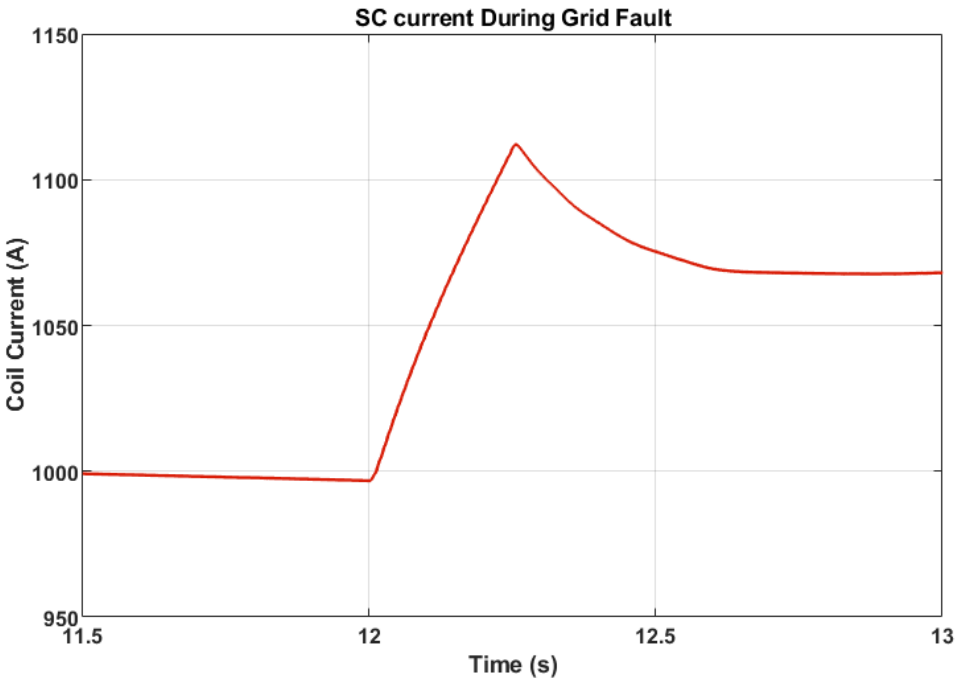

(b)

Figure 5.21 SC Current during Grid Fault (a) Response of SC-PI and SC-FOPI (b) SC Current in case of SC-FOPI

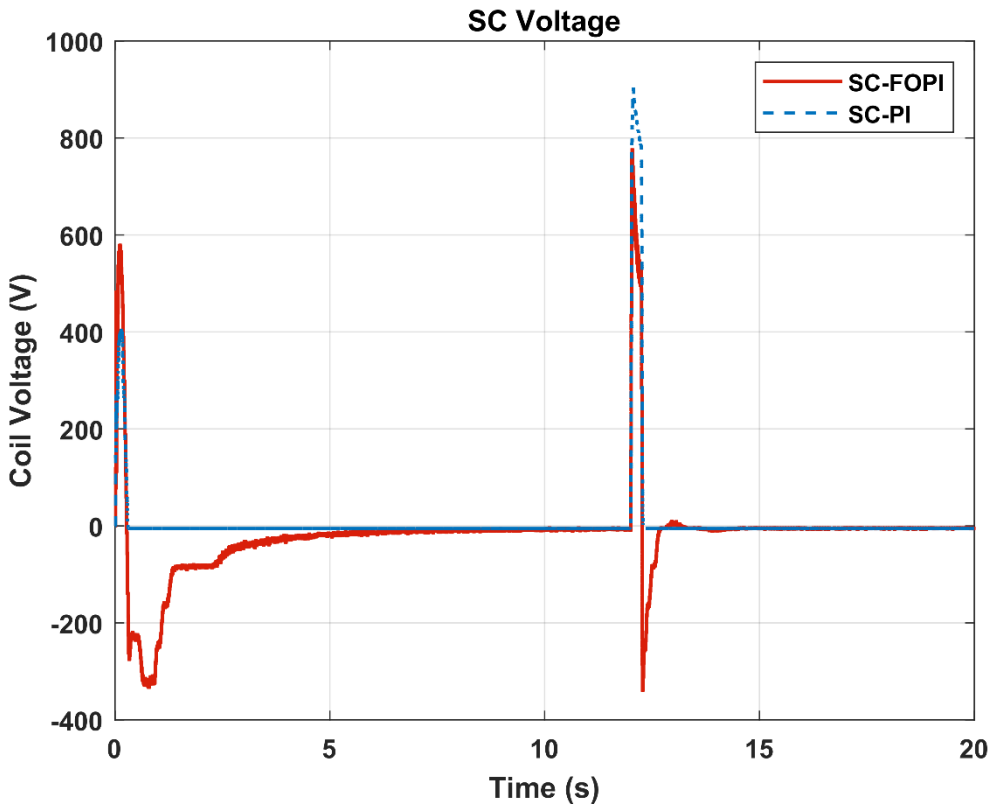

Figure 5.22 SC voltage during Grid Fault

The performance of SC is better with FOPI as compare to PI considering their response during short crcuit grid fault. Table 5.2 shows the Comparison of PI and FOPI based control of SC.

Table 5.3 Comparison of FOPI with PI during short circuit fault at PCC

Parameter value	No SC	SC-PI	SC-FOPI
PCC voltage (p.u)	0	0.15	0.4
PMSG active power (p.u)	0.42	0.437	0.7
Mechincal Speed (p.u)	1.14	1.12	1.11
Electromagnetic Torque (p.u)	0.85	0.845	0.84
DC Link votlage (p.u)	7.3	1.94	1.3

Chapter

6

Conclusion and Future Works

6.1 Conclusion

In this work, extensive investigation of application of SC in form of SMES for performance improvement of PMSG based WECS is done. It is shown in literature that the major two issues with any WECS are the output power fluctuations and FRT capability. PMSG based WECS being variable speed system suffers from output power fluctuations due to unpredictable variation of wind in form of wind gusts. Also WECS should be capable of keeping connection with the grid during grid faults by following grid codes. Numerous studies have been presented to tackle these issues of WECS by utilizing the energy storage based methods or coordinated control methods. Recently, among other storage technologies, Superconductors have gain popularity in power quality, stability of power systems. SMES can store and release power in short time even in case of small storage capacity. In addition to power absorb or discharge ability, SMES can also provide reactive power, which in turn makes it suitable for mitigation of voltage fluctuation in grid system. SMES unit have highest efficiency, which is 90-99% as compare to other storage technologies. The reason behind high efficiency of SMES due to minimal coil resistance and zero frictional losses. However, the economical factor of SC is the main concern. SMES has been used for performance improvement of PMSG in many studies either as sole functioning device or in combination with SFCL. But the size of the SC is not given more emphasis. In this thesis, integration of SC is employed for both issues of power fluctuation and FRT capability for PMSG based WECS. The integration of SC is done through two quarant DC chopper at the DC link of PMSG wind system. In addition, the presented control of SC utilizes the FOPI controller as it performs better againt transient disturbance as compare to conventional PI controller. The issue of size of SC is tackled in this work by using a Harmony search algorithm for finding parameters of FOPI/PI and SC parameters. The proposed system in investigated for different cases to analyz the performance of FOPI and PI based SC proposed control. In case of sudden change in wind speed at a specific time, the FOPI based control reduces power fluctuations peak to 1.027 p.u and PI based control gives peak value of 1.04 p.u as compare to 1.199 p.u value without SC unit integration. In case of wind gust, there is variation of 54.3% between max and min peak, w.r.t rated value of PMSG ouput power without SC integration. These fluctuations of output power are reduced to 17.7% with PI based proposed SC control. In this case, proposed FOPI based SC control gives better

response of keeping power variations within minimum range as compare to the PI based control and reduces output power fluctuations of PMSG to 15% with respect to rated value. In case of grid fault, performance of porposed control can be analyzed particularly from values of terminal voltage, output active power, rotor mechanical speed and voltage profile at DC link voltage as given in table. During grid fault, PCC voltage of PMSG based WECS experiences voltage sage of 100% without SC unit integration. The FOPI based SC control gives better response as compare to PI SC control by recovering PCC voltage to 40% with respect to 11% respectively. Similary, the dip in output power of PMSG is restored to 0.69 p.u in case of FOPI-SC and 0.435 p.u in case of PI-SC as compare to dip of 0.42 p.u without SC unit during grid fault. In addition, the mitigation of voltage rise at DC link is necessary for LVRT of WECS and in this case, there is a 7.3 p.u rise in DC link voltage during grid fault. Consequently, the comparison of voltage profiles at DC link during grid fault with and without SC unit shows that FOPI-SC effectively reduces the DC link voltage rise to 1.3 p.u as compare to 1.94 p.u in case of PI-SC control. From above comparison, It can be deduced that the performance FOPI based proposed SC control is much superior to that of PI based SC control.

Hence, the constribution and advantages of proposed work can be summarized as:

1. The proposed application of SC effectively provide multifunction benefits in terms of output power smoothing, power quality improvement and enhancement LVRT capability of PMSG based WECS.
2. The proposed work provide economical merits of SC as HS effectively optimizes the SC parameters to tackle cost converns.
3. Simulation results show that FOPI based proposed SC control provides better performance as compare to PI based SC control in terms of power fluctuations mitigation and LVRT improvments.
4. As compare to previous techniques that utilize external FACTS or modification in traditional controls of PMSG based WECS, The proposed approach is flexible and can be applied to both existing and new installations.

6.2 Future Works

The research work presented in this thesis highlighted the application of superconductors in PMSG based WECS in terms of better power quality and stable operation. The cost of SC is major issue in its application. The optimal integration of SC through more robust controller in FOPI in this thesis have presented an cost effective and better solution for performance improvement of PMSG based WECS. The optimized combined use of proposed strategy with Superconductor Fault Current Limiters (SFCL) can be researched to further enhance the performance and as an cost effective solution. Also the proposed technique can be investigated in coordination with modified converter controls to reduce strain on capacity of SC along with better control.

References

[1] R. E. N. Members, *Renewables 2019 global status report 2019*. 2019.

[2] GWEC, "Global wind energy council report 2018," *Wind Glob. Counc. Energy*, no. April, pp. 1–61, 2019.

[3] H. Polinder, F. F. A. Van Der Pijl, G. De Vilder, and P. J. Tavner, "Comparison of Direct-Drive and Geared Generator Concepts for Wind Turbines," vol. 21, no. 3, pp. 725–733, 2006.

[4] P. Ejnar, N. Antonio, L. Enrico, H. Donovan, and R. Kristoffersen, *Risø-R-Report*. 2009.

[5] A. M. Howlader, N. Urasaki, A. Yona, T. Senjyu, and A. Y. Saber, "A review of output power smoothing methods for wind energy conversion systems," *Renew. Sustain. Energy Rev.*, vol. 26, pp. 135–146, Oct. 2013, doi: 10.1016/j.rser.2013.05.028.

[6] Y. Li, Z. Xu, and K. P. Wong, "Transactions on Power Systems Advanced Control Strategies of PMSG - Based Wind Turbines for System Inertia Support," vol. 8950, no. c, 2016, doi: 10.1109/TPWRS.2016.2616171.

[7] J. I. Yoo, Y. C. Kang, D. Yang, K. Kim, and J. Park, "Power Smoothing of a Variable-Speed Wind Turbine Generator Based on a Two-Valued Control Gain," *IEEE Trans. Sustain. Energy*, vol. 11, no. 4, pp. 2765–2774, Oct. 2020, doi: 10.1109/TSTE.2020.2975061.

[8] H. M. Abdel-Mageed, "Simulation of the Different Transmission Line Faults for a Grid Connected Wind Farm with Different Types of Generators," *Int. J. Electr. Comput. Eng.*, vol. 2, pp. 35–45, 2011, doi: http://dx.doi.org/10.11591/ijece.v2i1.113.

[9] R. Mittal, K. S. Sandhu, and D. K. Jain, "LOW VOLTAGE RIDE-THROUGH (LVRT) OF GRID INTERFACED," vol. 4, no. 5, pp. 73–83, 2009.

[10] Li Yan, Chi Yongning, Wang Zhen, Wei Linjun, and Liu Chao, "Study on LVRT capability of D-PMSG based wind turbine," in *2011 IEEE Power Engineering and Automation Conference*, 2011, pp. 154–157, doi: 10.1109/PEAM.2011.6134824.

[11] V. Sekhar and K. Ravi, “Low-voltage ride-through capability enhancement of wind energy conversion system using an ant-lion recurrent neural network controller,” *Meas. Control*, vol. 52, no. 7–8, pp. 1048–1062, Sep. 2019, doi: 10.1177/0020294019858102.

[12] M. Molinas, J. A. Suul, and T. Undeland, “Low Voltage Ride Through of Wind Farms With Cage Generators : STATCOM Versus SVC,” vol. 23, no. 3, pp. 1104–1117, 2008.

[13] M. Ding and Q. Zhu, “Equivalent modeling of PMSG-based wind power plants considering LVRT capabilities: electromechanical transients in power systems,” *Springerplus*, vol. 5, no. 1, p. 2037, Dec. 2016, doi: 10.1186/s40064-016-3700-5.

[14] S. W. Mohod and M. V. Aware, “A STATCOM-Control Scheme for Grid Connected Wind Energy System for Power Quality Improvement,” *IEEE Syst. J.*, vol. 4, no. 3, pp. 346–352, Sep. 2010, doi: 10.1109/JSYST.2010.2052943.

[15] C. Wessels, F. Gebhardt, and F. W. Fuchs, “Fault Ride-Through of a DFIG Wind Turbine Using a Dynamic Voltage Restorer During Symmetrical and Asymmetrical Grid Faults,” *IEEE Trans. Power Electron.*, vol. 26, no. 3, pp. 807–815, Mar. 2011, doi: 10.1109/TPEL.2010.2099133.

[16] Ã. Bolund, H. Bernhoff, and M. Leijon, “Flywheel energy and power storage systems,” vol. 11, pp. 235–258, 2007, doi: 10.1016/j.rser.2005.01.004.

[17] C. Abbey and G. Joos, “Supercapacitor Energy Storage for Wind Energy Applications,” *IEEE Trans. Ind. Appl.*, vol. 43, no. 3, pp. 769–776, 2007, doi: 10.1109/TIA.2007.895768.

[18] T. H. Nguyen and D. Lee, “Ride-Through Technique for PMSG Wind Turbines using Energy Storage Systems,” pp. 733–738.

[19] P. Taylor, M. N. Eskander, and S. I. Amer, “Mitigation of Voltage Dips and Swells in Grid-connected Wind Energy Conversion Systems Mitigation of Voltage Dips and Swells in Grid- connected Wind Energy Conversion Systems,” no. March 2015, pp. 37–41, 2014, doi: 10.4103/0377-2063.92267.

[20] P. MUKHERJEE and V. V. RAO, “Superconducting magnetic energy storage for stabilizing grid integrated with wind power generation systems,” *J. Mod. Power Syst. Clean Energy*, vol. 7, no. 2, pp. 400–411, Mar. 2019, doi: 10.1007/s40565-018-0460-y.

[21] X. Luo, J. Wang, M. Dooner, and J. Clarke, “Overview of current development

in electrical energy storage technologies and the application potential in power system operation," *Appl. Energy*, vol. 137, pp. 511–536, Jan. 2015, doi: 10.1016/j.apenergy.2014.09.081.

[22] S. Kim, S. Member, B. Kang, S. Member, S. Bae, and S. Member, "Application of SMES and Grid Code Compliance to Wind / Photovoltaic Generation System," no. c, pp. 1–4, 2012.

[23] M. Y. Worku and M. A. Abido, "Fault Ride-Through and Power Smoothing Control of PMSG-Based Wind Generation Using Supercapacitor Energy Storage System," *Arab. J. Sci. Eng.*, vol. 44, no. 3, pp. 2067–2078, Mar. 2019, doi: 10.1007/s13369-018-3284-1.

[24] M. Y. Khamaira, A. Abu-Siada, and S. Islam, "Application of high temperature superconductor to improve the dynamic performance of WECS," in *2015 IEEE Power & Energy Society General Meeting*, 2015, pp. 1–6, doi: 10.1109/PESGM.2015.7285695.

[25] M. E. Elshiekh, D. E. A. Mansour, M. Zhang, W. Yuan, H. Wang, and M. Xie, "New technique for using SMES to limit fault currents in wind farm power systems," *IEEE Trans. Appl. Supercond.*, vol. 28, no. 4, pp. 1–5, 2018, doi: 10.1109/TASC.2018.2810512.

[26] P. Taylor *et al.*, "Electric Power Components and Systems Small Wind Energy Systems Small Wind Energy Systems," no. July 2015, doi: 10.1080/15325008.2015.1029057.

[27] P. W. Carlin and A. S. Laxson, "The History and State of the Art of Variable-Speed Wind Turbine Technology The History and State of the Art of Variable-Speed Wind Turbine Technology," no. February, 2001.

[28] J. M. Carrasco *et al.*, "Power Electronic Systems for the Grid Integration of Renewable Energy Sources : a Survey," pp. 1–14, 2000.

[29] A. D. Hansen and L. H. Hansen, "Wind turbine concept market penetration over 10 years (1995–2004)," *Wind Energy*, vol. 10, no. 1, pp. 81–97, Jan. 2007, doi: 10.1002/we.210.

[30] T. Ackermann, *Wind Power in Power Systems*. Chichester, UK: John Wiley & Sons, Ltd, 2012.

[31] M. R. Khadraoui and M. Elleuch, "Comparison between OptiSlip and Fixed Speed wind energy conversion systems," in *2008 5th International Multi-Conference on Systems, Signals and Devices*, 2008, pp. 1–6, doi:

10.1109/SSD.2008.4632796.

[32] L. Xu and P. Cartwright, “Direct Active and Reactive Power Control of DFIG for Wind Energy Generation,” *IEEE Trans. Energy Convers.*, vol. 21, no. 3, pp. 750–758, Sep. 2006, doi: 10.1109/TEC.2006.875472.

[33] I. Introduction, “Wind Power Interconnection into the Power System :,” 2009.

[34] J. G. Slootweg, S. W. H. De Haan, and H. Polinder, “General Model for Representing Variable Speed Wind Turbines in Power System Dynamics Simulations,” vol. 18, no. 1, pp. 144–151, 2003.

[35] N. Goudarzi and W. D. Zhu, “A review on the development of wind turbine generators across the world,” *Int. J. Dyn. Control*, vol. 1, no. 2, pp. 192–202, Jun. 2013, doi: 10.1007/s40435-013-0016-y.

[36] N. S. Hasan, M. Y. Hassan, M. S. Majid, and H. A. Rahman, “Review of storage schemes for wind energy systems,” *Renew. Sustain. Energy Rev.*, vol. 21, pp. 237–247, May 2013, doi: 10.1016/j.rser.2012.12.028.

[37] D. Lamsal, V. Sreeram, Y. Mishra, and D. Kumar, “Output power smoothing control approaches for wind and photovoltaic generation systems: A review,” *Renew. Sustain. Energy Rev.*, vol. 113, no. May, p. 109245, Oct. 2019, doi: 10.1016/j.rser.2019.109245.

[38] S. D. G. Jayasinghe, S. Member, D. M. Vilathgamuwa, and S. Member, “Flying Supercapacitors as Power Smoothing Elements in Wind Generation,” vol. 60, no. 7, pp. 2909–2918, 2013.

[39] H. Pham, J. Bourgeot, and M. Benbouzid, “Power Smoothing Control and Low-Voltage Ride-Through Enhancement of a 5-phase PMSG-based Marine Tidal Turbine using a Supercapacitor Energy Storage System,” no. 2.

[40] A. Pratap, T. Senju, A. Yona, N. Urasaki, and T. Funabashi, “A Hybrid Control Method for Output Power Smoothing of a PMSG-Based WECS,” *Int. J. Emerg. Electr. Power Syst.*, vol. 12, no. 6, Feb. 2012, doi: 10.1515/1553-779X.2756.

[41] M. A. Chowdhury, N. Hosseinzadeh, and W. X. Shen, “Smoothing wind power fl uctuations by fuzzy logic pitch angle controller,” *Renew. Energy*, vol. 38, no. 1, pp. 224–233, 2012, doi: 10.1016/j.renene.2011.07.034.

[42] Y. Zhu and Y. Gao, “Power Smoothing Control for the PMSG WECS Based on the Kinetic Energy,” *2018 13th IEEE Conf. Ind. Electron. Appl.*, no. 3, pp. 1068–1072, 2018.

[43] X. Zhao, Z. Yan, Y. Xue, and X. Zhang, “Wind Power Smoothing by Controlling

the Inertial Energy of Turbines With Optimized Energy Yield," *IEEE Access*, vol. 5, pp. 23374–23382, 2017, doi: 10.1109/ACCESS.2017.2757929.

[44] S. G. Varzaneh, G. B. Gharehpetian, and M. Abedi, "Output power smoothing of variable speed wind farms using rotor-inertia," *Electr. Power Syst. Res.*, vol. 116, pp. 208–217, Nov. 2014, doi: 10.1016/j.epsr.2014.06.006.

[45] A. Uehara *et al.*, "A Coordinated Control Method to Smooth Wind Power Fluctuations of a PMSG-Based WECS," *IEEE Trans. Energy Convers.*, vol. 26, no. 2, pp. 550–558, Jun. 2011, doi: 10.1109/TEC.2011.2107912.

[46] X. Lyu, J. Zhao, Y. Jia, Z. Xu, and K. Po Wong, "Coordinated Control Strategies of PMSG-Based Wind Turbine for Smoothing Power Fluctuations," *IEEE Trans. Power Syst.*, vol. 34, no. 1, pp. 391–401, Jan. 2019, doi: 10.1109/TPWRS.2018.2866629.

[47] M. Nasiri, J. Milimonfared, and S. H. Fathi, "A review of low-voltage ride-through enhancement methods for permanent magnet synchronous generator based wind turbines," *Renew. Sustain. Energy Rev.*, vol. 47, pp. 399–415, 2015, doi: 10.1016/j.rser.2015.03.079.

[48] Z. Ge, Y. Yiyun, X. Jing, G. Like, and X. Yuanyuan, "Coordinated Low Voltage Ride through strategies for Permanent Magnet Direct Drive Synchronous Generators," vol. 09003, 2016.

[49] C. N. Kendeck and A. K. Raji, "Control of Permanent Magnet Synchronous Generator based wind turbine and Fault Ride-through improvement during Faulty Grid Conditions," no. 1, 1906.

[50] M. Jahanpour-dehkordi, S. Vaez-zadeh, S. Member, and J. Mohammadi, "Development of a Combined Control System to Improve Performance of a PMSG Based Wind Energy Conversion System under Normal and Grid Fault Conditions," *IEEE Trans. Energy Convers.*, vol. PP, no. c, p. 1, 2019, doi: 10.1109/TEC.2019.2912080.

[51] C. Kim, Y. Gui, C. C. Chung, K. Yonghao, C. Kim, and K. Yonghao, "ScienceDirect Coordinated Control Control for," *IFAC-PapersOnLine*, vol. 50, no. 1, pp. 8758–8763, doi: 10.1016/j.ifacol.2017.08.1733.

[52] T. H. Nguyen, T. H. Phuong, T. H. Nguyen, S. St, and P. T. H. Nguyen, "ScienceDirect Wind Through in PMSG Wind Turbines Through," vol. 28, pp. 672–677, 2018, doi: 10.1016/j.ifacol.2018.11.782.

[53] D. Jeong, C. Kim, Y. Gui, and C. C. Chung, "Sliding mode control for LVRT of

a PMSG wind turbine using stored energy in rotor inertia," in *2016 IEEE Power and Energy Society General Meeting (PESGM)*, 2016, pp. 1–5, doi: 10.1109/PESGM.2016.7741404.

[54] H. Geng, S. Member, L. Liu, R. Li, and S. Member, "Synchronization and Reactive Current Support of PMSG based Wind Farm during Severe Grid Fault," vol. 3029, no. c, 2018, doi: 10.1109/TSTE.2018.2799197.

[55] M. Nasiri and R. Mohammadi, "Peak Current Limitation for Grid Side Inverter by Limited Active Power in PMSG-based Wind Turbines during Different Grid Faults," vol. 3029, no. c, 2016, doi: 10.1109/TSTE.2016.2578042.

[56] R. Vijayapriya, P. Raja, and M. P. Selvan, "A Modified Active Power Control Scheme for Enhanced Operation of PMSG Based WGs," vol. 3029, no. c, 2017, doi: 10.1109/TSTE.2017.2751744.

[57] M. A. Soliman, H. M. Hasanien, S. Member, H. Z. Azazi, and S. A. Mahmoud, "An Adaptive Fuzzy Logic Control Strategy for Performance Enhancement of a Grid - Connected PMSG - Based Wind Turbine," vol. 3203, no. c, 2018, doi: 10.1109/TII.2018.2875922.

[58] A. M. S. Yunus and M. Saini, "Overview of SMES units application on smart grid systems," in *2016 International Seminar on Intelligent Technology and Its Applications (ISITIA)*, 2016, vol. 60, pp. 465–470, doi: 10.1109/ISITIA.2016.7828705.

[59] M. N. Musarrat, M. R. Islam, K. M. Muttaqi, and D. Sutanto, "Enhanced Frequency Support From a PMSG-Based Wind Energy Conversion System Integrated With a High Temperature SMES in Standalone Power Supply Systems," *IEEE Trans. Appl. Supercond.*, vol. 29, no. 2, pp. 1–6, Mar. 2019, doi: 10.1109/TASC.2018.2882429.

[60] W. Guo *et al.*, "Development of a 1-MVA/1-MJ Superconducting Fault Current Limiter–Magnetic Energy Storage System for LVRT Capability Enhancement and Wind Power Smoothing," *IEEE Trans. Appl. Supercond.*, vol. 28, no. 4, pp. 1–5, Jun. 2018, doi: 10.1109/TASC.2018.2800000.

[61] S. Nagaya *et al.*, "Development of MJ-Class HTS SMES for Bridging Instantaneous Voltage Dips," *IEEE Trans. Appiled Supercond.*, vol. 14, no. 2, pp. 770–773, Jun. 2004, doi: 10.1109/TASC.2004.830105.

[62] Myungjin Park *et al.*, "Conceptual Design of HTS Magnet for a 5 MJ Class SMES," *IEEE Trans. Appl. Supercond.*, vol. 18, no. 2, pp. 750–753, Jun. 2008,

doi: 10.1109/TASC.2008.922533.

[63] J. Zhu, M. Qiu, B. Wei, H. Zhang, X. Lai, and W. Yuan, “Design, dynamic simulation and construction of a hybrid HTS SMES (high-temperature superconducting magnetic energy storage systems) for Chinese power grid,” *Energy*, vol. 51, pp. 184–192, Mar. 2013, doi: 10.1016/j.energy.2012.09.044.

[64] A. Morandi, A. Fiorillo, S. Pullano, and P. L. Ribani, “Development of a Small Cryogen-Free MgB 2 Test Coil for SMES Application,” *IEEE Trans. Appl. Supercond.*, vol. 27, no. 4, pp. 1–4, Jun. 2017, doi: 10.1109/TASC.2017.2653202.

[65] J. Zhu *et al.*, “Experimental demonstration and application planning of high temperature superconducting energy storage system for renewable power grids,” *Appl. Energy*, vol. 137, pp. 692–698, Jan. 2015, doi: 10.1016/j.apenergy.2014.07.022.

[66] M. R. I. Sheikh, S. M. Muyeen, R. Takahashi, T. Murata, and J. Tamura, “Minimization of fluctuations of output power and terminal voltage of wind generator by using STATCOM/SMES,” in *2009 IEEE Bucharest PowerTech*, 2009, pp. 1–6, doi: 10.1109/PTC.2009.5282099.

[67] G. H. Kim *et al.*, “A novel HTS SMES application in combination with a permanent magnet synchronous generator type wind power generation system,” *Phys. C Supercond. its Appl.*, vol. 471, no. 21–22, pp. 1413–1418, Nov. 2011, doi: 10.1016/j.physc.2011.05.206.

[68] M. R. I. Sheikh, S. M. Muyeen, R. Takahashi, and J. Tamura, “Smoothing control of wind generator output fluctuations by PWM voltage source converter and chopper controlled SMES,” *Eur. Trans. Electr. Power*, vol. 21, no. 1, pp. 680–697, Jan. 2011, doi: 10.1002/etep.469.

[69] W. Guo, L. Xiao, and S. Dai, “Enhancing low-voltage ride-through capability and smoothing output power of DFIG with a superconducting fault-current limiter-magnetic energy storage system,” *IEEE Trans. Energy Convers.*, vol. 27, no. 2, pp. 277–295, 2012, doi: 10.1109/TEC.2012.2187654.

[70] A. H. M. A. Rahim and M. H. Khan, “An adaptive optimum SMES controller for a PMSG wind generation system,” in *2013 IEEE Power & Energy Society General Meeting*, 2013, pp. 1–5, doi: 10.1109/PESMG.2013.6672187.

[71] H. M. Hasanien, “A Set-Membership Affine Projection Algorithm-Based Adaptive-Controlled SMES Units for Wind Farms Output Power Smoothing,”

IEEE Trans. Sustain. Energy, vol. 5, no. 4, pp. 1226–1233, Oct. 2014, doi: 10.1109/TSTE.2014.2340471.

[72] A. R. Ma and Y. J. Huang, "The Power Smoothing Control of PMSG Based on Superconducting Magnetic Energy Storage," *Adv. Mater. Res.*, vol. 898, pp. 493–496, Feb. 2014, doi: 10.4028/www.scientific.net/AMR.898.493.

[73] L. Chen, G. Li, H. Chen, and L. H. Koh, "Combined Use of SFCL and SMES for Augmenting FRT Performance and Smoothing Output Power of PMSG Based Wind Turbine," *2018 Asian Conf. Energy, Power Transp. Electrif. ACEPT 2018*, no. 51507117, pp. 1–5, 2019, doi: 10.1109/ACEPT.2018.8610758.

[74] C. Huang, X. Y. Xiao, Z. Zheng, and Y. Wang, "Cooperative Control of SFCL and SMES for Protecting PMSG-Based WTGs under Grid Faults," *IEEE Trans. Appl. Supercond.*, vol. 29, no. 2, pp. 8–13, 2019, doi: 10.1109/TASC.2019.2891908.

[75] L. Chen *et al.*, "Combined use of a resistive sfcl and dc-link regulation of a smes for frt enhancement of a dfig wind turbine under different faults," *IEEE Trans. Appl. Supercond.*, vol. 29, no. 2, p. 1, 2019, doi: 10.1109/TASC.2018.2881988.

[76] I. Ngamroo, "Optimization of SMES-FCL for Augmenting FRT Performance and Smoothing Output Power of Grid-Connected DFIG Wind Turbine," *IEEE Trans. Appl. Supercond.*, vol. 26, no. 7, pp. 1–5, Oct. 2016, doi: 10.1109/TASC.2016.2592945.

[77] T. Karaipoom and I. Ngamroo, "Optimal Superconducting Coil Integrated Into DFIG Wind Turbine for Fault Ride Through Capability Enhancement and Output Power Fluctuation Suppression," *IEEE Trans. Sustain. Energy*, vol. 6, no. 1, pp. 28–42, Jan. 2015, doi: 10.1109/TSTE.2014.2355423.

[78] M. H. Qais, H. M. Hasanien, S. Alghuwainem, and M. A. Elgendy, "Output Power Smoothing of Grid-Tied PMSG-Based Variable Speed Wind Turbine Using Optimal Controlled SMES," *2019 54th Int. Univ. Power Eng. Conf. UPEC 2019 - Proc.*, pp. 1–6, 2019, doi: 10.1109/UPEC.2019.8893530.

[79] H. M. Nguyen and D. S. Naidu, "Advanced Control Strategies for Wind Energy Systems : An Overview," in *IEEE/PES Power Systems Conference and Exposition*, 2011, no. March, pp. 20–23, doi: 10.1109/PSCE.2011.5772514.

[80] S. Mathew, *Wind Energy*. Berlin, Heidelberg: Springer Berlin Heidelberg, 2006.

[81] H. B. Zhang, J. Fletcher, N. Greeves, S. J. Finney, and B. W. Williams, "One-power-point operation for variable speed wind/tidal stream turbines with

synchronous generators," *IET Renew. Power Gener.*, vol. 5, no. 1, pp. 99–108, 2011, doi: 10.1049/iet-rpg.2009.0207.

[82] F. B. Tao Sun, Zhe Chen, "Voltage Recovery of Grid-Connected Wind Turbines with DFIG After a Short-Circuit Fault," in *2004 IEEE 35th Annual Power Electronics Specialists Conference, 2004. PESC 04.*, 2004, pp. 1991–1997.

[83] M. Ragheb and A. M. Ragheb, "Wind Turbines Theory - The Betz Equation and Optimal Rotor Tip Speed Ratio," vol. 1, no. 1, 1926.

[84] S. O. Ani, "Low Cost Small Wind Turbine Generators for Developing Countries," TU Delft, Delft University of Technology, 2011.

[85] J. H. Laks and L. Y. Pao, *Optimal Control of Wind Energy Systems*, 1st ed., no. June. London: Springer London, 2008.

[86] J. Pyrhönen, T. Jokinen, and V. Hrabovcová, *Design of Rotating Electrical Machines*. Chichester, UK: John Wiley & Sons Ltd, 2013.

[87] T. A. Lipo, *Analysis of Synchronous Machines*. CRC Press, 2017.

[88] B. Wu, Y. Lang, N. Zargari, and S. Kouro, *Power Conversion and Control of Wind Energy Systems*. Hoboken, NJ, USA: John Wiley & Sons, Inc., 2011.

[89] S. A. Azmi, K. H. Ahmed, S. J. Finney, and B. W. Williams, "COMPARATIVE ANALYSIS BETWEEN VOLTAGE AND CURRENT SOURCE INVERTERS IN GRID-CONNECTED APPLICATION," in *In Renewable Power Generation (RPG 2011), IET Conference*, 2011, pp. 1–6.

[90] F. I. F Blaabjerg, "Wind power–a power source now enabled by power electronics," in *COBEP 2007*, 2007.

[91] S. Bifaretti, P. Zanchetta, A. Watson, L. Tarisciotti, and J. C. Clare, "Advanced Power Electronic Conversion and Control System for Universal and Flexible Power Management," *IEEE Trans. Smart Grid*, vol. 2, no. 2, pp. 231–243, Jun. 2011, doi: 10.1109/TSG.2011.2115260.

[92] J. Clare, "Advanced power converters for universal and flexible power management in future electricity networks," in *2009 13th European Conference on Power Electronics and Applications*, 2009, pp. 1–29.

[93] N. Mohan, *Advanced Electric Drives*. Hoboken, NJ, USA: John Wiley & Sons, Inc., 2014.

[94] D. D. Banham-Hall, G. A. Taylor, C. A. Smith, and M. R. Irving, "Towards large-scale direct drive wind turbines with permanent magnet generators and full converters," in *IEEE PES General Meeting*, 2010, pp. 1–8, doi:

10.1109/PES.2010.5589780.

[95] H. Chen, T. N. Cong, W. Yang, C. Tan, Y. Li, and Y. Ding, “Progress in electrical energy storage system: A critical review,” *Prog. Nat. Sci.*, vol. 19, no. 3, pp. 291–312, 2009, doi: 10.1016/j.pnsc.2008.07.014.

[96] M. H. Ali, B. Wu, and R. A. Dougal, “An overview of SMES applications in power and energy systems,” *IEEE Trans. Sustain. Energy*, vol. 1, no. 1, pp. 38–47, 2010, doi: 10.1109/TSTE.2010.2044901.

[97] R. B. Schainker, “Executive overview: energy storage options for a sustainable energy future,” in *IEEE Power Engineering Society General Meeting, 2004.*, 2005, vol. 2, pp. 2310–2315, doi: 10.1109/PES.2004.1373298.

[98] S. C. Smith, P. K. Sen, and B. Kroposki, “Advancement of energy storage devices and applications in electrical power system,” *IEEE Power Energy Soc. 2008 Gen. Meet. Convers. Deliv. Electr. Energy 21st Century, PES*, pp. 1–8, 2008, doi: 10.1109/PES.2008.4596436.

[99] A. M. Shiddiq Yunus, A. Abu-Siada, and M. A. S. Masoum, “Improving dynamic performance of wind energy conversion systems using fuzzy-based hysteresis current-controlled superconducting magnetic energy storage,” *IET Power Electron.*, vol. 5, no. 8, p. 1305, 2012, doi: 10.1049/iet-pel.2012.0135.

[100] M. H. Khan and A. H. M. A. Rahim, “IPSO based SMES controller design for a PMSG wind system,” in *2012 IEEE International Energy Conference and Exhibition (ENERGYCON)*, 2012, pp. 599–604, doi: 10.1109/EnergyCon.2012.6348223.

[101] K. Zhang, C. Mao, J. Lu, D. Wang, X. Chen, and J. Zhang, “Optimal control of state-of-charge of superconducting magnetic energy storage for wind power system,” *IET Renew. Power Gener.*, vol. 8, no. 1, pp. 58–66, Jan. 2014, doi: 10.1049/iet-rpg.2013.0003.

[102] M. Ahnaf Abid Khan, M. Mofrat Shahriar, and M. Shahidul Islam, “Power Quality Improvement of DFIG and PMSG Based Hybrid Wind Farm Using SMES,” *2nd Int. Conf. Electr. Electron. Eng. ICEEE 2017*, no. December, pp. 1–4, 2018, doi: 10.1109/CEEE.2017.8412899.

[103] E. F. Shaaban, A. El-Wahab Hassan, D. E. A. Mansour, and W. Yuan, “Application of SMES for voltage stabilization of PMSG connected to DC grids,” *Proc. - 2018 53rd Int. Univ. Power Eng. Conf. UPEC 2018*, pp. 1–5, 2018, doi: 10.1109/UPEC.2018.8541934.

[104] P. Dey, M. Datta, N. Fernando, and T. Senjyu, “Fuzzy-based Coordinated Control to Reduce DC-link Overvoltage of a PMSG based Wind Energy Systems during Grid Faults,” *2018 5th Int. Conf. Electr. Power Energy Convers. Syst. EPECS 2018*, pp. 1–6, 2018, doi: 10.1109/EPECS.2018.8443560.

[105] C. Masetti, “Revision of European Standard EN 50160 on power quality: Reasons and solutions,” in *Proceedings of 14th International Conference on Harmonics and Quality of Power - ICHQP 2010*, 2010, pp. 1–7, doi: 10.1109/ICHQP.2010.5625472.

[106] M. S. Tavazoei, “From Traditional to Fractional PI Control: A Key for Generalization,” *IEEE Ind. Electron. Mag.*, vol. 6, no. 3, pp. 41–51, Sep. 2012, doi: 10.1109/MIE.2012.2207818.

[107] A. Jain and R. Saravanakumar, “Comparative analysis of fractional order PI and integer order PI based controller for hybrid standalone wind energy conversion system,” *Environ. Prog. Sustain. Energy*, vol. 39, no. 2, pp. 1–9, Mar. 2020, doi: 10.1002/ep.13293.

[108] H. Chen *et al.*, “Fractional-Order PI Control of DFIG-Based Tidal Stream Turbine,” *J. Mar. Sci. Eng.*, vol. 8, no. 5, p. 309, Apr. 2020, doi: 10.3390/jmse8050309.

[109] A. Beddar and H. Bouzekri, “Design and real-time implementation of hybrid fractional order controller for grid connected wind energy conversion system,” *Int. J. Model. Identif. Control*, vol. 29, no. 4, p. 315, 2018, doi: 10.1504/IJMIC.2018.092110.

[110] M. Samir and M. Said, “AT | E An Optimized Fractional Order PI Controller to Improve DFIG Active and Reactive Powers Control,” 2021.

[111] R. K. Arora, “1-D Optimization Algorithms,” in *Optimization*, Chapman and Hall/CRC, 2015, pp. 51–70.

[112] X. Z. Gao, V. Govindasamy, H. Xu, X. Wang, and K. Zenger, “Harmony Search Method: Theory and Applications,” *Comput. Intell. Neurosci.*, vol. 2015, pp. 1–10, 2015, doi: 10.1155/2015/258491.

[113] J. Ricart, G. Hüttemann, J. Lima, and B. Barán, “Multiobjective Harmony Search Algorithm Proposals,” *Electron. Notes Theor. Comput. Sci.*, vol. 281, pp. 51–67, Dec. 2011, doi: 10.1016/j.entcs.2011.11.025.

[114] A. A. Al-Omoush, A. A. Alsewari, H. S. Alamri, and K. Z. Zamli, “Comprehensive Review of the Development of the Harmony Search Algorithm

and its Applications," *IEEE Access*, vol. 7, pp. 14233–14245, 2019, doi: 10.1109/ACCESS.2019.2893662.

[115] M. I. Mosaad and H. S. Ramadan, "Power quality enhancement of grid-connected fuel cell using evolutionary computing techniques," *Int. J. Hydrogen Energy*, vol. 43, no. 25, pp. 11568–11582, Jun. 2018, doi: 10.1016/j.ijhydene.2018.02.001.

[116] L. Xu, R. Lin, L. Ding, H. Zhang, S. Li, and C. Huang, "A new frt method of pmsg under grid faults by using improved msc control and smes device," *IOP Conf. Ser. Mater. Sci. Eng.*, vol. 490, no. 7, 2019, doi: 10.1088/1757-899X/490/7/072032.